GEOCHEMICAL AND ISOTOPIC STUDIES OF THE PLATREEF WITH SPECIAL EMPHASIS ON SULPHIDE MINERLISATION.

Elizabeth Sharman-Harris

A dissertation submitted to the Faculty of Science, University of the Witwatersrand, in fulfilment of the requirements for the degree of Master of Science (by dissertation).

Johannesburg, 2006

DECLARATION

I declare that this dissertation is my own, unaided work. It is being submitted for the Degree of Master in Science in the University of the Witwatersrand, Johannesburg. It has not been submitted before for any degree or examination in any other University.

_____

Signature of Candidate

_____ day of _____ 2006

ABSTRACT

The Platreef has been the site of platinum mining since the 1920's. The reef itself comprises a series of pyroxenites, gabbronorites and norites that contain xenoliths/rafts of footwall rocks. The Platreef is irregularly mineralised with PGE, Cu and Ni, and has a greater abundance of sulphides than the Merensky Reef. The main base metal sulphides within the Platreef are pyrrhotite, pyrite, pentlandite, and chalcopyrite. Extremely varied platinum group minerals occur as tellurides, bismuthotellurides, antimonides and arsenides.

This study aimed to gain a clearer understanding of the formation of sulphides within the Platreef. In order to do this, cores from both the northern and southern sectors of the Platreef were sampled. A detailed study of the sulphides within these cores was conducted to identify different styles of mineralisation and their occurrences. Four different styles of mineralisation were identified: massive, net-textured, blebby and interstitial. In general, sulphides in the southern sector of the Platreef are concentrated in the lower portion of the package, whereas in the northern sector they are concentrated in the upper part although in both sectors the sulphide occurrences are associated with metasedimentary xenoliths.

Conventional and multiple sulphur isotope analyses were undertaken on sulphides from cores from both the southern and the northern sectors. This was done in order to determine the source of the sulphur. These analyses were also conducted to examine sulphur isotope variations with changing footwall. Previous sulphur isotope data predominantly obtained from the central sector of the Platreef indicated a crustal contribution to the sulphur budget but did not provide much data on footwall sulphides so the nature of the crustal component was only implied. In this thesis sulphur from an external source was identified as having contributed to the formation of sulphides in both the southern and the northern sectors of the Platreef, especially for sulphides in proximity to metasedimentary xenoliths. In the southern sector of the

Platreef this source was identified as most likely being pyritic shales of the Lower Duitschland Formation. In the northern sector, Malmani dolomites, which are suggested to have collapsed from the roof of the Platreef, are the most likely source of sulphur. Importantly, in the northern sector no sulphur is thought to have come from the Archaean granite footwall.

Oxygen isotope analyses were conducted on samples from the southern sector of the Platreef to verify the presence of crustal contamination. Data collected indicated that there had been a crustal oxygen component involved in the formation of silicates that led to their partial recrystallisation. When compared to oxygen isotope data from the central sector of the Platreef it appears that there are variations along strike that most likely result due to the changing footwall.

This data indicates a major contribution of oxygen-, sulphur- and other volatile-rich fluids to the Platreef. This led to the partial re-crystallisation of silicates, and in areas in close proximity to sulphur-bearing metasedimentary xenoliths aided in the formation of sulphides. These volatile-rich fluids most likely originated from metasedimentary xenoliths during metamorphism that then migrated through the Platreef package.

When the observations from both the southern and northern sectors of the Platreef are compared and combined with pre-existing data for the central sector, several general observations can be made.

1. The entire length of the Platreef has been affected by contamination from crustal sulphur sources to some degree. This contamination is suggested to be from volatile-rich fluids which were released from metasedimentary crustal xenoliths and footwall during metamorphism.

2. The proximity between sulphide enrichment and sulphur-bearing sediments (as footwall or xenoliths) is important and indicates the source of the sulphur which led to sulphide formation.
3. Contamination occurred on a localised scale, depending on the composition of the sedimentary lithologies and the proximity of the contaminant to the magma. In the southern sector of the Platreef the source of the sulphur is almost certainly pyritic shales of the Lower Duitschland Formation. In the central sector, sulphur has most likely come from sulphur-rich dolomites and evaporites from the Malmani dolomites. In the northern sector, sulphur-rich fluids were released from Malmani dolomite rafts that collapsed from the roof into the magma during the emplacement of the Platreef. The Archaean footwall in this area has had little or no control on the formation of the sulphides within the Platreef.

DEDICATION

To my husband Martin Tuchscherer,
my parents Angie and Philip Harris, and David Sharman.

For all their support.

THOUGHTS

“If we knew what we were doing, it wouldn’t be called research would it?”

Albert Einstein

ACKNOWLEDGEMENTS

I would firstly and most importantly like to thank my supervisor Prof. Judith Kinnaird for taking me on for an MSc and giving me this fantastic opportunity. Her constant support and guidance were invaluable in this endeavour.

This project would not be what it is without access to samples and funding. To that end I would like to thank Ivanhoe Nickel and Platinum Ltd., and especially Louis Schürmann for their continuous interest and support for this project including access to core and geochemical data as well as funding. I would similarly like to thank Gernot Wober at Hunter Dickinson/Anooraq Resources for providing access to samples and databases for the work conducted on the northern sector of the Platreef. I would also like to thank THRIP for providing funding for this project, particularly the costs of travelling to the United States to conduct multiple sulphur isotope analyses.

In the duration of this study I have had the opportunity to conduct many different types of analyses in many different places around the world. I would like to thank Uwe Horstmann at the iThemba Laboratories in Johannesburg for introducing me to sulphur isotope analyses. To Chris Harris at the University of Cape Town, thank you for a rewarding opportunity to learn what is required for oxygen isotope analyses. At the University of Maryland thanks must go especially to Boz Wing, for knowing how far to push me, and taking me for a beer when I could go no further. Also to Sarah Penniston-Dorland and Dave Johnston who helped me in the lab, and to Stephanie Mair, for her pep talks, and constant supply of coffee. These people made running multiple sulphur isotope analyses some of the hardest but most rewarding times of this thesis. Thanks also go to Dave Lowry and Nathalie Grassineau at Royal Holloway University College London for running sulphur isotope analyses, and Tim Atkinson at University College London for providing access to a microdrill. I would also like to thank Joe Aphane at the University of the Witwatersrand for helping me with the processes involved in the preparation of sulphide separates.

Acknowledgments and thanks must also go to Paul Nex, for help with anything digital from Corel Draw to Strater, as well as always patiently listening. I am also indebted to Tony Naldrett for allowing me to accompany him into the field, for always being there to discuss ideas, and providing invaluable support, insight and motivation. Thanks also to Dave Hutchinson for also being there to talk things through.

Finally, to my friends, who were always there with some respite when things got tough. Especially to my husband Martin for being there through thick and thin, and pushing me on no matter how much I wanted to quit. Also to those who were always happy to meet for lunch or a drink, you kept me sane, and for that I will be eternally grateful - you know who you are. Lastly to Torben, for making the best Thai food in Johannesburg, this thesis may not have been possibly without your satays.

CONTENTS **Page**

DECLARATION……i
ABSTRACT……ii
DEDICATION……v
ACKNOWLEDGEMENTS……vi
LIST OF FIGURES……x
LIST OF TABLES……xii

CHAPTER ONE – INTRODUCTION

Introduction……1
Regional Geology……2
Transvaal Supergroup……2
Bushveld Igneous Complex……6
Northern Limb of the Bushveld Complex……9
General Geology of the Platreef……13
Aims and Objectives……15

CHAPTER TWO – PETROGRAPHY

Introduction……16
Core Logs……18
ATS-046……18
ATS-057……18
AMK-021……22
ARF-08……24
PR-174……26
PR-175……26

CHAPTER THREE – SULPHIDE MINERALOGY

Introduction……29
Sulphide Mineralisation Theory and Concepts……29
Sulphide Mineralisation of the Platreef……30
Core ATS-046……33
Core ATS-057……36
Core AMK-021……38
Core PR-174……38
Core PR-175……40
Duitschland Formation……41
Vein Material……41

CHAPTER FOUR – SULPHUR ISOTOPE ANALYSES

Introduction……..……..44
Sulphur Isotope Theory and Concepts……44
Previous Work……...……46
Methodology……..……..48
Results……..……53
Southern Sector of the Platreef…….....……53
Northern Sector of the Platreef……57
Sedimentary Material……...……...60
Vein Material……...60
Discussion of Results……61

CHAPTER FIVE – MULTIPLE SULPHUR ISOTOPE ANALYSES

Introduction……65
Multiple Sulphur Isotope Theory and Concepts……65
Previous Work……...66
Methodology……...67
Results……68
Discussion of Results……..69

CHAPTER SIX – OXYGEN ISOTOPE ANALYSES

Introduction……71
Oxygen Isotope Theory and Concepts……71
Previous Work……...……72
Methodology……...……74
Results……75
Discussion of Results……..77

CHAPTER SEVEN – DISCUSSION AND CONCLUSIONS

Introduction……80
Discussion……...……80
Southern Sector of the Platreef……81
Northern Sector of the Platreef……88
Similar Global Deposits……..……93
Noril'sk, Siberia……...……93
Duluth Complex, North America……..95
Voisey's Bay, Canada……..96
Conclusions……98

REFERENCES……..……100

APPENDIX ONE: SAMPLE DESCRIPTIONS FOR CORE ATS-057……...106

APPENDIX TWO: THIN SECTION DESCRIPTIONS FOR CORE ATS-057……109

APPENDIX THREE: SAMPLE DESCRIPTIONS FOR CORE AMK-021……113

APPENDIX FOUR: POLISHED BLOCK DESCRIPTIONS FOR CORES AMK-021, ATS-056 AND ATS-046……..115

APPENDIX FIVE A: DESCRIPTION OF SULPHIDE MINERALISATION INTERVALS FOR CORE PR-174……119

APPENDIX FIVE B: DESCRIPTION OF SULPHIDE MINERALISATION INTERVALS FOR CORE PR-175……120

APPENDIX SIX: PUBLICATIONS ……122

LIST OF FIGURES

Figure 1.1: Stratigraphic column of the Transvaal Supergroup……...3
Figure 1.2: Geological Map of the area around the town of Mokopane……..5
Figure 1.3: Map of the Bushveld Complex……..7
Figure 1.4: Map of the Northern Limb of the Bushveld Igneous Complex…...…10
Figure 1.5: Map of the Northern Limb showing sectors and farm boundaries…..11

Figure 2.1: Map showing locations of boreholes for southern sector……16
Figure 2.2: Map showing locations of boreholes for northern sector……17
Figure 2.3: Examples of different lithologies from core ATS-046……19
Figure 2.4: Stratigraphic log of ATS-046……..20
Figure 2.5: Stratigraphic log of ATS-057……..21
Figure 2.6: Typical lithologies from core AMK-021…….……22
Figure 2.7: Stratigraphic log of AMK-021……...……..23
Figure 2.8: Typical lithologies from core ARF-08…….……...……24
Figure 2.9: Stratigraphic log of ARF-08……...……..25
Figure 2.10: Stratigraphic log of PR-174……...……..27
Figure 2.11: Stratigraphic log of PR-175...……..28

Figure 3.1: Diagram of different types of sulphide mineralisation……31
Figure 3.2: Scanning electron microprobe images of various sulphides……32
Figure 3.3: Photograph of polished blocks from core ATS-046……34
Figure 3.4: Photograph of polished blocks from core ATS-046……34
Figure 3.5: Core log of ATS-046 with sulphur concentrations and sulphide textures……..35
Figure 3.6: Image of polished blocks from ATS-057……36
Figure 3.7: Core log of ATS-057 with sulphur concentrations and sulphide textures……..37
Figure 3.8: Photograph of polished blocks from core AMK-021……..…38
Figure 3.9: Core log of PR-174 with sulphur concentrations and sulphide textures……..39
Figure 3.10: Core log of PR-175 with sulphur concentrations and sulphide textures……..40
Figure 3.11: Photograph of nodular pyrite in shale……..41
Figure 3.12: Photograph of sample ZN396-214.4……42
Figure 3.13: Photograph of sample PRS-17……42

Figure 4.1: $\delta^{34}S$ values for a variety of geological materials…….……45
Figure 4.2: Histograms for all previous sulphur isotope analyses……47
Figure 4.3: Photograph of the microdrill……50
Figure 4.4: Diagram of a continuous flow mass spectrometer…..……51
Figure 4.5: Histograms for sulphur isotope analyses for the southern sector…..56
Figure 4.6: Diagram showing variation of $\delta^{34}S$ values with depth for southern sector……57

Figure 4.7: Histograms for sulphur isotope analyses for the northern sector…..59
Figure 4.8: Diagram showing variation of $\delta^{34}S$ values with depth for the northern sector……..59
Figure 4.9: Stratigraphy of the Duitschland Formation with $\delta^{34}S$ values……60
Figure 4.10: Geological map of the Platreef showing non-magmatic sulphur isotope data for the Platreef……..64

Figure 5.1: Plot of $\Delta^{33}S$ vs. age……..……66
Figure 5.2: Diagram showing multiple sulphur isotope data for the Transvaal Supergroup…….……67
Figure 5.3: Diagram showing multiple sulphur isotope data from this study……69
Figure 5.4: Diagram plotting $\delta^{34}S$ vs. $\Delta^{33}S$……70

Figure 6.1: Diagram showing variation of $\delta^{18}O$ with depth……...……76
Figure 6.2: Diagram showing $\delta^{18}O$ data for different sectors of the Platreef……78

Figure 7.1: Sulphur contents at sulphide saturation vs. pressure and temperature……..……81
Figure 7.2: Core logs and sulphur concentration of cores ATS-57 and ATS-46……..83
Figure 7.3: Generalised core logs for the southern sector of the Platreef showing average sulphur isotope values……..84
Figure 7.4: Simplified core log of the Platreef with multiple-sulphur isotope data……..……86
Figure 7.5: Diagram plotting $\delta^{34}S$ vs. $\Delta^{33}S$……87
Figure 7.6: Core logs with sulphur concentration for cores PR-174 and PR-175…….……89
Figure 7.7: Generalised core of the Platreef package on Farm Drenthe with average sulphur isotope values……..……90
Figure 7.8: Geological cross-section of part of the Noril'sk deposits……94
Figure 7.9: Geological map of the Duluth Complex……..96
Figure 7.10: Geological map of the area of the Voisey's Bay Deposit……97

LIST OF TABLES

Table 4.1: Sulphur isotope data for the southern sector of the Platreef on Farms Turfpruit and Macalacaskop……54
Table 4.2: Sulphur isotope data for the southern sector of the Platreef on Farm Rietfontein……..55
Table 4.3: Sulphur isotope data for the northern sector of the Platreef……58
Table 4.4: Sulphur isotope data for the footwall and vein material……..61

Table 5.1: Multiple Sulphur Isotope Analyses on sulphides from three cores….68

Table 6.1: Details of all oxygen isotope analyses for this study……..76
Table 6.2: Results of Oxygen Geothermometry……...77

CHAPTER ONE
INTRODUCTION

Introduction

The Platreef has been the site of platinum prospecting and mining since the 1920s (White, 1994). The reef itself is a series of pyroxenites and norites, containing xenoliths/rafts of footwall rocks. The Platreef is irregularly mineralised with PGE, Cu and Ni, and there is a greater abundance of sulphides than in the Merensky Reef. There is an extremely varied platinum group mineralogy, occurring mainly as tellurides, bismuthotellurides, antimonides and arsenides of Pd, Pt, and Rh, (Hutchinson et al., 2004) which varies in relative proportions in different sectors of the Platreef. The main base-metal sulphides within the Platreef are pyrrhotite, pyrite, pentlandite, and chalcopyrite. This mineralisation was previously thought to be dominantly of magmatic origin, however, evidence for "post-magmatic fluid interaction" (Harris and Chaumba, 2001), and contamination of the magma by crustal material are now regarded as potential processes.

In order to gain a further understanding of the sources of sulphur within the Platreef, as well as mineralisation processes, a sulphur-isotope study has been undertaken on samples collected from the southern and northern Platreef and its footwall rocks. Previous sulphur isotope data (Liebenberg, 1968; Hulbert, 1983) obtained more than twenty years ago indicated that sulphides within the Platreef were of a magmatic origin. However sulphur isotope data presented by Buchanan et al. (1981) and Buchanan and Rouse (1984) indicated a crustal contribution from Malmani dolomites to the sulphur budget, but did not provide much data on footwall sulphides.

This study aims to undertake a more detailed examination of the role of sulphur contamination within the Platreef by an analysis of sulphur isotopes both within the footwall and through the Platreef at differing distances from the footwall. It will also use other stable isotope systems (oxygen and multiple-sulphur isotopes)

as an additional monitor of contamination of the Platreef magma, and to possibly identify different generations of magma. This research forms part of a larger research group that is currently investigating different aspects of the Northern Limb. It is hoped that this will help provide a fuller understanding of the magmatic processes that led to the formation of the Platreef. Other work that is being conducted by this group includes additional geochemistry (Prof. J. Kinnaird), platinum-group mineralogy (Dr. D. Hutchinson), and mineral chemistry (Victor Mothetha).

Regional Geology

Transvaal Supergroup

The Palaeoproterozoic Transvaal Supergroup (Figure 1.1) was deposited between 2.67 and 2.07 Ga (Coetzee, 2001; Eriksson et al., 2001) in the Transvaal and the Griqualand West Basins which are separated by the Vryburg Rise (Bekker et al., 2001). The Supergroup attains a maximum thickness of 12 km within the Transvaal Basin (Eriksson et al, 2001). The basement rocks of the Transvaal Supergroup are predominantly Archaean granites, gneisses and greenstones, as well as a Witwatersrand sedimentary succession and Ventersdorp lavas (Coetzee, 2001; Eriksson et al., 2001). The Transvaal Basin comprises the Wolkberg, Chuinespoort, and Pretoria Groups (Figure 1.1), however as there is an erosional contact between the Wolkberg and Chuniespoort Groups, Coetzee (2001) does not consider the Wolkberg group to be part of the Transvaal Basin *sensu stricto*.

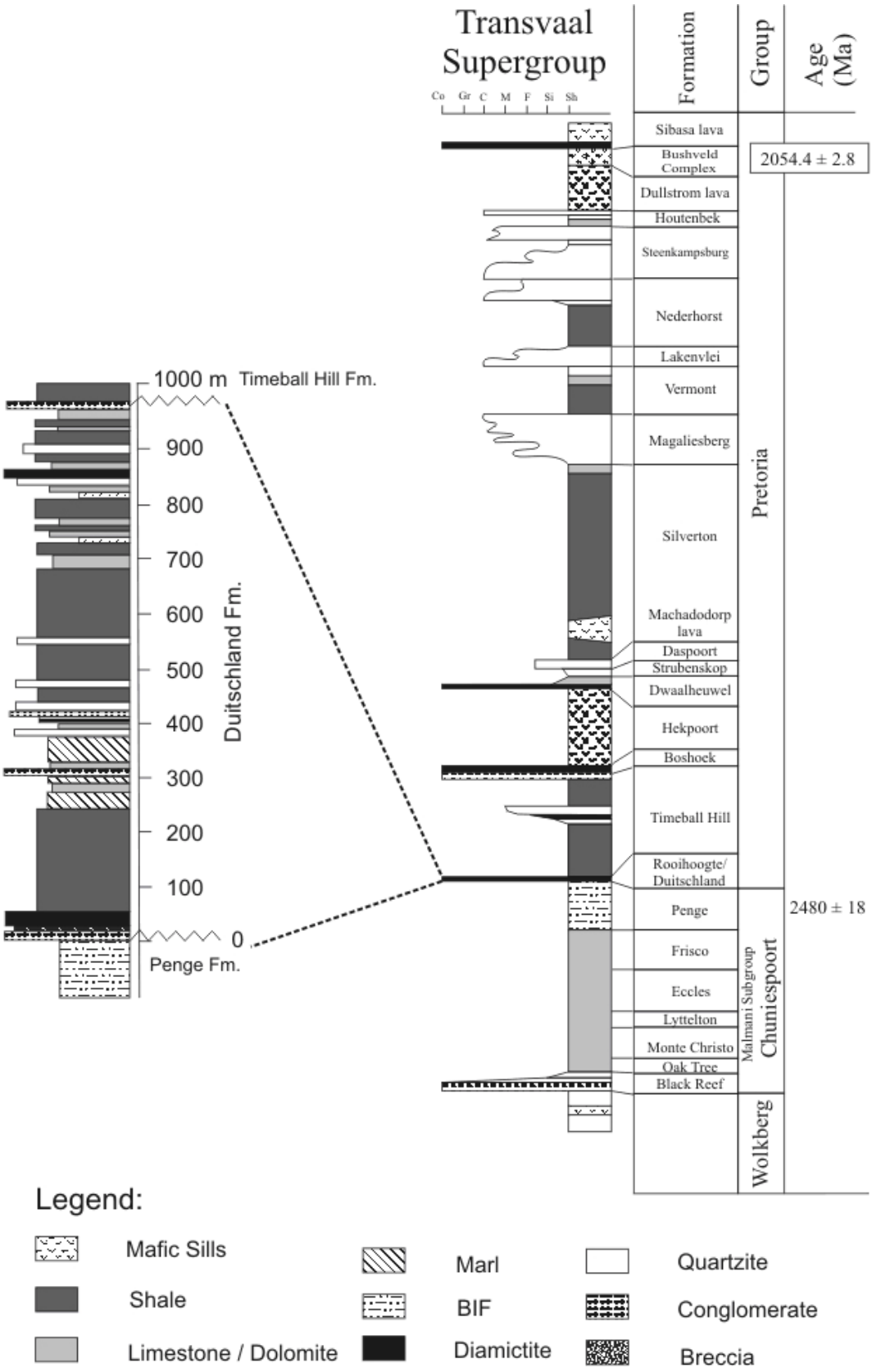

Figure 1.1: Stratigraphic Column of the Transvaal Supergroup, showing detail of the Duitschland Formation (Bekker et al., 2001; Coetzee, 2001).

The Wolkberg Group consists of upward-coarsening feldspathic quartzites and argillaceous sedimentary rocks, coarse quartz-sericite arenites, conglomerates, a basaltic lava and stromatolitic carbonate beds (Coetzee, 2001), and reaches a maximum thickness of 2000 m. It is unconformably overlain by the Black Reef Formation, which occurs at the base of the Chuniespoort Group. The Black Reef Formation comprises quartzites, and a basaltic lava unit. According to Coetzee (2001), the Black Reef Quartzite grades into the Malmani Subgroup through a 10 to 200 m-thick unit comprising iron and manganese-rich dolomite, carbonaceous shale and quartzite. The Malmani subgroup reaches a maximum thickness of 2400 m, and comprises limestone, chert-rich, and chert-poor dolomite. Conformably overlying the Malmani subgroup is the Penge Formation which is composed of quartz, magnetite, hematite, stilpnomelane, riebeckite, minnesotaite, grunerite and carbonates, either in mixed or monomineralic layers. It is micro-, meso- and macrobanded, with the laminae being laterally very persistent (Coetzee, 2001). This unit also contains subordinate carbonaceous shale beds. The transition from the Chuniespoort to the Pretoria Group marks a transition from mainly chemical to mainly clastic sedimentation.

In the southern sector of the Platreef, where this study is focused, the footwall is often comprised of Duitschland Formation which marks the base of the Pretoria Group and disconformably overlies the Chuniespoort Group. It comprises diamictite, an alternating sequence of fine-grained laminated shales; occasionally containing pyrite; and dolomite, along with some minor sequences of quartzite and mudrock (Figure 1.1). The Formation is exposed in two areas near Mokopane (Figure 1.2) and has a maximum thickness of 1000 m (Martini, 1979). The Duitschland Formation is thought to have been deposited in a relatively shallow marine environment (Bekker et al., 2001; Martini, 1979), this is supported by the presence of stromatolites. Carbonaceous shales represent the deepest depositional environment within the Formation (Martini, 1979). The base of the Formation is marked by a diamictite, and the top of the Formation is characterised by an ivory-white dolomite containing bornite and chalcopyrite. It is bounded at its base in the north by the Penge Formation which is composed predominantly of quartz,

magnetite and hematite (Coetzee, 2001) and also contains subordinate carbonaceous shale beds. The top of the sequence, in the south, is marked by the Timeball Hill Formation which is composed of shale, quartzite, and diamictite.

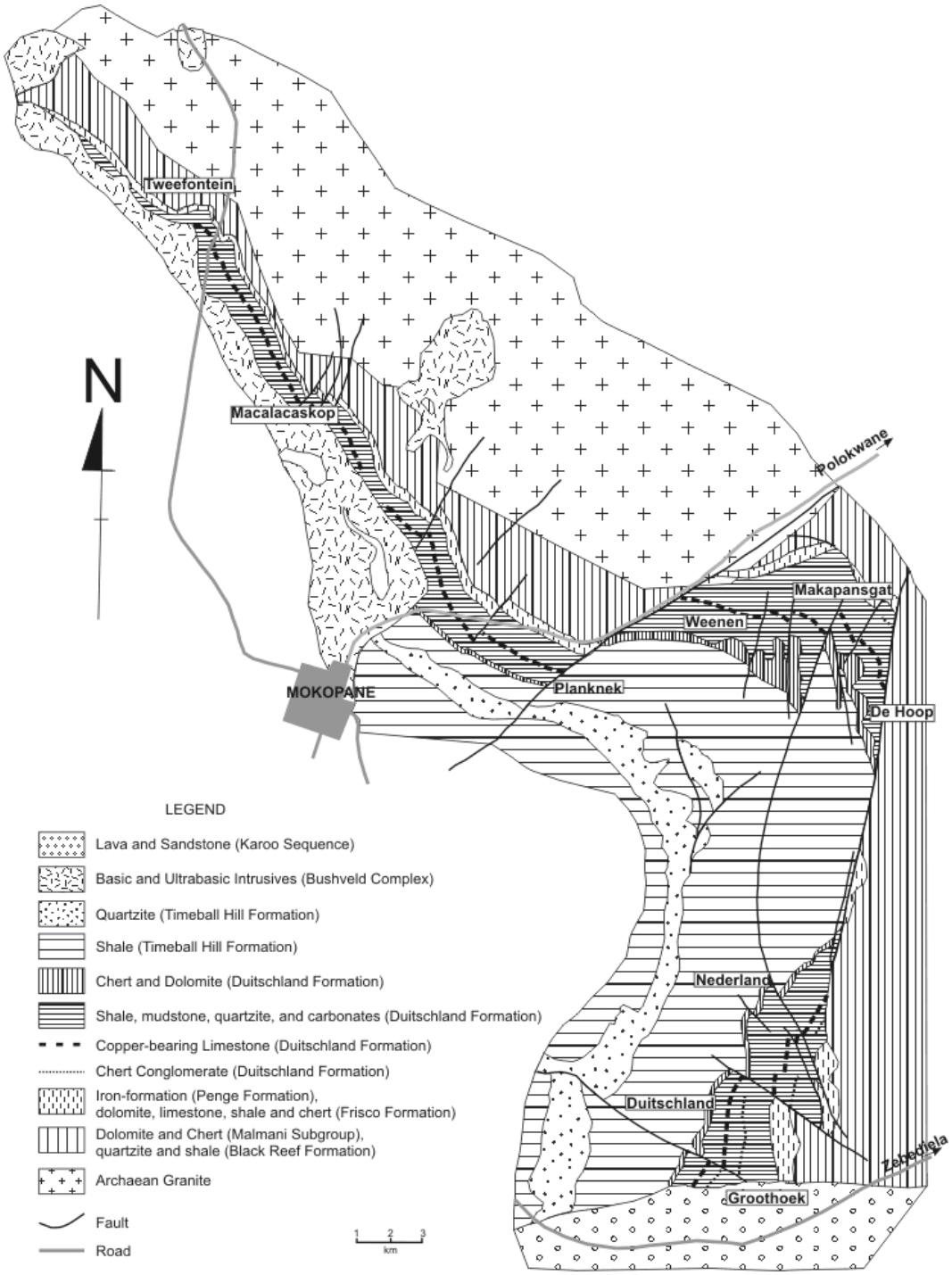

Figure 1.2: Geological Map of the area around the town of Mokopane (previously Potgietersrus) showing the location of Farm Duitschland (modified from Martini, 1979)

The Timeball Hill Formation is subsequently unconformably overlain by the Boeshoek Formation (Figure 1.1). This is then conformably overlain by altered basaltic lavas of the Hekpoort Formation. Overlying the Hekpoort lavas is a palaeosol, represented by the Dwaalheuwel Formation, which comprises diamictite, conglomerate, and sandstone (Catuneanu and Eriksson, 1999). Conformably above this is the Strubenkop Formation, which is finer-grained, and comprises mudstones with subordinate sandstones. The overlying Daspoort Formation is coarser-grained and comprises sandstones. This is then followed by the Silverton Formation mudstones [commonly tuffaceous] with some sandstone, and interrupted by the Machadodorp volcanics) and the Magaliesberg Formation (sandstone with mudstone lenses and interbeds) (Reczko, 1994; Catuneanu and Eriksson, 1999). This alternating sequence of mudstones and sandstones is then repeated through the Vermont, Lakenvlei, and Nederhorst Formations, followed by the Steenkampsberg Formation which comprises sandstones. The top of the Pretoria Group sedimentary succession is marked by the Houtenbek Formation, which comprises tuffaceous mudstones, followed by limestone, sandstone, and finally mudstones (Reczko, 1994; Catuneanu and Eriksson, 1999). The Dullstroom Lavas mark the top of the Transvaal Supergroup (Coetzee, 2001). However, as these lavas are Bushveld in age they do not truly belong to the Transvaal Supergroup.

Bushveld Igneous Complex

The Bushveld Igneous Complex (BIC) is a sequence of layered mafic and ultramafic rocks, with varying lithologies ranging from dunite and pyroxenite, to anorthosite and pure oxide layers (Eales and Cawthorn, 1996). The BIC covers an area of approximately 65 000 km^2, with a thickness of 3-9 km (Figure 1.3). The lithologies occur as a succession of layers of varying thickness, and despite their age of 2060 ± 1 Ma (Buick et al., 2001) have experienced no metamorphism, but only mild or local alteration (Eales and Cawthorn, 1996). The Complex comprises five major limbs, the Western Limb, the Far Western Limb, the Northern Limb, the Eastern Limb (all of which outcrop at surface) and the

Southeastern or Bethal Limb which is covered by younger sediments (Figure 1.3). The Western and Eastern Limbs are the best known, being the most extensive, with average strike lengths of ~200 km. The Northern Limb is partially concealed beneath younger rocks of the Waterberg Supergroup, the Far Western Limb is an eroded remnant, and the Bethal Limb is only identifiable through a gravity high, with its location confirmed by bore-core data (Eales and Cawthorn, 1996).

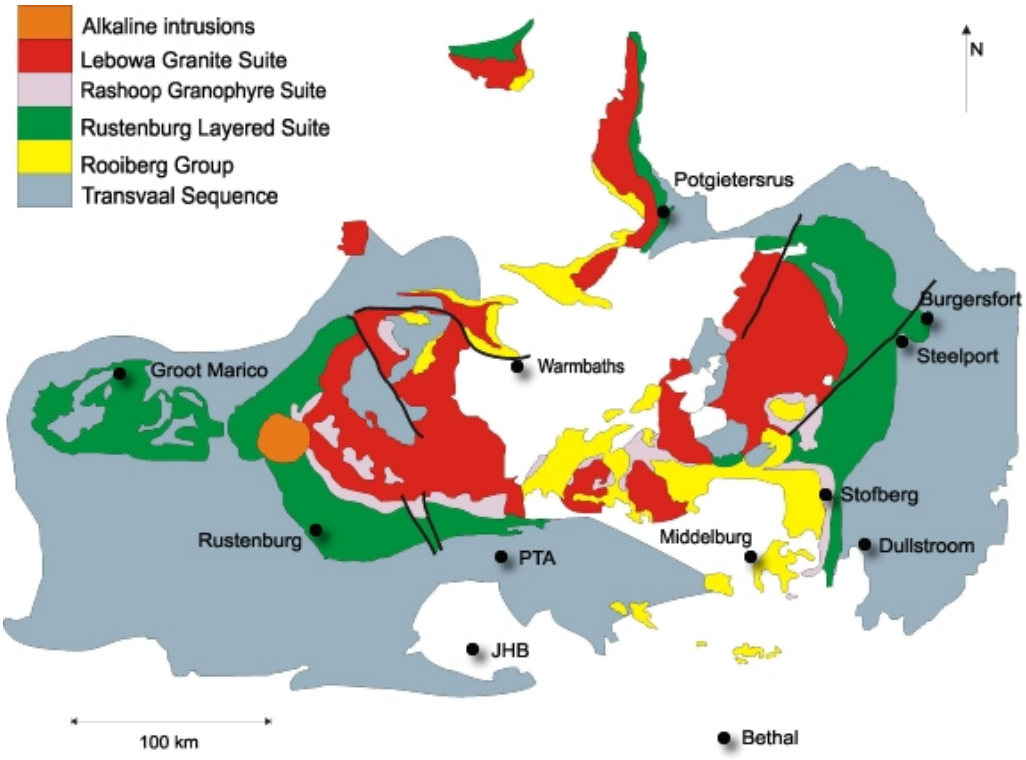

Figure 1.3: Map of the Bushveld Igneous Complex showing the major limbs (modified from Kinnaird, 2003).

The BIC intruded into the Transvaal Supergroup with the footwall of different limbs comprising different units of the sedimentary sequence. The floor of the Western and Far Western Limbs is composed of Magaliesurg quartzite; the Eastern Limb has a floor of Magaliesburg quartzite to the north, and transgresses upwards through 2 km of sediments towards the south into the Dullstroom basaltic volcanics (Eales and Cawthorn, 1996). The Northern Limb was intruded into Magaliesburg quartzites in the south, and transgresses downwards to the north, where the mafic rocks occur adjacent to the Archaean basement. The Bethal Limb was emplaced into Malmani dolomites (Eales and Cawthorn, 1996).

The BIC is divided into five zones, the Marginal, Lower (LZ), Critical (CZ), Main (MZ), and Upper (UZ) Zones (Eales and Cawthorn, 1996). Not all of the zones are represented in all of the limbs, in particular the Northern Limb, where the existence of units from the Critical Zone is yet to be proved north of Mokopane (Potgietersus). Units from the Lower Zone are present south of Mokopane (Buchanan et al, 1981; Harris and Chaumba, 2001) and as satellite bodies.

The Marginal Zone comprises medium-grained, heterogeneous noritic rocks thought to represent composite sills, or the distal facies of evolved magmas from within the chamber (Eales and Cawthorn, 1996). The Lower Zone is variable in composition, occurrence and thickness across the BIC. In the Western Limb the LZ is an 800 m thick olivine- and orthopyroxene-rich sequence. In the Eastern Limb, the LZ is divided into four units: basal feldspathic pyroxenite with minor harzburgite, lower pyroxenite, harzburgite, and upper pyroxenite (Eales and Cawthorn, 1996).

The Critical Zone of the BIC is subdivided into two major sub-zones, the Lower, and Upper CZ. The Lower Critical Zone is comprised of a thick succession of orthopyroxene-rich cumulates which overlie the LZ harzburgites. The Upper Critical Zone is made-up of up to eight partial or complete cyclic units. These sequences start from a base of ultramafic cumulates (chromitite, harzburgite, pyroxenites) through norite to anorthosite (Eales and Cawthorn, 1996). There are three packages of chromitites in the Critical Zone (CZ): A lower group within pyroxenites of the lower CZ, a middle Group straddling the boundary between the lower and upper CZ and an upper group within norites and anorthosites of the upper CZ. The Upper Group 2 (UG2) chromitite is one of the world's largest platinum-bearing ore-bodies.

The Merensky Reef (or Merensky Unit) comprises basal chromitite, pyroxenite (sometimes with olivine), norite and anorthosite (Eales and Cawthorn, 1996) and occurs at the base of the Main Zone.

In contrast to the units below it, the Main Zone is a thick succession of cumulates, without any olivine or chromium spinel. It also lacks the fine-scale layering and lithological diversity of the lower units. Minerals which occur as cumulates include augite and inverted pigeonite however, pyroxenites are rare and anorthosites are confined mainly within two short intervals (Eales and Cawthorn, 1996). The boundary between the Main and Upper Zones is marked by the first appearance of magnetite according to the S.A.C.S (1980), and by a Pyroxenite Marker according to Kruger (1990). The UZ is well-layered and approximately 2000 m thick. The diagnostic feature of this zone is the magnetite layers that occur in four clusters. The zone itself has been divided into three subzones: "a", "b", and "c". Subzone "a" comprises anorthosite and magnetite ferrogabbro. Subzone "b" is made-up of anorthosite, trocolite, diorite, and ferrogabbro. The 1000 m thick Subzone "c" is composed of olivine diorite, anorthosite, and magnetite-rich diorite (Eales and Cawthorn, 1996).

Northern Limb of the Bushveld Complex

The northern limb (Figure 1.4) occurs as a slightly sinuous, north-west striking sequence with a length of 110 km and a maximum width of 15 km (Armitage et al., 2002; Vennemann and Smith, 1990). It is generally divided up into three different sectors, the Southern, Central and Northern sectors (Figure 1.5). The Southern Sector comprises all of the farms from the town of Mokopane northwards to Farm Tweefontein where the footwall is Penge, Duitschland or Timeball Hill Formation; the Central Sector runs from, and includes, Farm Tweefontein northwards until Farm Zwartfontein with a footwall of Malmani dolomite. The Northern Sector comprises the farms Overysel and Drenthe where the footwall is Archaean granite.

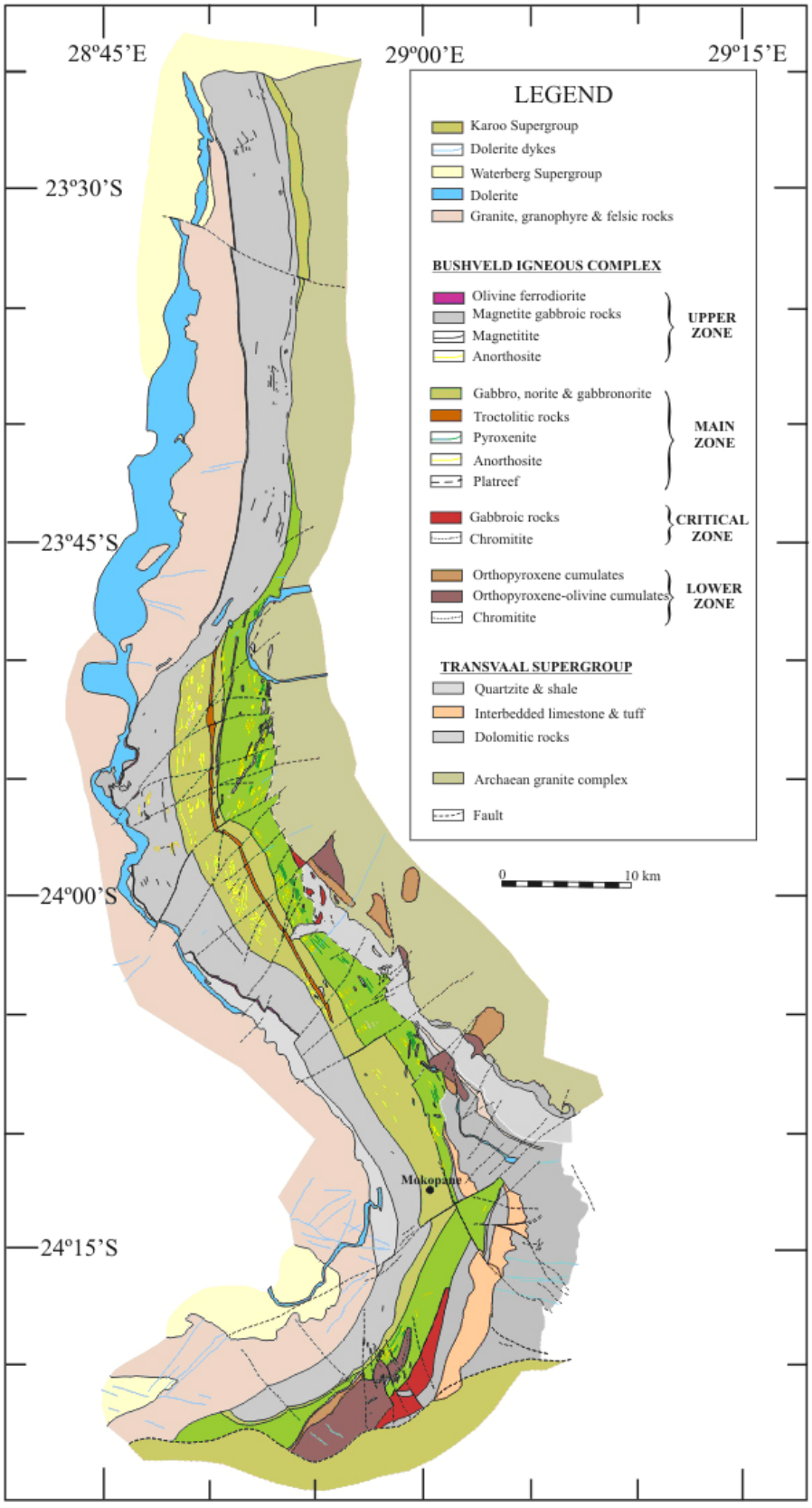

Figure 1.4: Map of the Northern Limb of the Bushveld Igneous Complex (based on Van der Merwe, 1978 and coloured by Ashwal et al, 2005).

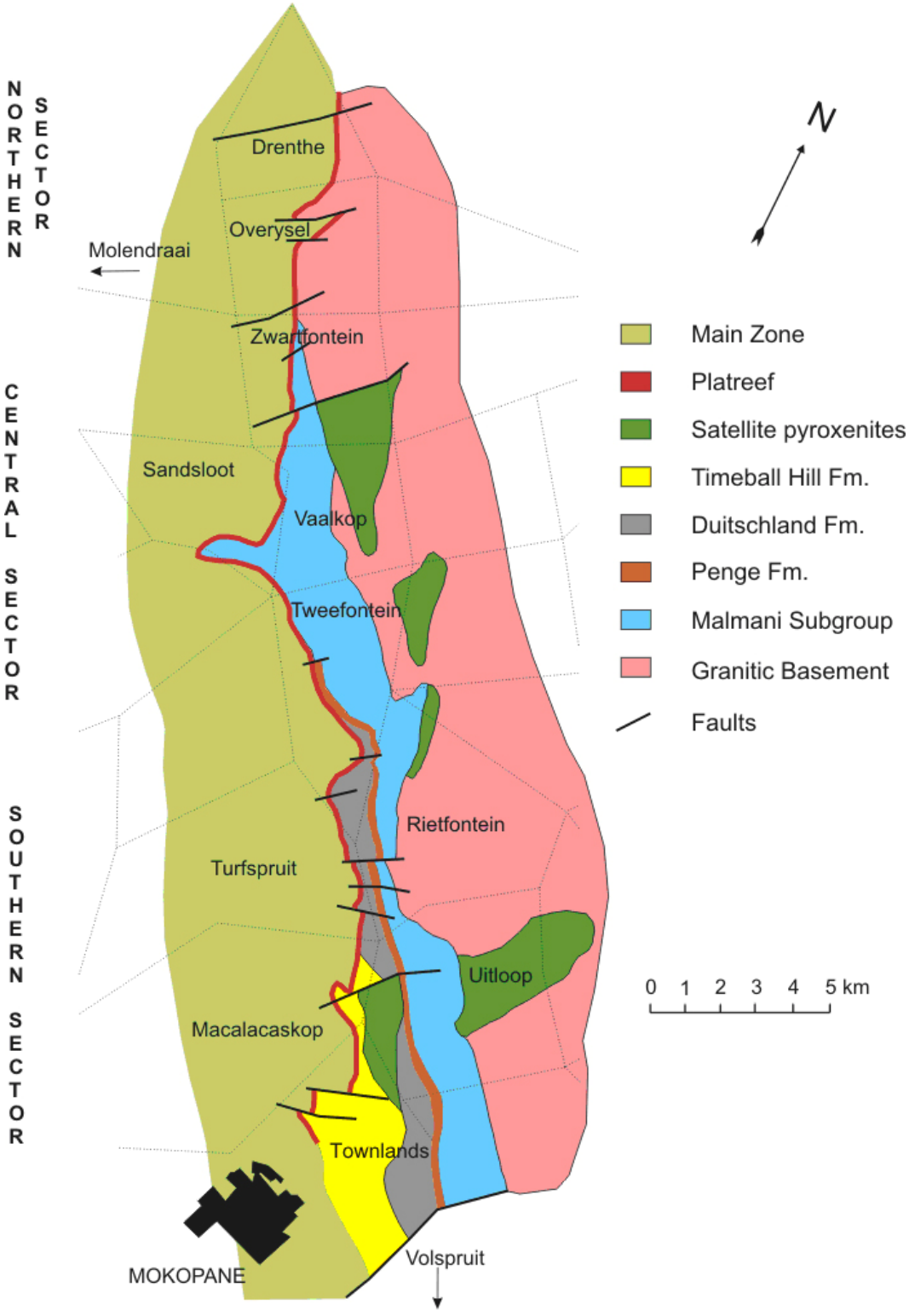

Figure 1.5: Diagram showing the location of the Southern, Central and Northern Sectors of the Northern Limb as well as major farm boundaries.

The Northern Limb of the Bushveld Complex differs in several ways from the Eastern and Western Limbs. Previously, not all of the zones of the Bushveld Complex were thought to be represented in the northern limb, where the existence of units from the Critical Zone was yet to be identified north of Mokopane (formerly Potgietersus) and units from the Lower Zone were thought to only be present south of Mokopane (Buchanan et al., 1981; Harris and Chaumba, 2001) and as satellite bodies. Current work however indicates that a Lower Zone component comprising pyroxenites and harzburgites occurs at the base of the succession south of Farm Tweefontein, as well as in satellite bodies (Figure 1.3) (Kinnaird et al., 2005). These satellite bodies occur as 7 distinct offshoots, and are described as satellite pyroxenites. These pyroxenites also occur in a zone south of Mokopane as the Grasvally Body which is a cyclic succession of alternating olivine - orthopyroxene and orthopyroxene cumulates with some chromitite layers (van der Merwe, 1978).

Marginal Zone norite also occurs sporadically within the succession on farms Macalacaskop 243KR and Turfspruit 241KR. These sequences are followed by the Platreef itself, and it appears that the entire magmatic sequence has an onlapping relationship with the floor rocks, with each subsequent magmatic event being intruded over a wider area than the previous sequences (Kinnaird, 2005).

The hanging-wall rocks of the Platreef are generally PGE-poor Main Zone comprising predominantly gabbronorite and are up to 2000 m in thickness (Vennemann and Smith, 1990). The thickness of the MZ in the northern limb is much less than in the Eastern and Western limbs of the Bushveld Complex. This Main Zone is followed by Upper Zone cyclic units of magnetite, magnetite gabbro, gabbro and anorthosite, which are approximately 1500 m thick (Ashwal et al., 2005). In the west, the hanging wall includes a variety of Bushveld granites and metasedimentary rocks (Kinnaird et al., 2005).

An important feature of the northern limb is that the layered rocks have a transgressive relationship with the country rocks of the Transvaal Supergroup i.e.

they are younger in the south. To the south of the town of Mokopane the floor rocks comprise Magaliesburg quartzites. Northwards the floor rocks first comprise the Pretoria Group, the banded Iron-Formations and dolomites of the Chuniespoort Group, and finally the Archaean granites (Harris and Chaumba, 2001). The entire layered sequence pinches out to the north (Buchanan et al., 1981; Harris and Chaumba, 2001; Vennemann and Smith, 1990).

General Geology of the Platreef:

The Platreef, which is the major PGE bearing layer of the northern limb, occurs at the base of the layered rocks. The Platreef comprises a complex series of medium- to coarse-grained pyroxenites and norites that contains xenoliths of the floor rocks (Gain and Mostert, 1982). More recently it has been defined as "the lithologically variable unit, dominated by pyroxenite, which is irregularly mineralised with PGE, Cu and Ni, between the Transvaal metasedimentary footwall or Archaean basement and the overlying Main Zone gabbronorite" (Kinnaird, 2004) whilst Kinnaird and MacDonald (2005) define it as "mafic units enriched in Ni–Cu–PGE that occur between the Archaean granite–gneiss basement or the Transvaal Supergroup and the gabbros and gabbronorites of the Main Zone, north of the Planknek Fault". It is observed as being a highly inhomogeneous body, comprising different rock types including pyroxenites, para-pyroxenites, feldspathic pyroxenites (pyroxenites with >10% interstitial plagioclase), serpentinites, gabbronorites and norites. It should also be noted that Platreef and its floor rocks have been extensively faulted along its entire strike length (Figure 1.3). The Platreef itself, has been equated with the Critical Zone, and specifically the Merensky Reef, of the Bushveld Complex proper (Wagner, 1929; White, 1994), although other authors have regarded the Platreef as the base of the Main Zone (Van der Merwe, 1976; Kruger, 2005).

The Platreef also contains xenoliths of altered footwall, which vary depending on the footwall; however the composition of these rafts is not always the same as the direct footwall. For example, the hornfels rafts within the Platreef; where there is

a Duitschland Formation footwall of dolomitic marble; have a mineral composition of aluminous cordierite-spinel hornfels. These rafts comprise mainly cordierite, with disseminated green spinel, and accessory corundum, sillimanite and andalusite, which indicates a high temperature metamorphism of a shale protolith. Another example is the occurrence of calc-silicate rafts in the Northern Sector of the Platreef on Farm Drenthe, where the direct footwall is Archaean granite.

In the southern sector of the Platreef, three or four feldspathic pyroxenites are separated by interlayers which include cordierite spinel hornfels, clinopyroxenites, calc-silicates, serpentinites (of both meta-sedimentary and igneous origin) and pyroxenites (Kinnaird, 2005). Hornfels layers which were originally pyritic black shales are predominant and at one point a major hornfels layer can be traced for 1500 m along strike. There are also minor occurrences of clinopyroxenite xenoliths, which are calc-silicate skarns. On farm Macalacaskop metaquartzite xenoliths are observed. These are very fine-grained with relict bedding defined by fine sulphides along the original bedding planes (Kinnaird, 2005). All of these xenoliths have been highly metamorphosed.

In general the geology of the northern sector of the Platreef comprises a complex package of norites, melanorites, pyroxenites, serpentinites and xenoliths of dolomite (Gain and Mostert, 1982). On the farm Drenthe the Platreef is an approximately 250 m thick package between the base of the Main Zone and the Archaean granites that comprise the floor (Gain and Mostert, 1982). At the base of the package is a feldspathic pyroxenite that has been chilled against the floor, which occasionally contains fragments of the footwall granite. This is followed by a sequence of norites and melanorites capped by a pyroxenite, all of which commonly contain calc-silicate xenoliths. These calc-silicate xenoliths have a high-temperature metamorphic assemblage, and are associated with extensive zones of alteration in the surrounding rocks (Gain and Mostert, 1982).

Aims and Objectives

This project aims to make a comprehensive study to extend the preliminary work presented by Sharman-Harris (2004) and to confirm the role of localised contamination of the Platreef by footwall material. This project has also examined the different possible sources of external sulphur for the Platreef and to incorporate this into current understanding of the formation of the Northern Limb.

Several cores from the southern Platreef, as well as cores from the northern Platreef were sampled. These samples were used to conduct a detailed petrographic study of the sulphides in different areas of the Northern Limb. The sulphides in these cores were also examined using an electron microprobe to further determine their composition. This will help to identify different styles and possibly generations of sulphides in the Platreef. A detailed study of the footwall of these cores was also conducted through detailed core logging and petrographic analysis.

These samples were also used to conduct detailed sulphur isotope analyses at Royal Holloway University of London and at the iThemba Environmental Laboratory, multiple sulphur isotope analyses at the University of Maryland and oxygen isotope analyses at the University of Cape Town. Data from this study will contribute to the assessment of the role of contamination in the Northern Limb, and to what extent it occurs. Sulphur isotopes were used to examine the variations in sources of sulphur both with depth, as well as within different generations of sulphides. Multiple sulphur isotopes were used to confirm the origin of the sulphur within sulphides in the Platreef, and to possibly correlate the source of sulphur to specific stratigraphic units within the Transvaal Supergroup. Oxygen isotopes were used as a further correlation of the possible presence of crustal contamination within the Platreef and compare with data from Harris and Chaumba (2001).

CHAPTER 2
PETROGRAPHY

Introduction

Six cores were examined and sampled for this project; four were taken from farms in the southern Platreef, and two were taken from the northern sector of the Platreef. Core ARF-08 comes from Farm Rietfontein, cores ATS-046 and ATS-057 from Farm Turfspruit, and core AMK-021 is from Farm Macalacaskop. The location of the boreholes is shown in Figure 2.1. Cores PR-174 and PR-175 both come from Farm Drenthe in the north (Figure 1.4 and 2.2).

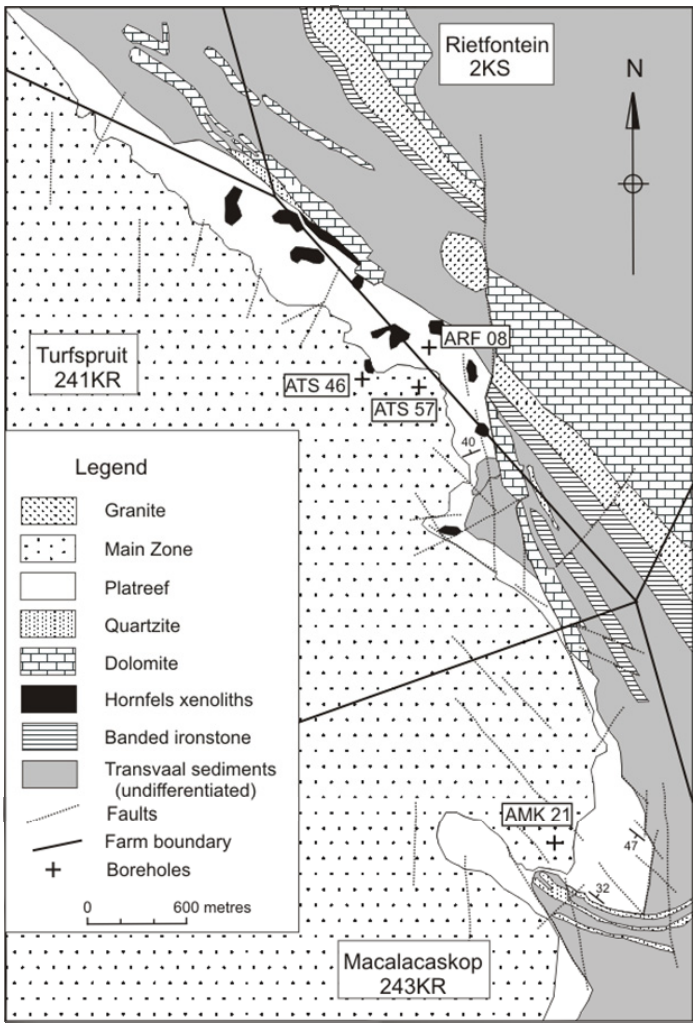

Figure 2.1: Map showing locations of boreholes from the southern sector of the Platreef that were sampled for this study.

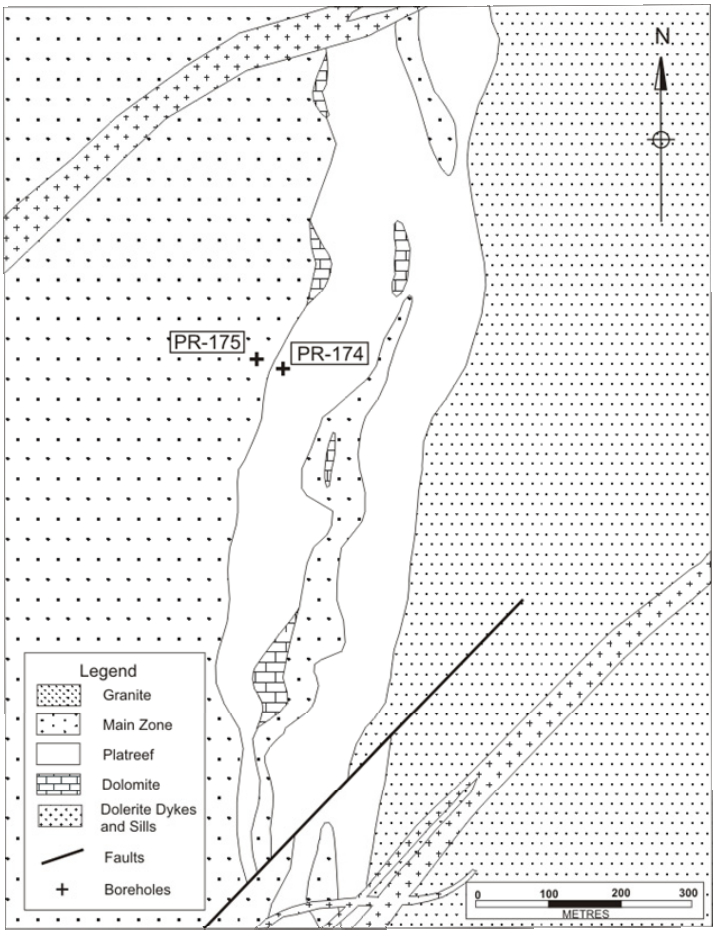

Figure 2.2: Map showing locations of boreholes from the northern sector of the Platreef (Farm Drenthe) that were sampled for this study.

Each core was sampled for a specific purpose in this study i.e. to reflect different footwall lithologies. Cores ATS-046 and ATS-057 were chosen as they had a footwall comprising altered dolomite of the Duitschland Formation, and were sampled to provide sulphide mineralisation and sulphur isotope data for the area of the Platreef with a Duitschland Formation footwall. Core AMK-021 was sampled in order to examine the variation of sulphide mineralisation and sulphur isotope values with a variation in footwall. The footwall of this core comprises quartzite of the Timeball Hill Formation. Core ARF-08 was also studied and sampled. It was chosen because it is particularly rich in sulphides, and the footwall of this core is also dolomite from the Duitschland Formation.

Cores PR-174 and PR-175 from the northern sector both have a footwall of Archaean granite, which is markedly different from the footwall lithologies of the cores from the southern sector of the Platreef. This pair of cores was chosen as they are relatively close together however core PR-175 has altered dolomite rafts within it, whereas PR-174 is free of sedimentary xenoliths.

Core Logs

ATS-046

This core from Farm Turfspruit is approximately 500 m long and has a footwall of serpentinised dolomite (Figure 2.3). The base of the sequence comprises ~90 m of feldspathic pyroxenite (Figure 2.3 and 2.4)) followed upwards by 100 m of serpentinised peridotite with occasional layers of feldspathic pyroxenite up to 8 m thick (Figure 2.4). This is succeeded by an ~45 m thick package of Marginal Zone norites and a ~20 m thick hornfels xenolith. Following this is a feldspathic pyroxenite ~200 m thick with layers of pegmatoidal gabbronorite, quartz-feldspar veins, melanorites, serpentinised peridotites, and dolomite (Figure 2.4). The pyroxenite varies texturally from being medium-grained, to locally pegmatoidal. There is approximately 14 m of weathered material at the top of the core.

ATS-057

This core is similar to ATS-046, and also has a footwall of altered dolomite. The core is approximately 360 m in thickness, and is dominated by feldspathic pyroxenite (Figure 2.5). The bottom of the intrusive package is marked by interlayered feldpathic pyroxenite and hornfels. This is followed by 30 m of hornfels with norites, and 20 m of serpentinite; followed by 200 m of feldspathic pyroxenite interlayered with pegmatoidal feldspathic pyroxenites and gabbronorites, pyroxenites, serpentinites, melanorites and cross-cut by quartzo-feldspathic veins (Figure 2.5). The top of the core comprises approximately 40 m of gabbronorite and mottled anorthosite, with the top one metre comprising weathered material. See Appendices I and II for more detailed sample and thin section descriptions.

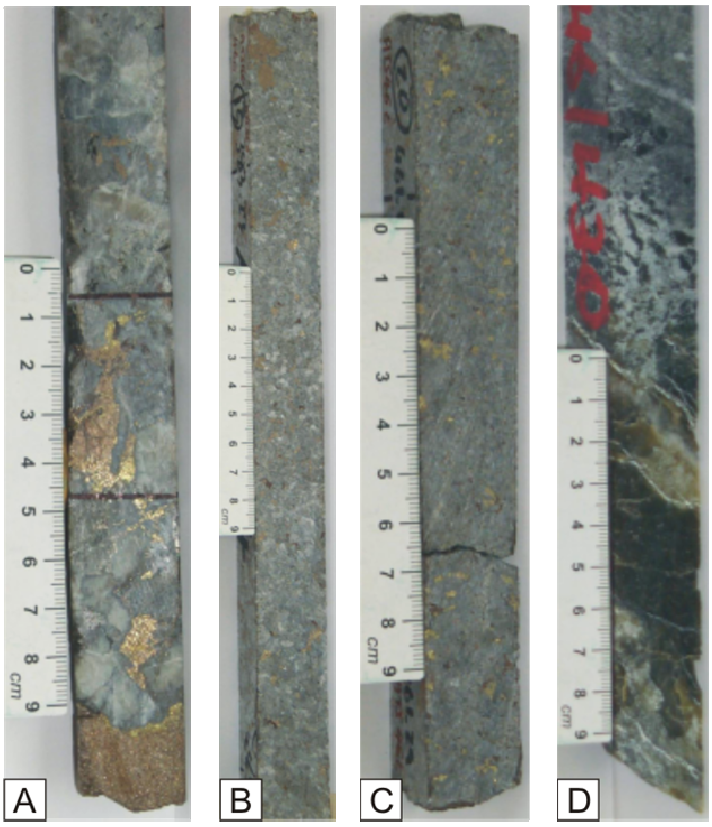

Figure 2.3: Examples of different lithologies from core ATS-046. A – Pegmatoidal Norite (60.34 m depth), B – Feldspathic Pyroxenite (383.38 m depth), C – Pyroxenite (461.21 m depth), D – Serpentinised Dolomite (469.38 m depth).

LEGEND FOR CORE LOGS

- Soil
- Mottled Anorthosite
- Leuco-Norite
- Norite
- Mela-Norite
- Gabbronorite
- Pegmatoidal Gabbronorite
- Feldspathic Pyroxenite
- Pegmatoidal Feldspathic Pyroxenite
- Pyroxenite
- Pegmatoidal Pyroxenite
- Serpentinite
- Massive Sulphide
- Quartz - Feldspar Vein
- Hornfels
- Dolomite / Calc-Silicate
- Quartzite
- Granite

Note: All core logs show depths in metres.

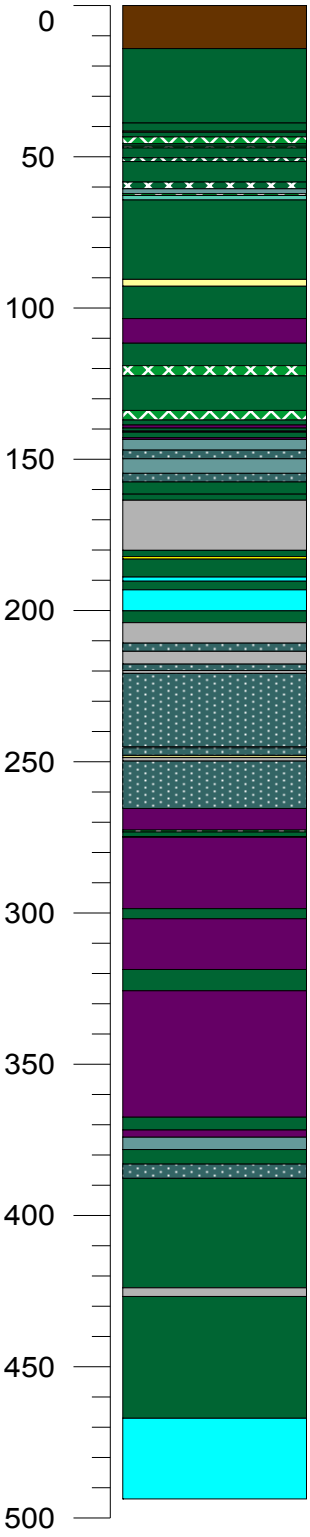

Figure 2.4: Stratigraphic log of ATS-046

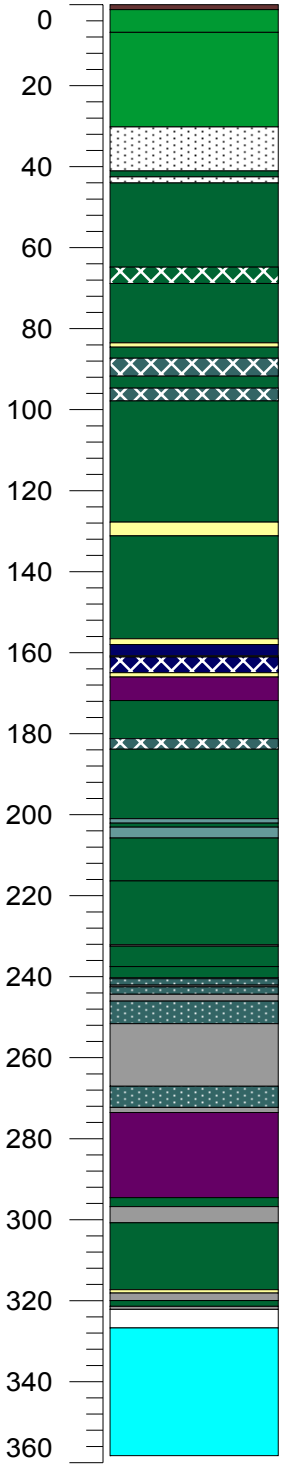

Figure 2.5: Stratigraphic log of ATS-057

AMK-021

The footwall of this core from Farm Macalacaskop comprises quartzites from the Timeball Formation (Figure 2.6). The floor rocks are intruded by thin sills of pyroxenite and feldspathic pyroxenite. The succeeding 300 m of core is predominantly feldspathic pyroxenite (Figure 2.6) which is pegmatoidal in places (Figure 2.7). This pyroxenite package includes a ~35 m thick dolomite xenolith, with associated serpentinite and gabbronorite, at ~340 m depth (Figure 2.7). This feldspathic pyroxenite unit also includes layers of melanorite, serpentinite (Figure 2.6), and norite of variable thickness. This package is topped by ~50 m of mottled anorthosite, followed by ~40 m of gabbronorite, which mark the top of the core (Figure 2.7). See Appendix III for detailed samples descriptions.

Figure 2.6: Typical lithologies from core AMK-021. A – Feldspathic Pyroxenite (90.25 m depth), B – Serpentinite (222.06 m depth), C – Pyroxenite (232.62 m depth), D – Timeball Hill Quartzite (393.33 m depth).

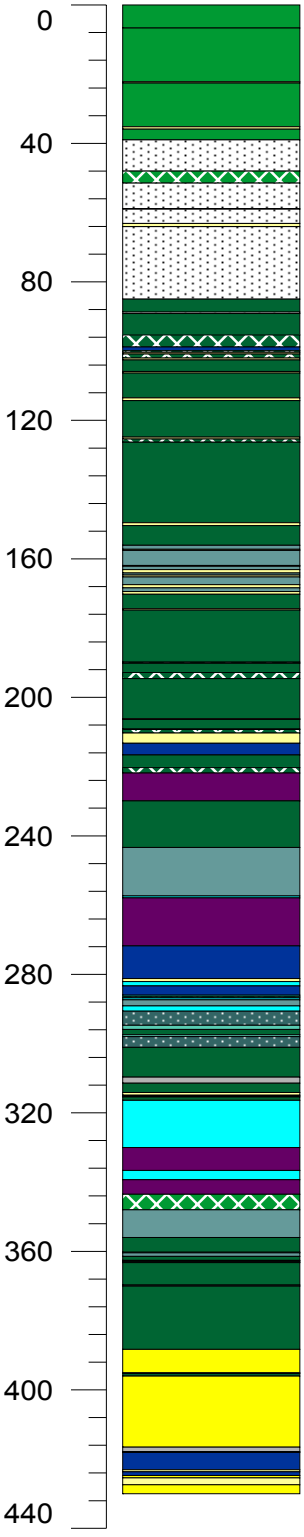

Figure 2.7: Stratigraphic log of AMK-021

ARF-08

This core, taken from Farm Rietfontein, is approximately 160 m thick, and has a footwall of dolomite (Figure 2.8). Above the footwall is a granite sill, which is followed by a ~10 m thick footwall xenolith of cordierite-spinel hornfels, and then a ~10 m thick layer of norite (Figure 2.9). At ~124 m depth, directly above the norite there is a 50 cm thick massive sulphide layer (Figure 2.8). This is succeeded by a 60 m thick, medium-grained gabbronorite (Figure 2.8), which contains layers of altered footwall, pegmatoidal gabbronorite, and granitic veins (Figure 2.9). The gabbronorite then becomes fine-grained for ~45 m and contains several footwall xenoliths ranging from ~60 cm to ~7 m in thickness. The top 25 m of the core consists of weathered regolith and broken core (Figure 2.9).

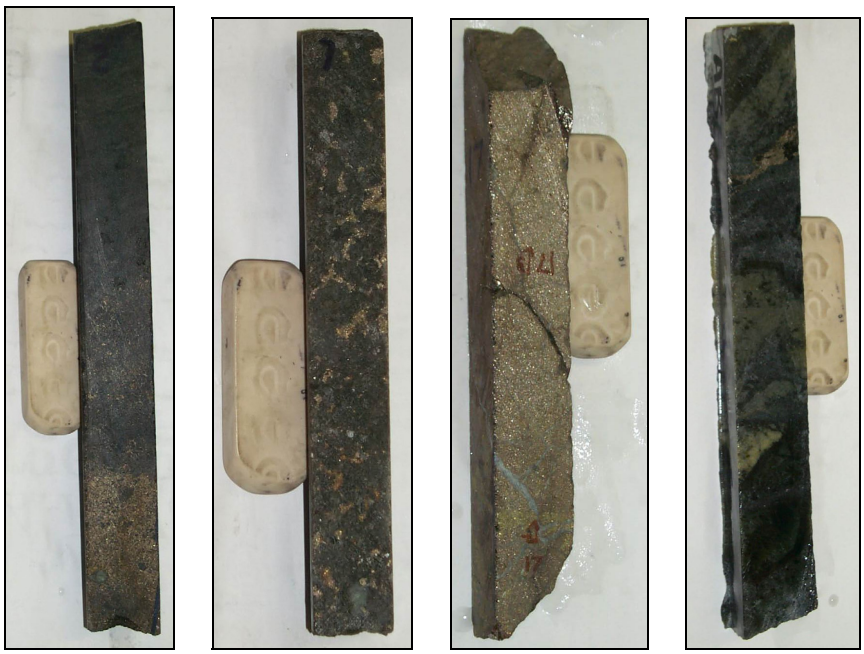

A B C D

Figure 2.8: Typical lithologies from core ARF-08. A-Hornfels (ARF08/35.47), B-Gabbronorite (ARF08/53.39), C-Massive Sulphide (ARF08/123.26), and D-Marble-Skarn (ARF08/152.44).

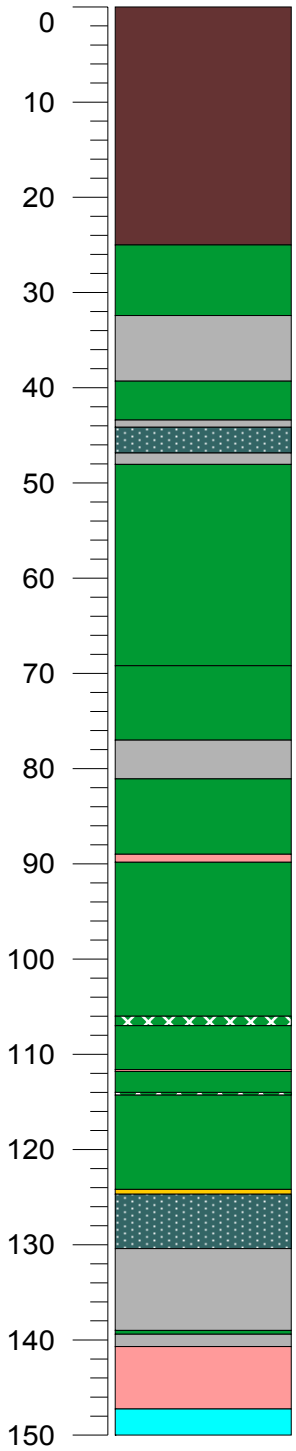

Figure 2.9: Stratigraphic log of ARF-08

PR-174

This core is 320m thick and is dominated by feldspathic pyroxenites, which vary from fine-grained to pegmatoidal (Figure 2.10). The pegmatoidal feldspathic pyroxenites are concentrated in the top 100 m of the core. The mafic package is intruded by norites, varying in thickness from 5 to 30 m (Figure 2.10). The end of the core does not extend into footwall. The core was chosen for the lack of dolomite xenoliths as a comparison to core PR-175.

PR-175

This core is 350 m in thickness and is also dominated by feldspathic pyroxenites (Figure 2.11). These feldspathic pyroxenites vary in grain size from medium to coarse grained. The feldspathic pyroxenites are interrupted by norites throughout the package, which vary in thickness from 5 to 25 m (Figure 2.11). There are also two altered dolomites within the sequence (Figure 2.11), the first occurs at approximately 20 m depth, and is ~5 m in thickness . The second is 25 m thick, and occurs from ~ 180 – 200 m depth. As with PR-174, the footwall is not intercepted in this core.

As the main focus of this study is the sulphide mineralisation of the Platreef, the style and distribution of sulphide minerals in these cores was examined in greater detail.

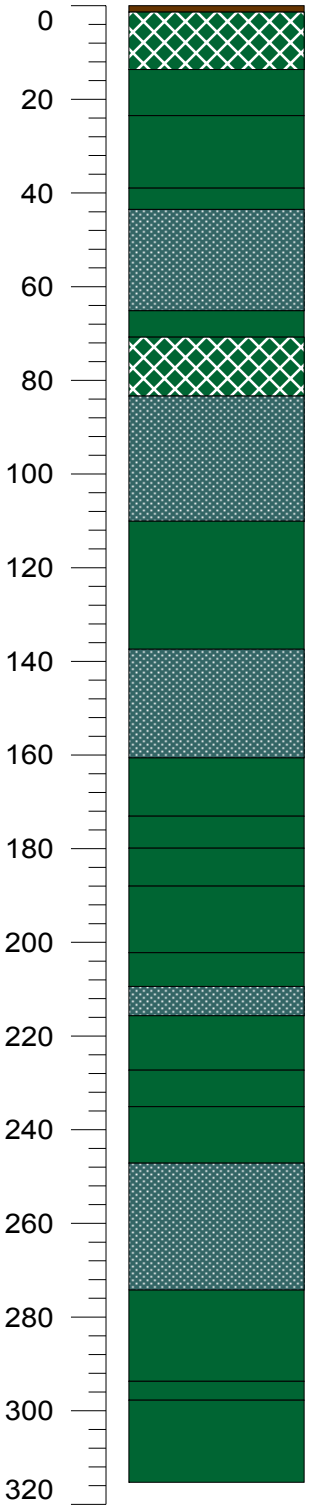

Figure 2.10: Stratigraphic log of PR-174

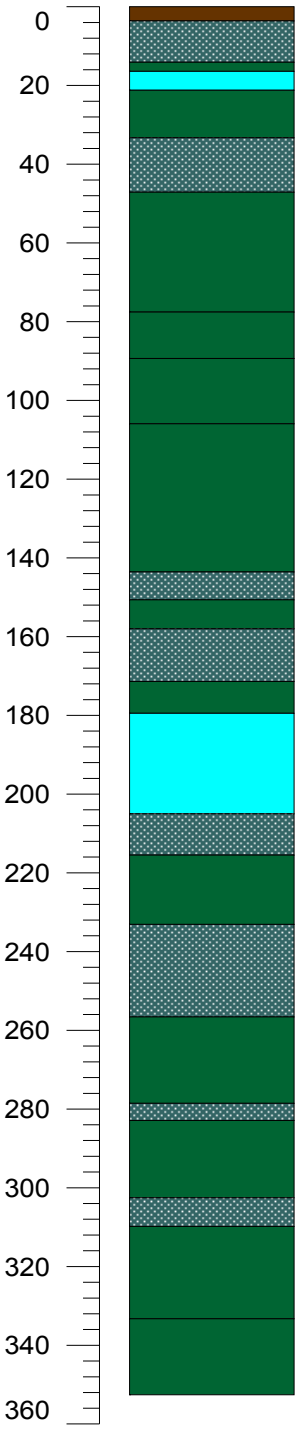

Figure 2.11: Stratigraphic log of PR-175

CHAPTER THREE
SULPHIDE MINERALOGY

Introduction

A detailed study of the sulphide mineralisation of cores ATS-046, ATS-057, AMK-21, PR-174 and PR-175 was conducted in order to identify different types and zones of sulphide mineralisation. Footwall and vein material were also examined for sulphide and sulphate occurrences. This was done through hand sample, polished block, and thin section descriptions, as well as through detailed core logging. The identification of these different sulphides not only allows for an understanding of their formation, but also aided in selection of samples for subsequent isotopic analysis.

Sulphide Mineralisation Theory and Concepts

Sulphide mineralisation occurs in a magma when that magma reaches sulphur saturation. This can occur in several ways, but the two main mechanisms for sulphur saturation are the addition of sulphur from an external source, or the felsification of a mafic magma (Naldrett, 2004). The quantity of sulphide minerals that forms is directly related to the percentage of sulphur within the system itself i.e. the larger the amount of sulphur in the magma, the more sulphides will form.

Once a sulphide liquid has formed, due to liquid immiscibility, it cools relatively slowly, and this cooling occurs in two phases (Naldrett, 2004). The first phase is termed monosulphide solid solution (*mss*) and is characterised by the formation of nickel-rich pyrrhotites. This phase usually starts at between 1160 and 1120 °C, and will continue until approximately 850 °C, when pentlandite begins to exsolve. During this first phase of crystallisation the remnant sulphide liquid becomes enriched in nickel and copper. This remnant liquid is termed intermediate solid solution (*iss*). The beginning of the second stage is marked by the first

appearance of pentlandite, which then causes the remnant liquid to become a copper-rich monosulphide solid solution. Subsequent cooling then leads to the formation of chalcopyrite. Because the *iss* is liquid while pyrrhotite is forming, it can move away from the pyrrhotite. It is therefore generally not unusual to have some areas of a deposit rich in pyrrhotite, and other areas being rich in chalcopyrite and pentlandite. Equally it is common to see pyrrhotite grains with pentlandite and chalcopyrite occurring as rims. This sequence of formation aids in interpreting sulphide deposits, as areas rich in pyrrhotite have probably formed at higher temperatures, and areas rich in chalcopyrite and pentlandite have formed at lower temperatures.

Sulphide Mineralisation of the Platreef

The base- and precious- metal mineralisation of the Platreef is unevenly distributed, and occurs over a zone that is up to 400 m thick. In the southern sector, sulphide minerals occur throughout the succession. They comprise < 1% to >25% (mode and occasionally to 45% over short intersections of core. Generally, these occur as centimetre to millimetre-sized blebs and interstitial grains of pentlandite, pyrrhotite and chalcopyrite. A wide range of accessory minerals are also present including sphalerite, galena, molybdenite, pyrite, chalcocite, and covellite among others. Where present, zones of massive sulphides rich in chalcopyrite are found close to the footwall contact. More compositionally complex sulphides are associated with felsic melt phases that pervasively infiltrate the package soon after its partial or complete crystallization (Hutchinson and Kinnaird, 2005). There is a close correlation between Cu and Ni concentrations but a poor correlation between PGE and base metal contents. Thus high Cu+Ni values do not necessarily indicate high PGE grade, although the highest PGE grades are located within sulphide-rich zones towards the floor (Hutchinson and Kinnaird, 2005). Sulphides are also concentrated towards the footwall on Farm Tweefontein but further north, the abundance of sulphides is dramatically reduced.

The sulphides studied for this research within the Platreef usually occur as a combination of pyrrhotite, pentlandite, chalcopyrite and occasionally pyrite, sphalerite and bornite, and exist as several different styles or phases of mineralisation. In many cores, massive sulphides are up to several metres in thickness, and often contain an assemblage of sulphide minerals (Figure 3.1a). Typically these massive sulphides are dominated by pyrrhotite. Chalcopyrite usually occurs around the rims of the pyrrhotite, and has pentlandite associated with it. Pentlandite also occurs as veins up to 2 mm thick, and as exsolution lamellae within the pyrrhotite (Figure 3.2a). More rarely the massive sulphides are dominated by chalcopyrite, which have pyrrhotite veins running through them.

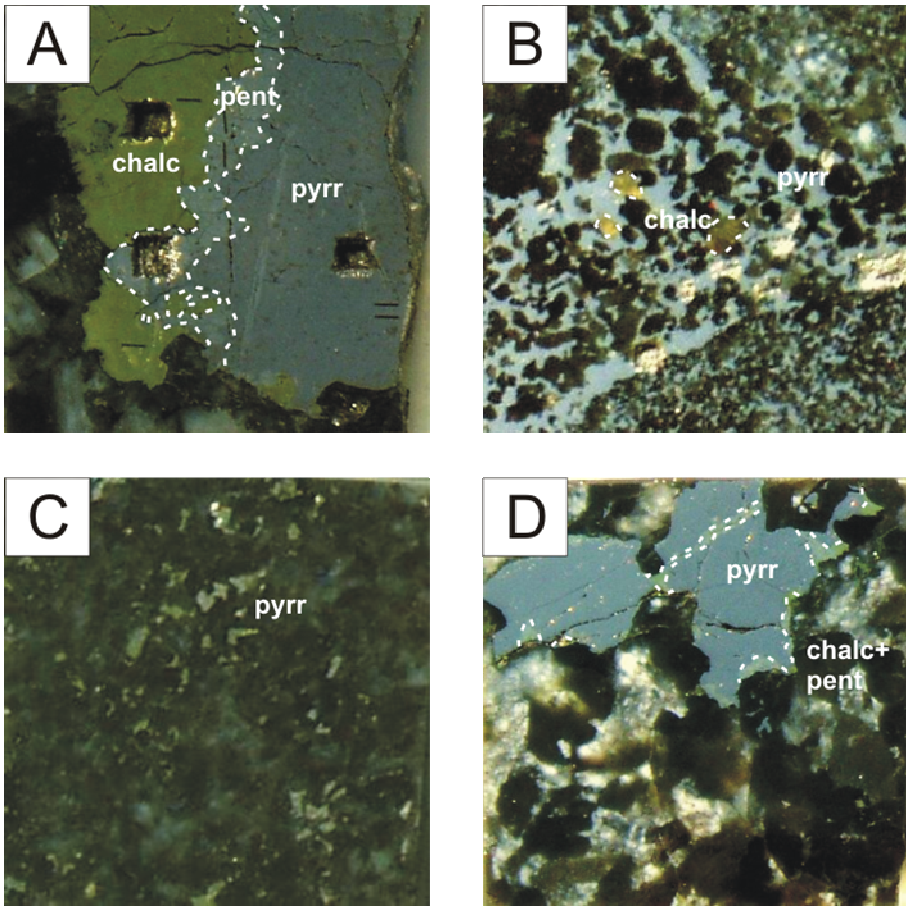

Figure 3.1: Diagram showing different types of sulphide mineralisation in the Platreef. A – Massive sulphide showing pyrrhotite, pentlandite and chalcopyrite (ATS46/61.05). B – Net-textured sulphides, dominated by pyrrhotite (ATS46/154.55). C – Fine-grained, interstitial sulphides (ATS46/461.03). D – Blebby sulphide, dominated by pyrrhotite with minor pentlandite and chalcopyrite (ATS46/383.23). Photos taken in natural light, each block is 25 x 25 mm. Note: pent – pentlandite, pyrr – pyrrhotite, chalc – chalcopyrite.

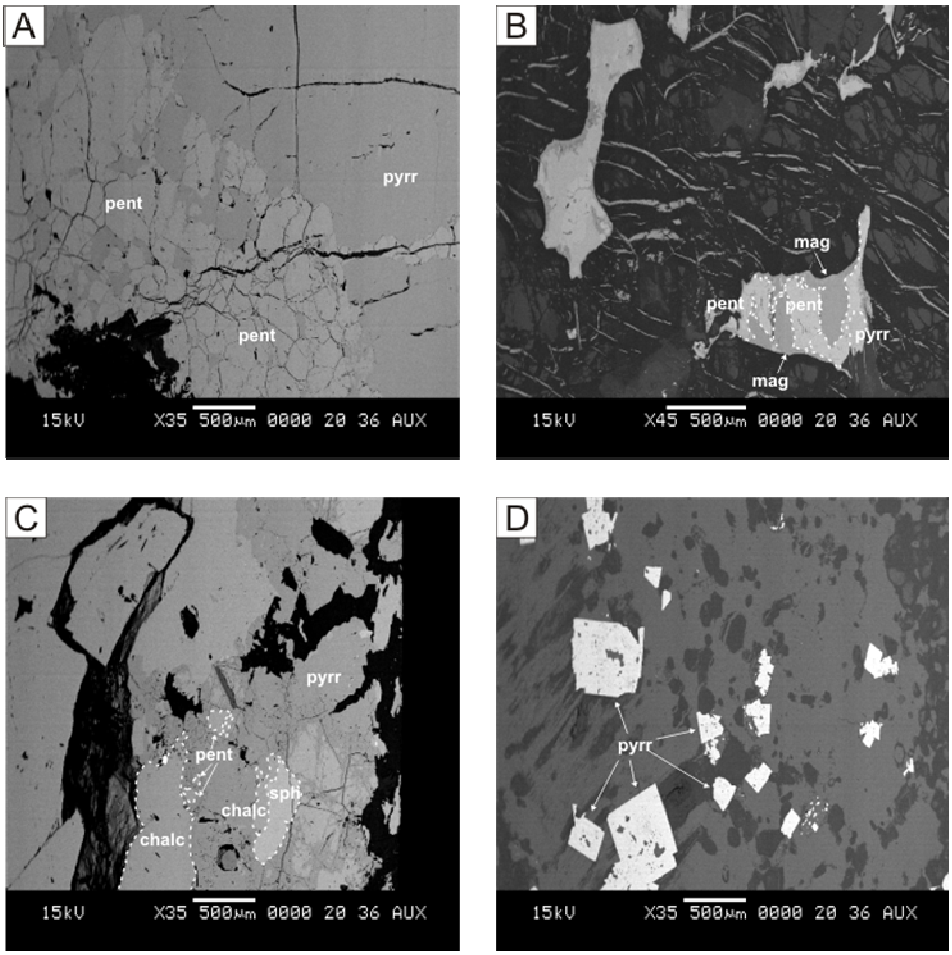

Figure 3.2: Electron Microprobe images of various sulphides from the southern sector of the Platreef. A – Portion of a massive sulphide showing the relationship between pyrrhotite and pentlandite including veins and exsolution lamellae of pentlandite (AMK21/125.76). B – Fine-grained interstitial sulphide grain (AMK21/222.06). C – Coarse-grained sulphide bleb showing complex mineralogy (ATS57/72.48). D – Cubic pyrrhotite grains within footwall calc-silicate (ATS57/335.07). Note: pent – pentlandite, pyrr – pyrrhotite, mag – magnetite, chalc – chalcopyrite, sph – sphalerite.

Associated with massive sulphides, and often within serpentinites are 'net-textured' sulphides that occur as a matrix to the silicate minerals, with samples having 50-80 modal percent sulphides (Figure 3.1b). 'Net-textured' sulphides are dominated by pyrrhotite, with minor chalcopyrite and pentlandite.

Fine- to medium-grained disseminated sulphides typically 1 to 4 mm in size are common in the finer-grained lithologies of the Platreef, and are often interstitial. These are often associated with interstitial quartz-feldspar symplectites. These sulphides have a different modal mineralogy than that of the massive or 'net-

textured' sulphides. They usually comprise approximately 50% pentlandite, 40% chalcopyrite, as well as pyrrhotite and occasional bornite and magnetite (Figure 3.1c, 3.2b).

'Blebby' sulphides also occur commonly ranging in size from 3 to 25 mm, and contain a similar combination of sulphide minerals to that of the interstitial sulphides. These blebby sulphides are often observed as pyrrhotite with chalcopyrite rims (Figure 3.1d), and can contain other accessory sulphides such as sphalerite (Figure 3.2c).

Sulphides also occur within the metamorphosed footwall of the Platreef, particularly within calc-silicates, but also occasionally within cordierite spinel hornfels. Typically these sulphides are cubic pyrite, but pyrrhotite has also been observed (Figure 3.2d), also sometimes occurring in a cubic form which may be due to the conversion of pyrite to pyrrhotite during the metamorphism of the footwall.

Sulphide mineralisation also occurs around calc-silicate rafts within the Main Zone of the northern limb, especially in the northern sector of the Platreef, and shows a similar Platreef-style mineralisation.

Core ATS-046

This core has a relatively high percentage of sulphides through its entire length. In general the sulphides are fine-grained and interstitial, and are dominated by pyrrhotite (Figure 3.3, 3.4). Pyrrhotite occurs within the calc-silicate footwall of the core, which has a remnant cubic shape, and has probably been altered from pyrite. See Appendix IV for full sample descriptions. Following this is a zone of medium to coarse-grained blebby sulphides within feldspathic pyroxenites (Figure 3.5). Within a serpentinised zone which occurs from ~260 – 370 m there are generally net-textured sulphides (Figure 3.5). There is a zone at ~60 m depth within a pegmatoidal feldspathic pyroxenite (Figure 3.5) which comprises very coarse-grained to massive sulphides, which clearly show pyrrhotite, chalcopyrite

and pentlandite. In general sulphides within the core become more enriched in chalcopyrite and pentlandite, and depleted in pyrrhotite, closer to the footwall. Concentrations of sulphides are generally associated with the presence of hornfels rafts, some of which contain sulphides themselves.

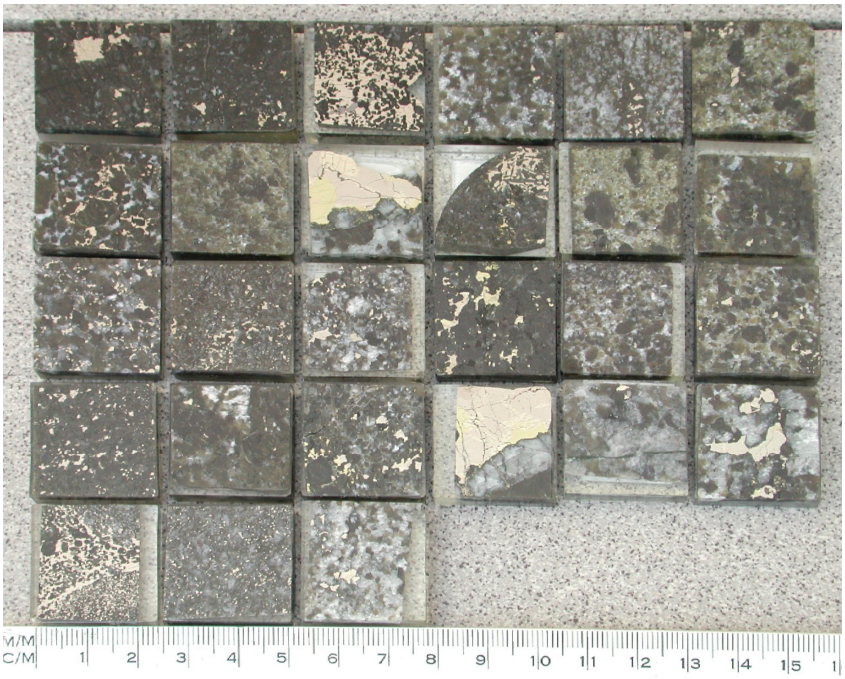

Figure 3.3: Photograph of polished blocks from core ATS-046 taken in natural light (from D. Hutchinson).

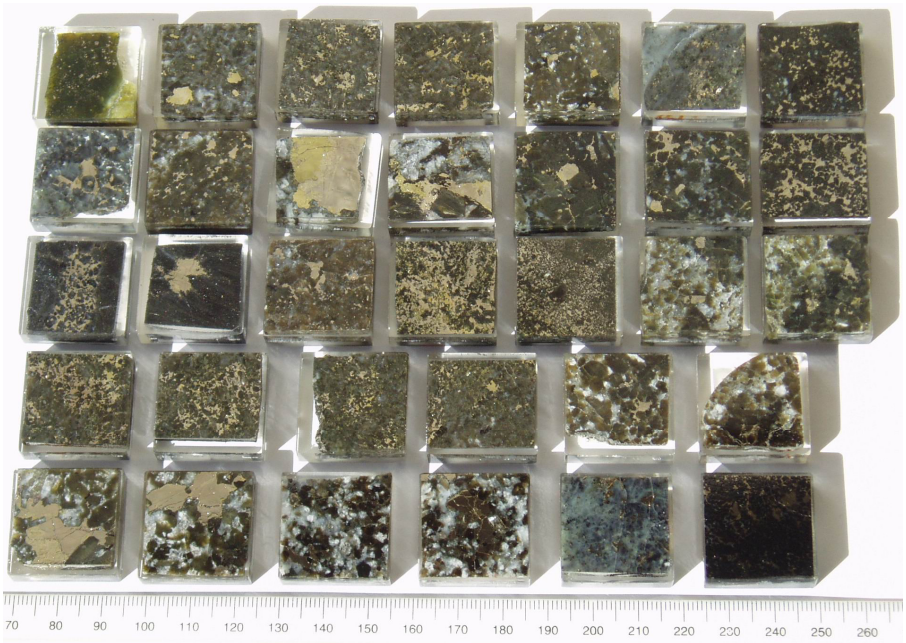

Figure 3.4: Photograph taken in natural light of polished blocks from core ATS-046 (from D. Hutchinson).

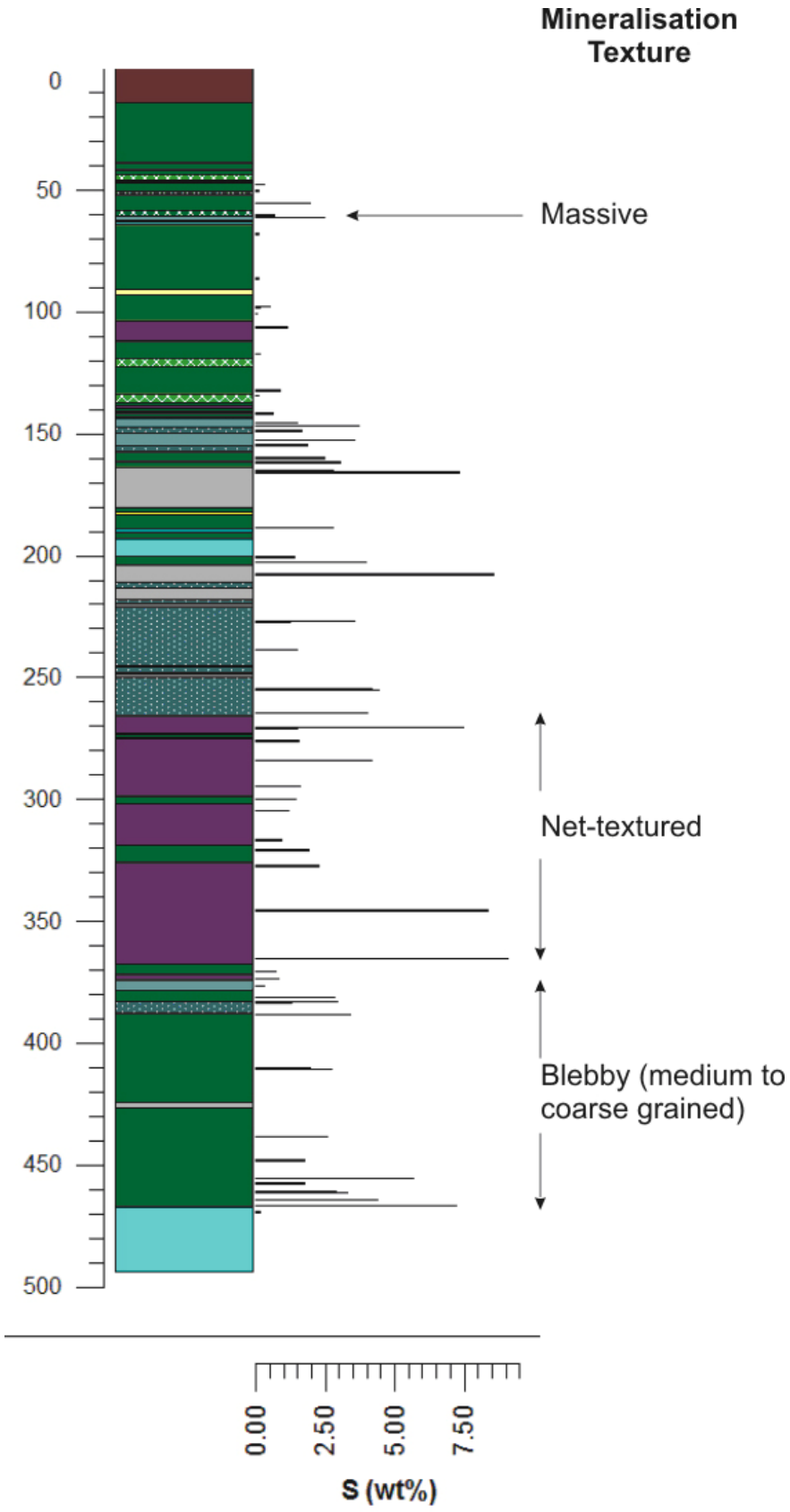

Figure 3.5: Core log of core ATS-046 with sulphur concentrations in weight % from whole rock analysis and main sulphide interval textures.

Core ATS-057

The sulphides in ATS-057 are concentrated in the lower half of the core predominantly within feldspathic pyroxenites, with a large concentration occurring just above a thick hornfels raft at ~260 m (Figure 3.6). This concentration of sulphides is predominantly massive and net-textured sulphides, which are dominated by pyrrhotite (Figure 3.7). Several samples from the top 100 m of core are almost 100% chalcopyrite, and there is a 30 m thick zone occurring at ~150 m which contains sulphides which are dominated by pentlandite (Figure 3.7). The altered dolomite footwall contains disseminated grains of cubic pyrite, as well as pyrrhotite. Appendix IV comprises detailed sample descriptions.

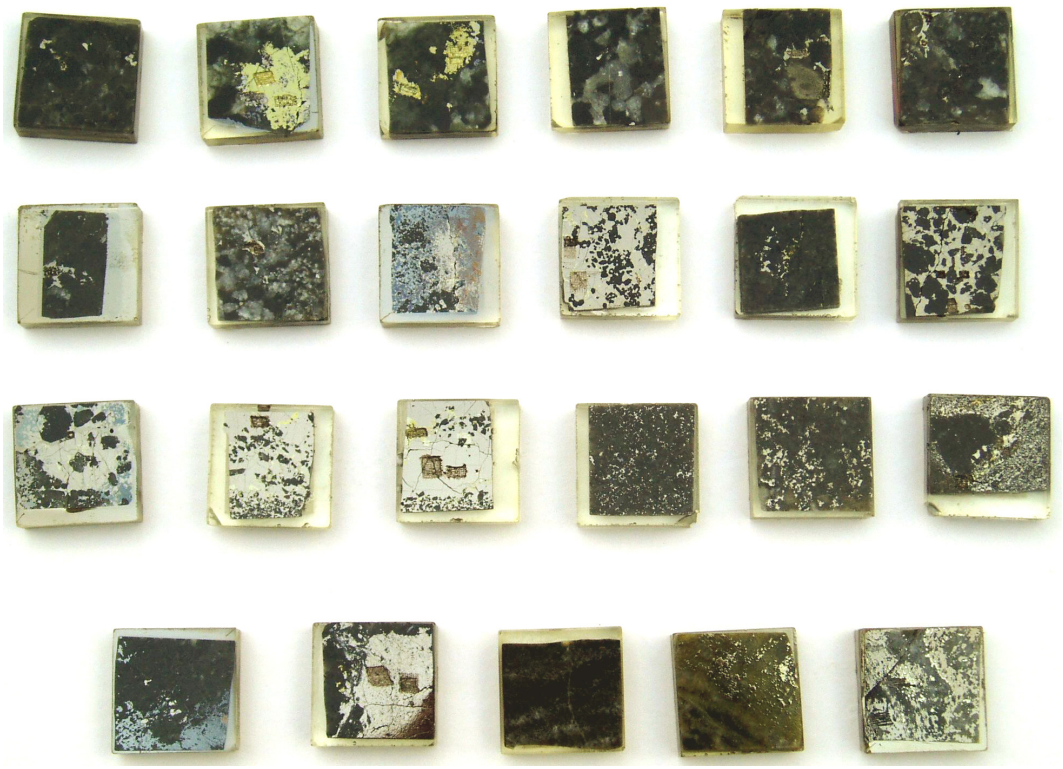

Figure 3.7: Image showing polished blocks of samples from ATS-057.

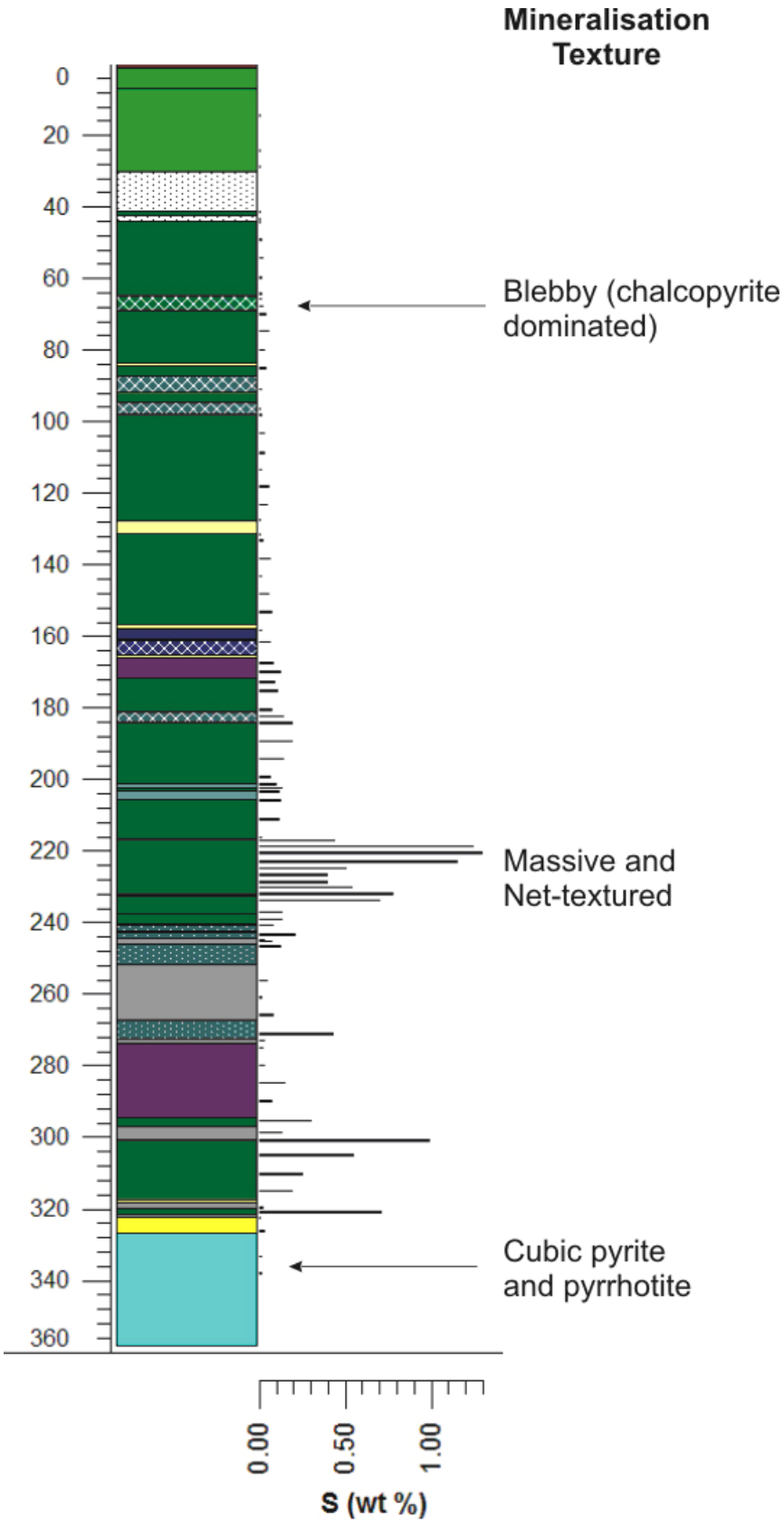

Figure 3.6: Core log of core ATS-057 with whole rock sulphur concentrations (wt%) and main sulphide textures plotted with depth.

Core AMK-021

This core has relatively low concentrations of sulphides, and they are predominantly fine-grained and interstitial and usually occur within feldspathic pyroxenites, although occasional blebs of sulphide occur. The sulphides are dominated by pyrrhotite, with pentlandite and chalcopyrite occurring around the rims. However, one sample is chalcopyrite dominated blebby sulphide, with a cross-cutting vein of pyrrhotite. See Figure 3.8 for images of all samples from AMK-021. See Appendix IV for a detailed description of all sulphide samples.

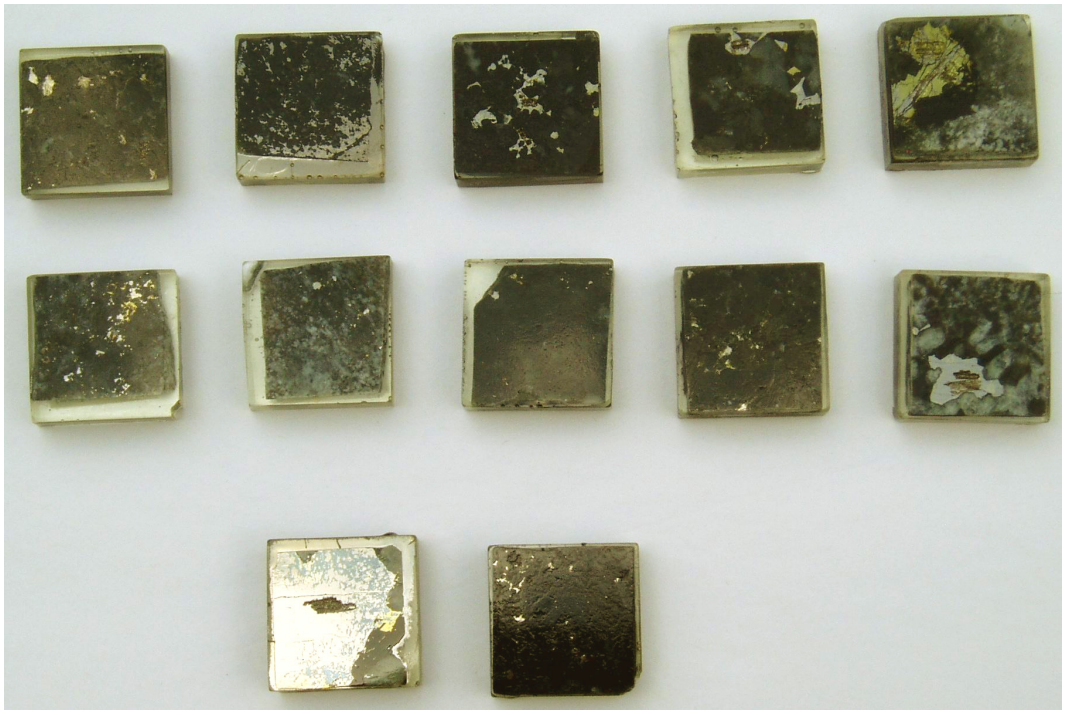

Figure 3.8: Photograph of polished blocks from AMK-021.

Core PR-174

The sulphide mineralisation in the core can be divided into several different zones, with no zone exceeding 25 m in thickness. Sulphides dominantly occur in norites, although mineralisation is also seen with feldspathic pyroxenites (Figure 3.9). All of the zones are dominated by pyrrhotite, with pentlandite and chalcopyrite occurring as rims to the pyrrhotite. Rarely zones occur where chalcopyrite forms

blebs, without associated pentlandite or pyrrhotite. The percentage of sulphides within the core decreases dramatically with depth. The bottom half of the core is dominated by blebby sulphides, whereas the top half of the core also contains fine-grained interstitial sulphides. See Appendix V for a detailed description of the sulphide zones.

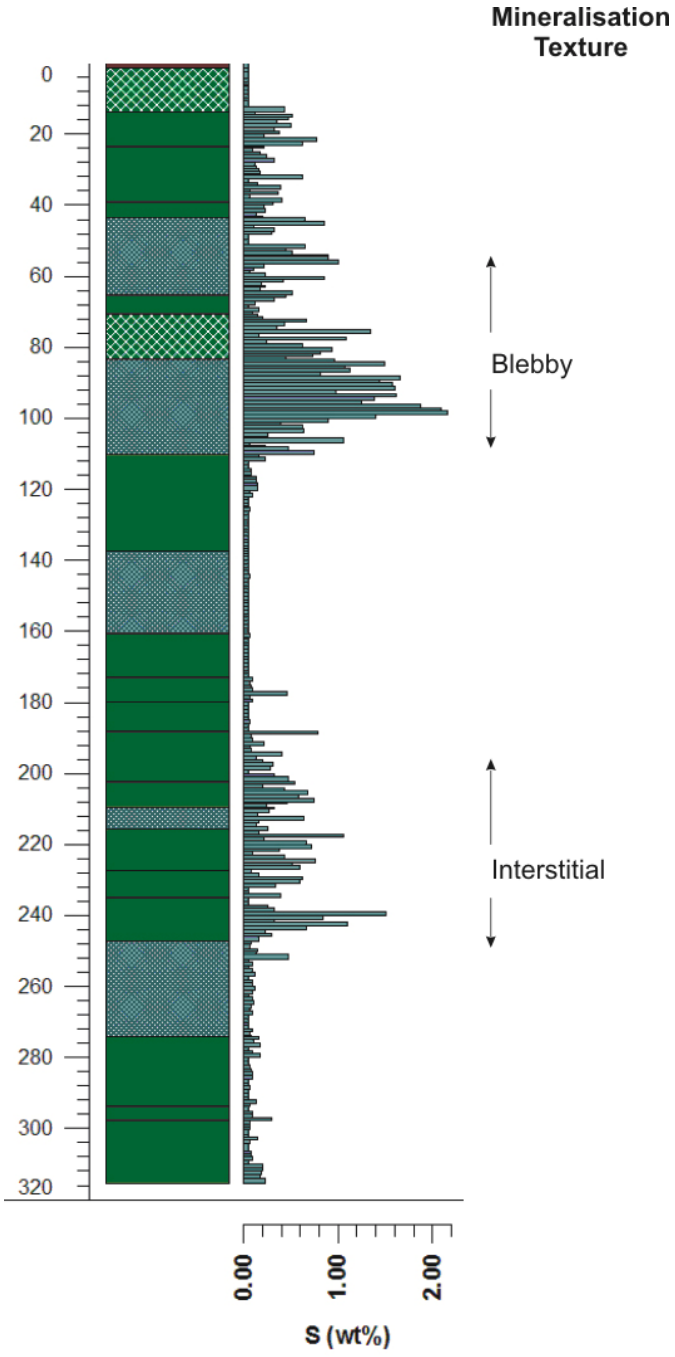

Figure 3.9: Core log of core PR-174 with sulphur content (wt %) and main sulphide textures plotted with depth.

Core PR-175

As with PR-174, this core from the northern sector has several discrete sulphide zones. In general, the percentage of sulphides in the top half of the core is markedly higher than in the lower half of the core (Figure 3.10). The sulphides occur more frequently within the feldspathic pyroxenites, although they do also occur within norites (Figure 3.10). The sulphides are dominated by pyrrhotite, with pentlandite and chalcopyrite occurring as accessory minerals on the rims of the pyrrhotite grains. The sulphides occur as either interstitial or blebby sulphides, and are generally fine-grained. See Appendix V for a detailed description of the sulphide zones.

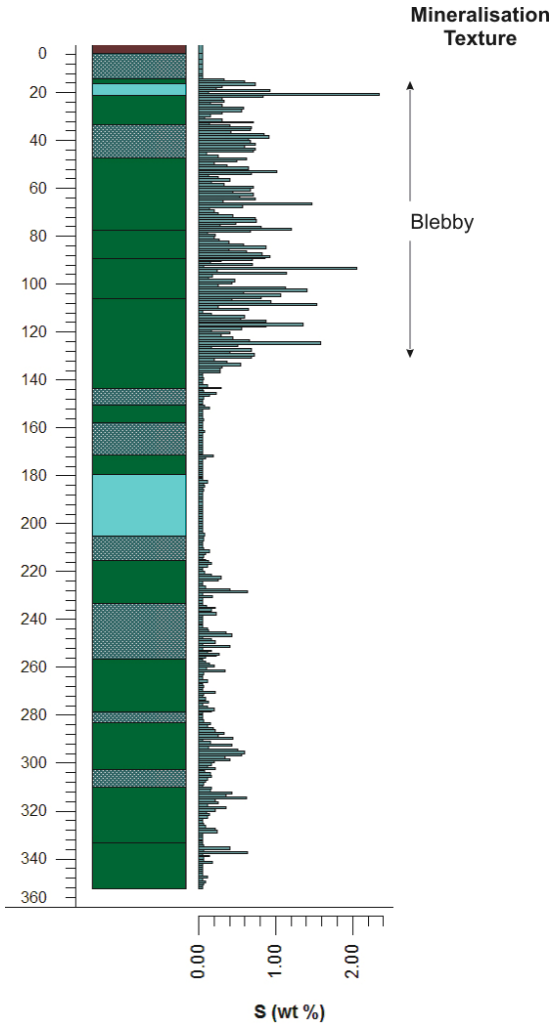

Figure 3.10: Core log of core PR-175 with sulphur content in weight percent and main sulphide intervals plotted with depth.

Duitschland Formation

Several samples containing sulphides were collected from Farm Duitschland. DL1 comprises a dolomite, which contains a thin vein of chalcopyrite and bornite, which appears to be secondary. DL2 and DL3 are both fine-grained shales from the Lower Duitschland Formation, which contain nodular pyrite (1 – 4 mm) that has formed along bedding planes (Figure 3.11).

Figure 3.11: Photograph of nodular pyrite within a shale from the Lower Duitschland Formation (from P. Nex).

Vein Material

Veins of varying composition occur throughout the Platreef, and various types were sampled. Several anhydrite veins from the central sector of the Platreef were collected (TN75, VK75-305) and comprised 100% anhydrite. Galena was also collected from a quartz-feldspar vein (ZN396 – 214.4) (Figure 3.12). Calcite crystals were collected which contain crystalline chalcopyrite occuring along crystal planes. Finally a quartz-calcite vein (PRS17) (Figure 3.13) containing crystalline sphalerite, chalcopyrite and galena was sampled. These veins are all confined within but cross-cut the Platreef package.

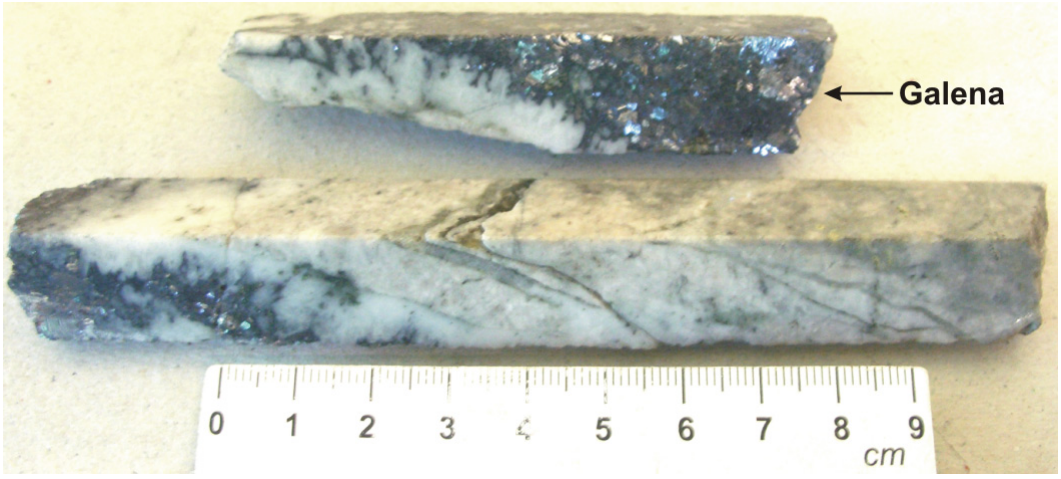

Figure 3.12: Photograph of sample ZN396-214.4 showing galena associated with a quartz-feldspar vein (from P. Nex).

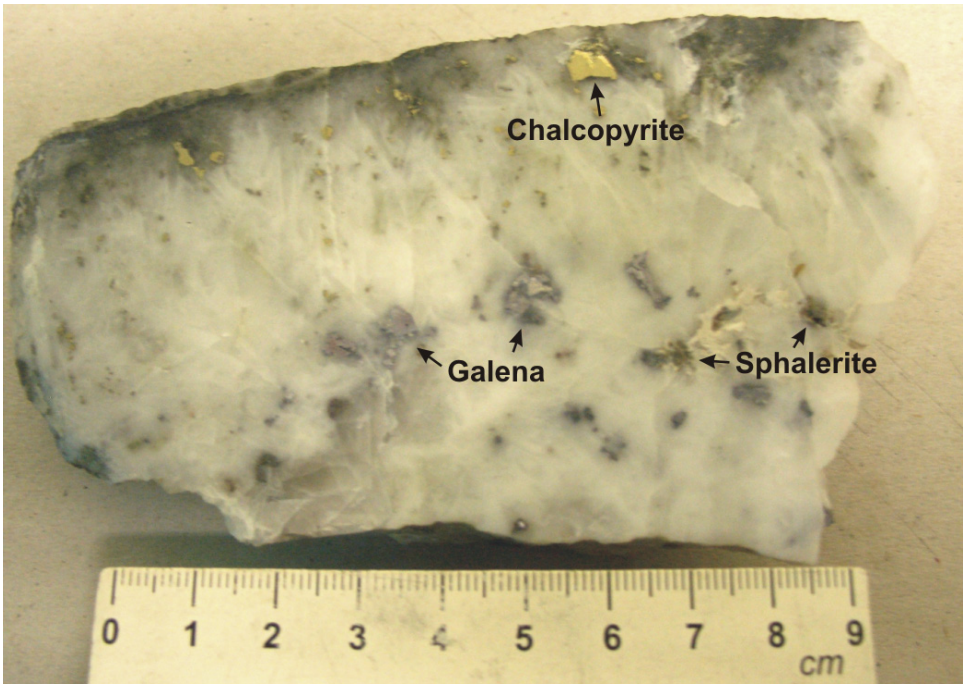

Figure 3.13: Photograph of sample PRS-17, a quartz-calcite vein with chalcopyrite, galena and sphalerite (from P. Nex).

Discussion

It is clear from this study and previous work (Hutchinson and Kinnaird, 2005; Armitage et al., 2002) that sulphides are abundant in the southern sector, but very minor in the central and northern sectors of the Platreef. Since footwall rocks in these different sectors vary with sulphide-bearing Duitschland Formation

comprising the dominant footwall in the southern sector, dolomites of the Malmani Subgroup comprising the central sector footwall, and the northern sector footwall comprising Archaean granites, it was thought that this may be a controlling factor in the distribution of sulphide mineralisation. Particularly it was thought that the sulphide abundances in the southern sector may be due to a contribution of sulphur from footwall pyrite in Duitschland Formation shales or from anhydrite in Duitschland Formation dolomites. Sulphur isotope studies were therefore undertaken on sulphides and sulphates from different footwall lithologies, from throughout the Platreef and from metasedimentary xenoliths and vein material from various lithologies of the Platreef package in order to test this hypothesis.

CHAPTER FOUR
SULPHUR ISOTOPE ANALYSES

Introduction

Sulphur isotopes are a complex, but powerful tool in the determination of the genesis of ore deposits (White, 2001). For this study, sulphide samples were collected from cores ATS-046, ATS-057, AMK-021, PR-174 and PR-175 to compare $\delta^{34}S$ values of sulphides from cores with different footwall rocks, as well as to examine possible variations through stratigraphy. The sulphide-bearing samples included pyrrhotite, pentlandite and chalcopyrite which occur as co-existing sulphides. Samples of bornite and pyrite were also collected from the sulphide bearing horizons on Farm Duitschland, as well as anhydrites and associated galena from cores on Farm Tweefontein. Sulphides from vein material were also analysed. All of these samples were collected in order to obtain $\delta^{34}S$ values for a variety of footwall materials that may have been the source of sulphur within the Platreef. Samples were analysed at Royal Holloway, University of London in the United Kingdom as well as at the iThemba Laboratories in South Africa. Repeats of samples were included in each set of analyses as an internal standard.

Sulphur Isotope Theory and Concepts

Sulphur exists as four stable isotopes, ^{32}S, ^{33}S, ^{34}S, and ^{36}S, with ^{32}S having the highest abundance (95.02%), followed by ^{34}S (4.21%), ^{33}S (0.75%) and with ^{36}S being the least abundant (0.02%) (Rollinson, 1993). The ratio between the two most abundant isotopes is used in geochemistry, as they are easier to measure and hence allow for more precision. In geochemistry, the isotopic composition of sulphur is recorded as $\delta^{34}S$, and is presented as parts per thousand relative to a standard (Brownlow, 1996). The standard used is the Cañon Diablo Troilite (CDT) taken from an iron meteorite. The $\delta^{34}S$ values are calculated as follows:

$$\delta^{34}S\ ‰ = [(^{34}S/^{32}S\ (sample) - {}^{34}S/^{32}S\ (standard)) / (^{34}S/^{32}S\ (standard))] \times 1000.$$

In addition, sulphur can form four different valences (-2, 0, +4, and +6). Each of these valence states can form a variety of compounds, and equilibrium isotopic fractionations can occur between different valence states, and between compounds with sulphur of the same valence states (Rollinson, 1993).

Sulphide and sulphate minerals have different $\delta^{34}S$ values, depending on the processes which provided the sulphur. There are two main reservoirs of sulphur on the Earth, each of which has uniform sulphur isotope values; the first is the mantle, which has a $\delta^{34}S$ of approximately zero compared to meteoritic values, and modern sea water which has a $\delta^{34}S$ of approximately +20‰ (Rollinson, 1993). Sulphur from different sources can be characterised by their range of $\delta^{34}S$ values (Figure 4.1). Thus sulphide or sulphate minerals will have a specific range of $\delta^{34}S$ values depending on the processes which lead to their formation. Therefore, by measuring the $\delta^{34}S$ values for particular minerals in a suite of rocks, the origin of the sulphur in these rocks may be indicated.

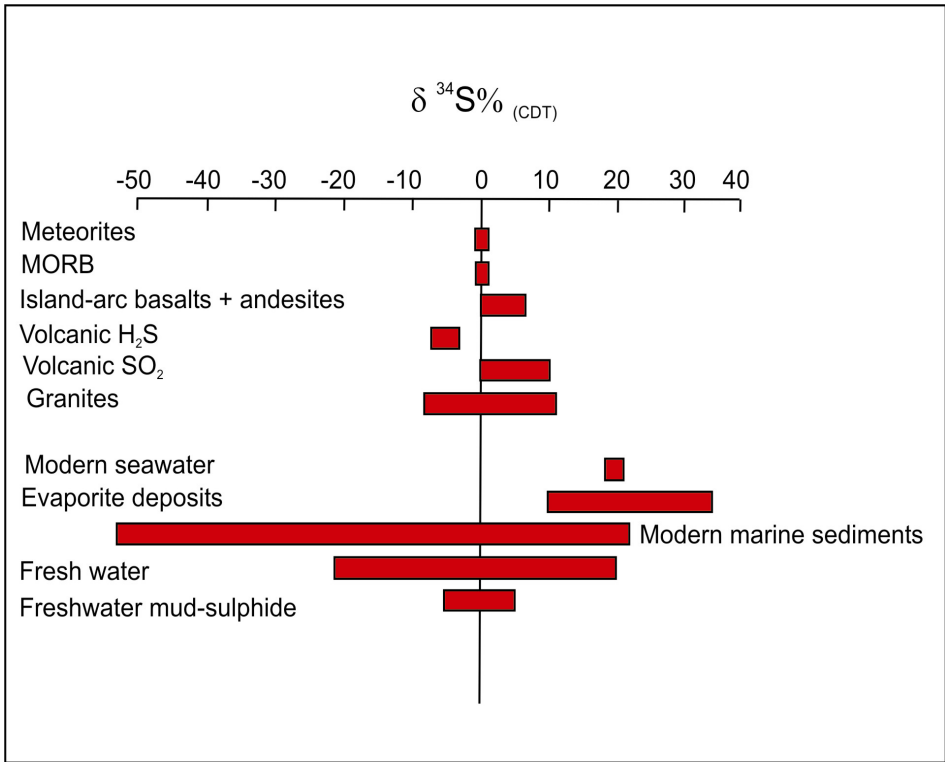

Figure 4.1: $\delta^{34}S$ values for a variety of geological materials (after Rollinson, 1993).

Previous Work

The first sulphur isotope analyses conducted on the northern limb was by Liebenberg (1968). He recorded two $\delta^{34}S$ values for the farm Zwartfontein 818LR, both of which had approximately magmatic values of +0.7‰ for a calc-silicate and +1.9‰ from a pegmatoidal norite (Figure 4.2). Hulbert (1983) presented data from Lower Zone pyroxenites and chromitites south of Mokopane, as well as pyroxenites, chromitites and anorthosites from the Critical Zone. These yielded $\delta^{34}S$ values from +0.96‰ to +7.54‰ (Figure 4.2). He also analysed two samples of Upper Zone material from the northern sector of the Platreef on farm Molendraai, which also had $\delta^{34}S$ values of approximately +2‰ (Figure 4.2). Hulbert interpreted this data as indicating that the majority of sulphur associated with sulphides was of mantle origin. Elevated $\delta^{34}S$ values were ascribed to an increased fo_2 which the author proposed was due to the release of volatiles from sedimentary material.

The majority of the sulphur isotope data available for the Platreef itself was presented by Buchanan et al. (1981) and Buchanan and Rouse (1984) and was for a variety of sulphide samples taken from farms Tweefontein and Turfspruit (Figure 4.2). These samples indicated $\delta^{34}S$ values in pyrrhotite of +6‰ to +9‰, which they suggested might have originated from contamination by anhydrite within the Malmani Dolomite (Buchanan et al. 1981). Sulphides from graphite layers on Farm Turfspruit yielded values of -2.42‰ to +2.0‰ (Buchanan and Rouse, 1984). From this data the authors proposed that the sulphides within the Platreef were enriched in $\delta^{34}S$ by the melting of anhydrite when rafts of the Malmani Dolomite were assimilated into the Platreef magma. This enrichment of sulphur then allowed for the precipitation of an immiscible sulphide liquid (Buchanan et al, 1981).

Manyeruke et al. (2005) examined samples taken from a core on farm Townlands (Figure 4.2), and identified three different units separated by hornfels rafts, which they called the Upper, Middle and Lower Platreef. Sulphur isotope values from

this core indicated that the Upper and Lower Platreefs had elevated $\delta^{34}S$ values of ~ +8‰, whereas the Middle Platreef had $\delta^{34}S$ values of ~ +4‰. These elevated values were also attributed to the addition of sulphur of crustal origin.

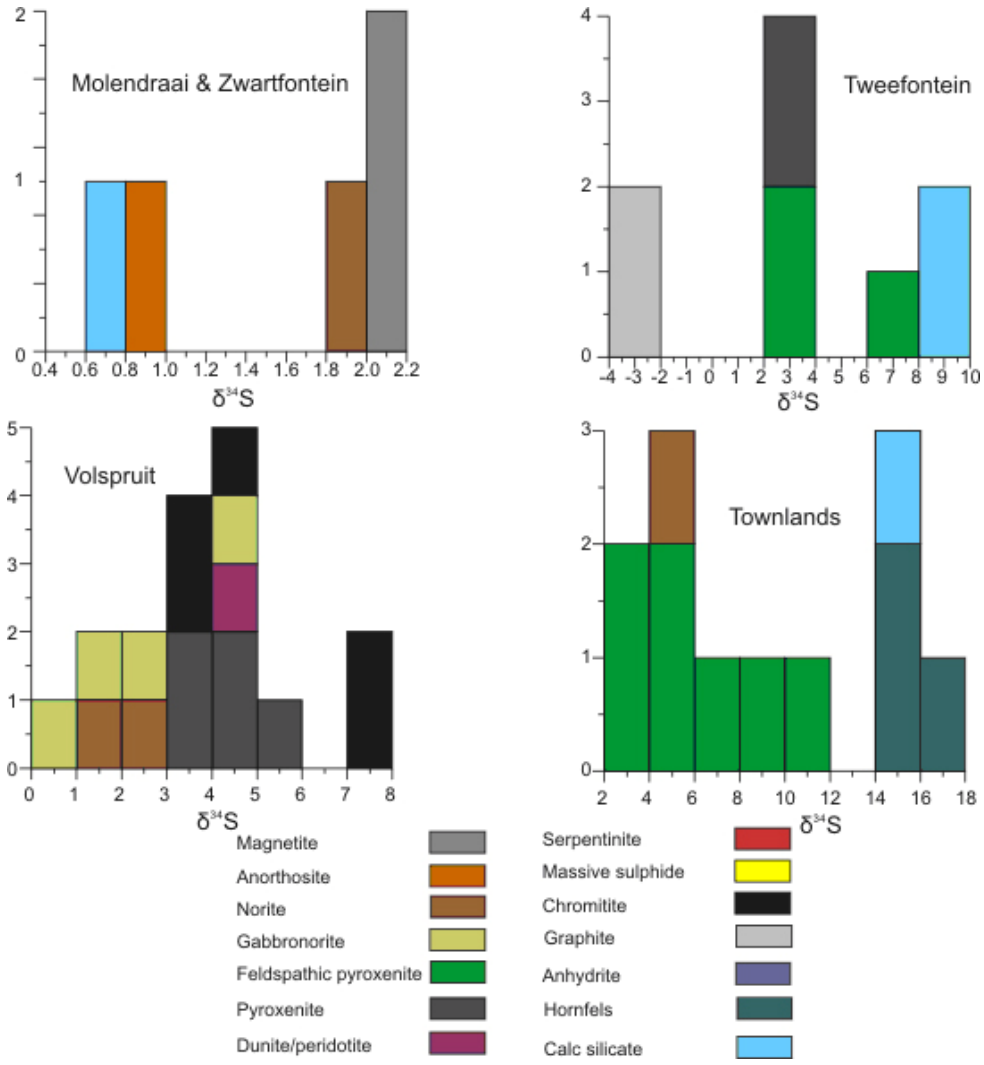

Figure 4.2: Histograms showing all previous sulphur isotope analyses of sulphide minerals vs. number of analyses for the northern limb of the Bushveld Complex. Data from Buchanan et al. (1981), Buchanan and Rouse (1984), Hulbert (1983), Liebenberg (1968), and Manyeruke (2003). Note: For location of farms see Figure 4.10. Graphite and magnetite refer to the dominant mineralogy of the host rock rather than minerals analysed. Scale on each diagram is different.

Li et al. (2002) examined sulphur isotope variations for the Uitkomst Complex, which is considered to be a satellite body of the eastern Bushveld Complex. In the unmineralised lithologies of the complex, as well as the basal gabbro, $\delta^{34}S$ values are recorded as being close to magmatic (-0.9‰ to +2.6‰). However, in

the sulphide-bearing harzburgites, the $\delta^{34}S$ values indicated a contribution of crustal sulphur (-2.6‰ to -7.1‰), which the authors proposed was probably from either the Malmani Subgroup or the Timeball Hill Formation.

Cameron (1982) investigated sulphur isotope variations for the Transvaal Supergroup, specifically for the Timeball Hill shale, Penge Iron Formation, the Malmani Subgroup, and the Black Reef Quartzite. The Timeball Hill Formation yielded $\delta^{34}S$ values of -12‰ to -18‰, and the Penge Formation has $\delta^{34}S$ values of -3‰ to -6‰. Pyrite-bearing shales from the Malmani Subgroup showed some variations, with the upper three-quarters yielding $\delta^{34}S$ values of 0‰ to -8‰, and the lower quarter yielding values of +3‰ to +10‰. Pyrite in quartzites of the Black Reef Formation gave $\delta^{34}S$ values of approximately +3‰.

Methodology

Sulphides for this study were collected through a vertical Platreef profile of 450 m and from sulphide-bearing footwall lithologies. Samples in the southern sector of the Platreef were chosen from selected cores on Farms Macalacaskop (AMK021), Turfspruit (ATS046, ATS057, ITS033) and Rietfontein (ARF08). In the northern sector of the Platreef two cores were chosen from Farm Drenthe (PR174 and PR175). These cores had footwall of sulphur-poor Archaean granite, and one core contained xenoliths of calc-silicate (PR175). Sulphides from the Platreef in both the southern and northern sectors were collected systematically from top to bottom and included disseminated, blebby, net-textured and massive ore together with sulphides from hornfels and calc-silicate xenoliths. Samples were also collected from several footwall lithologies of the Platreef including pyritic shales and sulphide-bearing dolomite from the Duitschland Formation, anhydrite veins from cores from the central sector of the Platreef, and a variety of late-stage vein material including a chalcopyrite-bearing calcite vein, and a quartz-calcite vein containing chalcopyrite, sphalerite and galena. Chosen samples were either crushed or prepared into polished blocks.

Samples that were crushed were then milled, and sieved to -125 + 90 microns in size. These fractions were then washed and dried to remove any very fine material. Samples were also cleaned of any heavily magnetic minerals (i.e. magnetite or pyrrhotite) using a hand magnet, then separated according to magnetic susceptibility on a Frantz Isodynamic Separator using various amperages. Separates were then further cleaned to remove any remaining silicates using heavy liquid separation (bromoform) resulting in pure sulphide fractions.

In the case of the samples from the northern sector, there were little or no sulphides in the sieved fraction used for separation. It was decided therefore to analyses the sulphur isotopes using bulk sample analysis. The finest sieved fraction (<90 microns) was used for analysis on the basis that sulphides have a lower hardness than silicates and are therefore more likely to be in the finest milled fraction than in coarser fractions.

For samples in the southern sector where it was not possible to separate out pure sulphides, mineral separates were extracted by microdrill (Figure 4.3) from polished blocks at University College London. This drill allows for the extraction of mineral separates on a small scale as its tip is approximately 50 μm in diameter. Different sulphides within polished blocks were targeted and extracted using a variety of drilling methods. One method involved drilling a grid of holes at 150 μm depth at a spacing of 300 μm, followed by an identical grid of holes at 300 μm, and another at 500 μm if further material was required. The spacing of the hole was small enough that it created fracturing, removing the sulphide phase between the holes. The second method of extracting sulphides from the polished block involved drilling a line raster with a 200 μm spacing at a depth of 150 μm, followed by one at a depth of 300 μm, and one at 500 μm – again if further material was required.

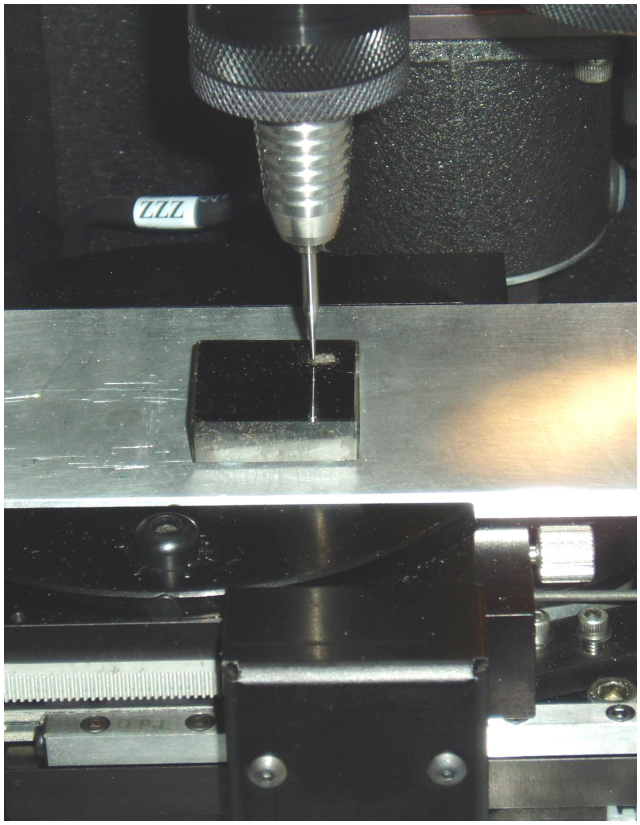

Figure 4.3: Photograph of the microdrill used for extracting sulphide minerals, as well as a polished block.

Sulphur isotopes analyses were conducted on pyrrhotite, pentlandite and chalcopyrite mineral separates from the Platreef, pyrrhotite and pyrite from hornfels and calc-silicates within cores, and on bulk samples from the northern sector of the Platreef. Sulphur isotope analyses were also conducted on pyrite and bornite from footwall material of the Duitschland Formation, anhydrite samples from core which occurs in the Central Sector of the Platreef, and chalcopyrite, sphalerite and galena from vein material. Sulphur isotope analyses were conducted at the Environmental Isotope Laboratory of the iThemba Laboratories in South Africa, and microdrilled, bulk and vein samples were analysed at Royal Holloway, University of London in the United Kingdom.

Samples for sulphur isotope analysis in South Africa were prepared using the procedure outlined by Horstmann and Malinga (2003) and analysed using a continuous-flow isotope ratio mass-spectrometer (GEO 20-20). Samples weighing between 0.3 and 2.2 mg depending on the sample composition were

weighed into tin capsules. Vanadium pentoxide (V_2O_5) weighing at least double the weight of the sample was then added to the capsule to aid combustion. Samples were then loaded into a carousel on the ANCA–GSL (automated nitrogen and carbon analysis for gases, solids and liquids). They were then dropped into a furnace held at 1020°C where they were combusted in the presence of oxygen (Figure 4.4). The combusted gases were swept in a helium stream over a combustion and reduction catalyst to purify the gas to sulphur dioxide. Water was removed by a Nafion™ membrane and magnesium perchlorate chemical trap. SO_2 gas was separated from N_2 and CO_2 by a gas chromatograph (Figure 4.4). The resultant chromatographic peak of SO_2 entered the ion source of the GEO 20-20 CF–IRMS where it was ionised and accelerated (Figure 4.4).

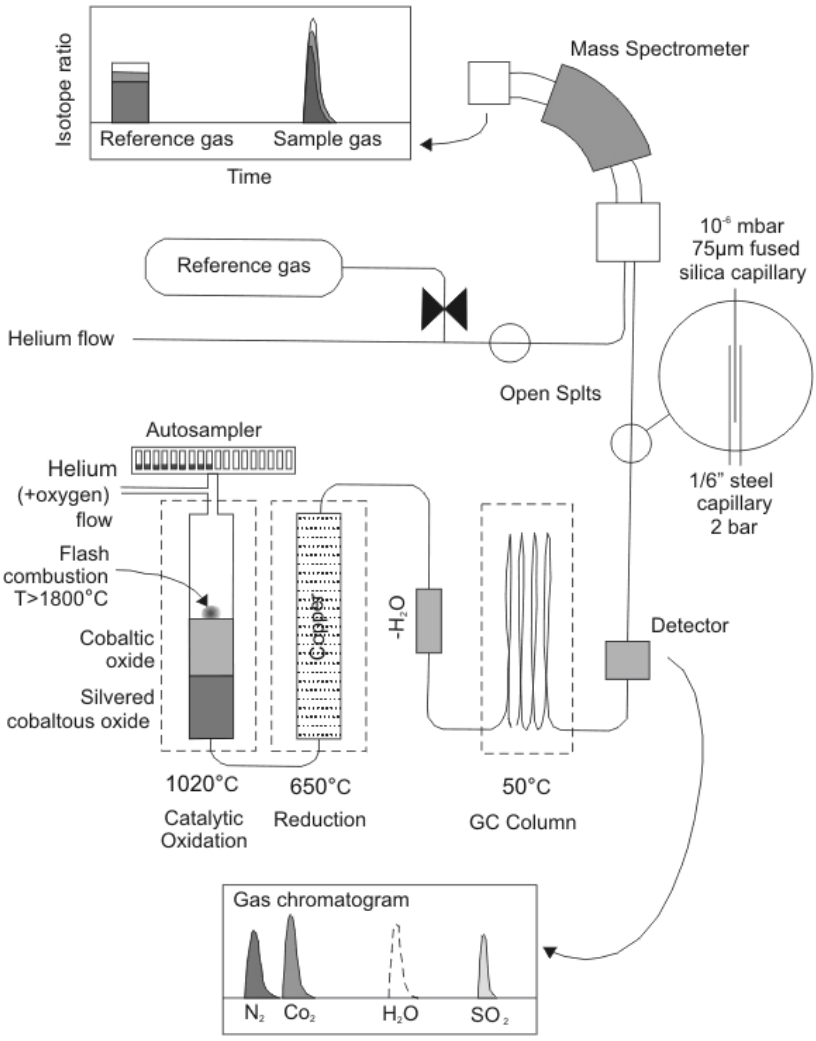

Figure 4.4: Diagramatic representation of a continuous flow mass spectrometer (modified from Gill, 1999).

^{32}S and ^{34}S were separated in a magnetic field then simultaneously measured on a Faraday cup universal collector array. Analysis time was about five minutes per sample. The raw data were linearly regressed using international and internal standards, and are reported relative to the Cañon Diablo troilite (CDT) standard (Table 4.1). The reproducibility of duplicate determinations yielded aliquot differences between 0.1‰ and 0.8‰.

Sulphur isotope analyses conducted in the United Kingdom were done using procedures outlined in Grassineau et al. (2001). A continuous flow – isotope ratio mass spectrometry (CF-IRMS) method was used in the analyses, with prepared samples being dropped successively into a catalytic combustion furnace at 1000 – 1200 °C. The catalytic combustion furnace is constantly purged with He carrier gas. A temperature of 1800 °C, in the presence of oxygen ensures complete oxidation of the sample, with copper being used to absorb any excess oxygen. Chemical scrubbing and gas chromatography are used to selectively remove or separate the products of the combustion (CO_2, N_2, H_2O, SO_2) (Figure 4.4). These products, with the He carrier gas, are introduced into the IRMS. The monitoring of ion beam intensities relative to background values allows for the determination of the isotope ratios of the gas peaks. All corrected isotope results are expressed relative to the CDT standard. The reproducibility of the samples is validated through the analyses of standards during the analyses of the samples and is between 0.03‰ and 0.22‰.

For the bulk samples that were analysed in the United Kingdom the procedure is essentially the same as that used for the sulphide separates. Much larger samples (up to 30 mg) are analysed to guarantee that sufficient sulphur is present for an accurate analysis. Before the analytical run is started the linearity of the machine is tested to ensure that the difference in isotopic values between large and small samples from the same sample is negligible.

Results

Southern Sector of the Platreef:

Data obtained from Platreef sulphides varied according to the type of footwall lithology. On farm Turfspruit (Table 4.1), where the footwall is Duitschland Formation dolomites, $\delta^{34}S$ values can be separated into two distinct groups, one with an average of +5.2‰, the other with an average of +1.4‰ (Table 4.1, Figure 4.5). These two groups occur at different depths in the sampled cores, with higher values occurring towards the base (Figure 4.6). On farm Rietfontein (Table 4.2), where the footwall is also Duitschland Formation dolomites, $\delta^{34}S$ values all grouped together, with an average of +5.0‰ (Table 4.2, Figure 4.5). Hornfels xenoliths from the two farms also split into two groups, with hornfels from farm Rietfontein having an average $\delta^{34}S$ of +5.2‰, and a hornfels from farm Turfspruit yielding a $\delta^{34}S$ value of +9.7‰ (Table 4.1, Table 4.2, Figure 4.5). Calc-silicates from the two farms generally showed two different sets of results, with pyrite and pyrrhotite within calc-silicates from farm Turfspruit having average $\delta^{34}S$ values of +16.6‰, and a pyrrhotite from farm Rietfontein, yielding an average $\delta^{34}S$ of +4.5‰. Analysis of a coarse-grained sulphide bleb which occurs within a calc-silicate at the base of core ATS 57 yielded anomalously high $\delta^{34}S$ values of +27.69‰ to +28.17‰.

Sulphides from magmatic rocks sampled from farm Macalacaskop, which has a footwall of Timeball Hill Formation quartzite, showed slightly less variation. Analyses yielded an average $\delta^{34}S$ value of +2.9‰ (Table 4.1), although a slight decrease in sulphur isotope values (from +3.6‰ to +2.2‰) is seen from the bottom to the top of the sampled core. A serpentinite from the same core yielded a $\delta^{34}S$ value of +3.3‰ and a pyrrhotite from the calc-silicate footwall has a $\delta^{34}S$ value of +3.6‰ (Table 4.1).

Table 4.1: Sulphur isotope data for the southern sector of the Platreef on Farms Turfpruit (ATS, ITS) and Macalacaskop (AMK). RSA and UK refer to the location of the laboratory where the samples were analysed.

Sample Number	Rock Type	Mineral	Sulphide/Sulphate Texture	$\delta^{34}S‰$ CDT	Analysed
ATS 46/60.34	Pegmatoidal Norite	Pyrrhotite	Coarse grained bleb	**1.1**	RSA
ATS 46/60.34	Pegmatoidal Norite	Chalcopyrite	Coarse grained bleb	**1.1**	RSA
ATS 46/61.12	Feldspathic Pyroxenite	Pyrrhotite	Coarse grained bleb	**1.1**	UK
ATS 46/61.12	Feldspathic Pyroxenite	Chalcopyrite	Coarse grained bleb	**1.3**	UK
ATS 46/61.12	Feldspathic Pyroxenite	Pentlandite	Coarse grained bleb	**0.9**	UK
ATS 46/146.71	Feldspathic Pyroxenite	Pyrrhotite	Fine to medium grained disseminated	**5.9**	UK
ATS 46/154.67	Gabbro Norite	Pyrrhotite	Net-textured vein	**6.3**	UK
ATS 46/207.50	Hornfels	Pyrrhotite	Medium grained bleb	**9.7**	UK
ATS 46/316.62	Peridotite	Pyrrhotite	Medium to coarse grained interstitial	**4.8**	UK
ATS 46/345.60	Dunite / Peridotite	Pyrrhotite	Net-textured	**5.3**	UK
ATS 46/457.49	Pyroxenite	Pyrrhotite	Fine grained interstitial	**5.4**	RSA
ATS 46/461.21	Feldspathic Pyroxenite	Chalcopyrite	Medium grained interstitial	**5.5**	UK
ATS 46/469.25	Calc-silicate	Pyrrhotite	Fine grained disseminated	**16.4**	UK
ATS 57/72.48	Pyroxenite	Chalcopyrite	Coarse grained bleb	**1.0**	UK
ATS 57/118.78	Pyroxenite	Pyrrhotite	Fine to coarse grained interstitial	**2.2**	UK
ATS 57/180.64	Feldspathic Pyroxenite	Pyrrhotite	Fine to medium grained disseminated	**4.5**	UK
ATS 57/218.39	Pyroxenite	Pyrrhotite	Net-textured	**5.0**	UK
ATS 57/218.39	Pyroxenite	Chalcopyrite	Net-textured	**4.9**	UK
ATS 57/221.39	Massive Sulphide / Pyroxenite	Pyrrhotite	Massive sulphides	**5.3**	UK
ATS 57/221.39	Massive Sulphide / Pyroxenite	Pentlandite	Massive sulphides	**5.4**	UK
ATS 57/268.15	Feldspathic Pyroxenite	Pyrrhotite	Fine-grained disseminated	**4.6**	UK
ATS 57/325.32	Calc-silicate	Pyrrhotite	Coarse grained bleb	**28.2**	UK
ATS 57/325.32	Calc-silicate	Pyrrhotite	Coarse grained bleb	**27.7**	UK
ATS 57/325.32	Calc-silicate	Pyrrhotite	Coarse grained bleb	**28.7**	UK
ATS 57/335.07	Calc-silicate	Pyrite	Fine grained disseminated	**16.9**	UK
AMK 21/125.76	Pyroxenite	Pyrrhotite	Coarse grained bleb	**2.2**	UK
AMK 21/125.76	Pyroxenite	Pyrrhotite	Very coarse grained bleb	**2.1**	UK
AMK 21/227.15	Serpentinite	Pyrrhotite	Interstitial	**3.3**	UK
AMK 21/232.62	Pyroxenite	Pyrrhotite	Interstitial	**3.6**	UK
AMK 21/232.62	Pyroxenite	Chalcopyrite	Interstitial	**3.6**	RSA
AMK 21/235.31	Calc-silicate	Pyrrhotite	Vein within chalcopyrite bleb	**3.5**	UK
ITS 33/241.16	Feldspathic Pyroxenite	Pyrrhotite	Coarse grained interstitial	**1.8**	RSA
ITS 33/241.16	Feldspathic Pyroxenite	Chalcopyrite	Coarse grained interstitial	**1.7**	RSA

Table 4.2: Sulphur isotope data for the southern sector of the Platreef on Farm Rietfontein.

Sample Number	Rock Type	Mineral	Sulphide/Sulphate Texture	$\delta^{34}S‰$ CDT	Analysed
ARF 08/36.42	Cordierite-Spinel Hornfels	Pyrrhotite	Fine grained disseminated	**5.3**	RSA
ARF 08/36.42	Cordierite-Spinel Hornfels	Chalcopyrite	Fine grained disseminated	**5.6**	RSA
ARF 08/36.53	Cordierite-Spinel Hornfels	Pyrrhotite	Fine grained disseminated	**5.0**	RSA
ARF 08/44.65	Norite	Pyrrhotite	Medium grained disseminated	**5.2**	RSA
ARF 08/49.26	Norite	Pyrrhotite	Fine grained disseminated	**4.5**	RSA
ARF 08/49.26	Norite	Chalcopyrite	Fine grained disseminated	**4.8**	RSA
ARF 08/49.26	Norite	Pyrrhotite	Fine grained disseminated	**5.2**	RSA
ARF 08/52.42	Gabbronorite	Pyrrhotite	Fine grained disseminated	**5.4**	RSA
ARF 08/73.24	Gabbronorite	Pyrrhotite	Fine grained disseminated	**5.1**	RSA
ARF 08/76.80	Cordierite-Spinel Hornfels	Pyrrhotite	Fine to coarse grained blebs	**5.0**	RSA
ARF 08/82.74	Gabbronorite	Pyrrhotite	Medium grained disseminated	**4.9**	RSA
ARF 08/96.32	Gabbronorite	Pyrrhotite	Medium grained disseminated	**4.1**	RSA
ARF 08/106.67	Gabbro	Pyrrhotite	Coarse grained blebs	**4.2**	RSA
ARF 08/124.64	Massive Sulphide	Pyrrhotite	Massive sulphide	**4.9**	RSA
ARF 08/124.64	Massive Sulphide	Pyrrhotite	Massive sulphide	**4.9**	RSA
ARF 08/124.64	Massive Sulphide	Pyrrhotite	Massive sulphide	**4.9**	RSA
ARF 08/124.64	Massive Sulphide	Pyrrhotite	Massive sulphide	**5.4**	RSA
ARF 08/124.64	Massive Sulphide	Pyrrhotite	Massive sulphide	**5.4**	RSA
ARF 08/126.27	Norite	Pyrrhotite	Fine to coarse grained interstitial	**5.6**	RSA
ARF 08/129.78	Norite	Pyrrhotite	Medium to coarse grained blebs	**5.0**	RSA
ARF 08/129.78	Norite	Chalcopyrite	Medium to coarse grained blebs	**5.4**	RSA
ARF 08/130.89	Norite	Pyrrhotite	Very coarse grained bleb	**5.3**	RSA
ARF 08/153.46	Marble-Skarn	Pyrrhotite	Fine grained disseminated	**4.5**	RSA

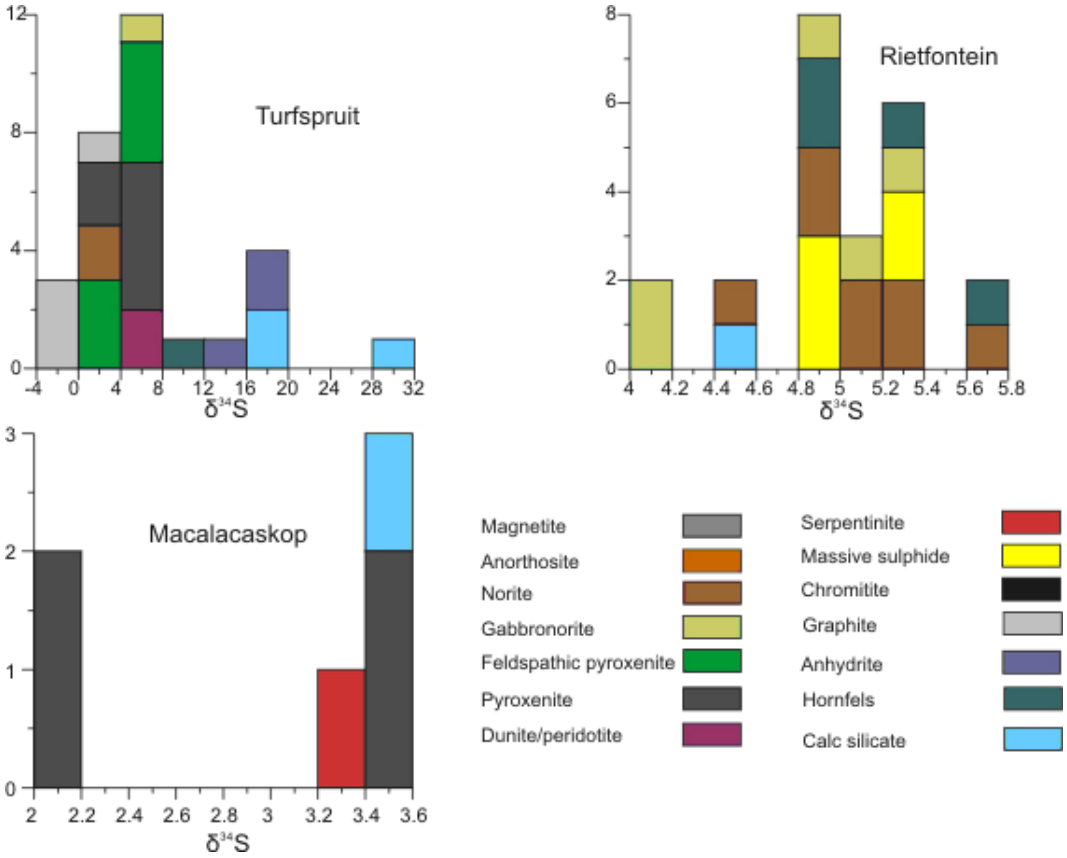

Figure 4.5: Histograms showing sulphur isotopes vs. number of analyses for the southern sector of the Platreef depending on location. The footwall on Farms Turfspruit and Rietfontein comprise Duitschland Formation, on Farm Macalacaskop it comprises Timeball Hill Formation. Note: the scale of each of the diagrams is different. Also graphite and magnetite refer to the dominant mineralogy of the host rocks rather than minerals analysed.

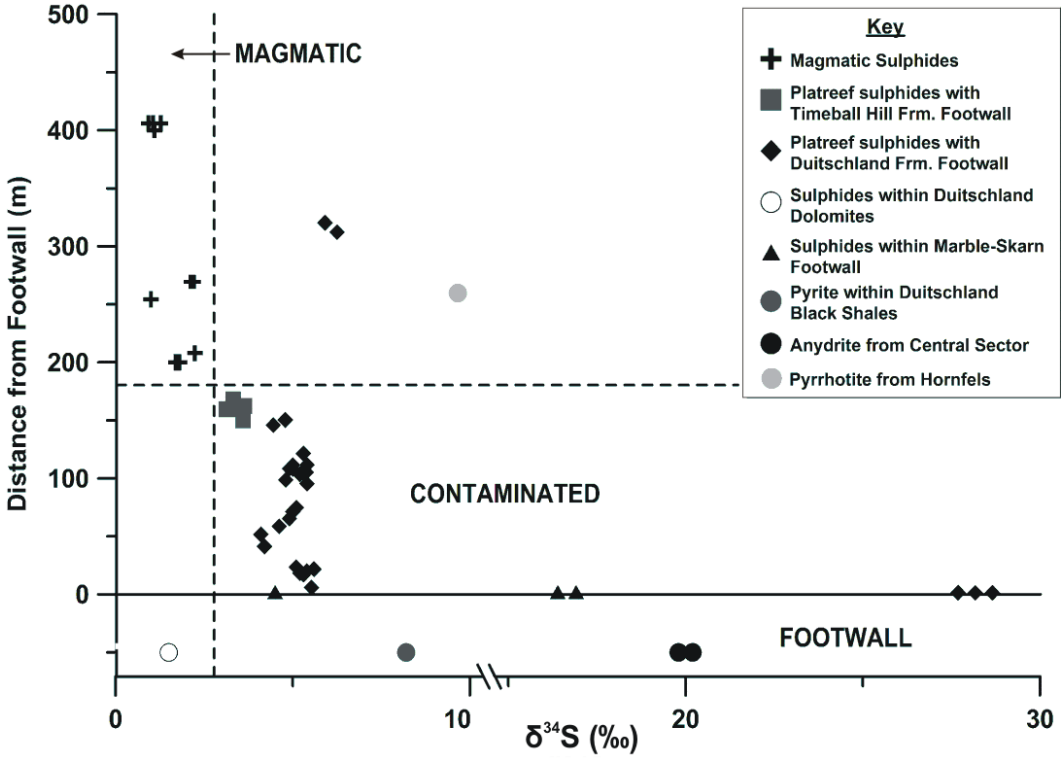

Figure 4.6: Diagram showing variation of $\delta^{34}S$ values with depth and increasing distance from the footwall in the southern sector of the Platreef, as well as $\delta^{34}S$ values from various sulphur-bearing footwalls of the Northern limb. The phrase contaminated refers to samples which have $\delta^{34}S$ values which are higher than those accepted for mantle sulphur. The term magmatic refers to those samples which have $\delta^{34}S$ values close to that of mantle sulphur. Horizontal dashed line indicates distance from footwall at which $\delta^{34}S$ values become magmatic, vertical dashed line represents the $\delta^{34}S$ value where sulphides become contaminated. Solid horizontal line represents the depth of the footwall contact.

Northern Sector of the Platreef:

In the northern sector of the Platreef $\delta^{34}S$ values can also be separated into two distinct groups, one with an average of +6.4‰, the other with an average of +3.3‰ (Table 4.3, Figure 4.7). These two groups also occur at different depths in the sampled cores, but as opposed to the southern sector of the Platreef, the higher values occur towards the top of the core (Figure 4.8). There are two analyses (PR175/102.50) which are included in the upper group that have comparatively high values of +10.7‰ and +11.0‰ (Table 4.3, Figure 4.8).

Table 4.3: Sulphur isotope data for the northern sector of the Platreef in percent per mil relative to CDT.

Sample Number	Rock Type	Sulphide/Sulphate Texture	$\delta^{34}S‰$ CDT
PR174/21.50	Feldspathic Pyroxenite	Very fine grained, disseminated	4.87
PR174/56.00	Contaminated Norite	Medium grained blebs	4.47
PR174/75.50	Serpentinised Pyroxenite	Fine to medium grained blebs	5.94
PR174/80.50	Feldspathic Pyroxenite	Medium grained blebs	5.61
PR174/84.50	Contaminated Norite	Fine grained, interstitial	5.58
PR174/88.50	Contaminated Norite	Fine grained, interstitial	5.33
PR174/88.50	Contaminated Norite	Fine grained, interstitial	5.56
PR174/97.50	Contaminated Norite	Fine grained, interstitial	6.09
PR174/97.50	Contaminated Norite	Fine grained, interstitial	5.47
PR174/106.13	Serpentinised Pyroxenite	Fine to coarse grained blebs	5.98
PR174/109.54	Contaminated Norite	Fine grained, interstitial	5.40
PR174/188.50	Feldspathic Pyroxenite	Net-textured	3.78
PR174/188.50	Feldspathic Pyroxenite	Net-textured	3.31
PR174/207.50	Granofels	Fine grained, interstitial	3.13
PR174/217.50	Granofels	Fine grained, interstitial	3.37
PR174/224.50	Granofels	Fine grained, interstitial	3.09
PR174/240.50	Serpentinite	Fine to coarse grained blebs	3.29
PR174/240.50	Serpentinite	Fine to coarse grained blebs	3.18
PR175/16.50	Calc-Silicate	Fine grained, disseminated	7.11
PR175/19.08	Calc-Silicate	Fine grained, disseminated	7.19
PR175/19.08	Calc-Silicate	Fine grained, disseminated	7.93
PR175/19.08	Calc-Silicate	Fine grained, disseminated	6.07
PR175/32.35	Feldspathic Pyroxenite	Fine grained, disseminated	5.96
PR175/38.50	Contaminated Norite	Medium grained blebs	4.89
PR175/44.50	Contaminated Norite	Medium grained blebs	5.43
PR175/66.50	Feldspathic Pyroxenite	Medium to coarse grained, interstitial	5.35
PR175/77.18	Feldspathic Pyroxenite	Medium to coarse grained, interstitial	6.40
PR175/84.50	Feldspathic Pyroxenite	Medium to coarse grained, interstitial	7.30
PR175/84.50	Feldspathic Pyroxenite	Medium to coarse grained, interstitial	7.87
PR175/88.35	Feldspathic Pyroxenite	Medium to coarse grained, interstitial	5.91
PR175/91.79	Feldspathic Pyroxenite	Coarse grained blebs	6.55
PR175/91.79	Feldspathic Pyroxenite	Coarse grained blebs	6.87
PR175/102.50	Feldspathic Pyroxenite	Fine grained, disseminated	11.03
PR175/102.50	Feldspathic Pyroxenite	Fine grained, disseminated	10.70
PR175/115.35	Feldspathic Pyroxenite	Medium grained blebs	5.72
PR175/116.81	Feldspathic Pyroxenite	Medium grained blebs	6.65
PR175/116.81	Feldspathic Pyroxenite	Medium grained blebs	6.77

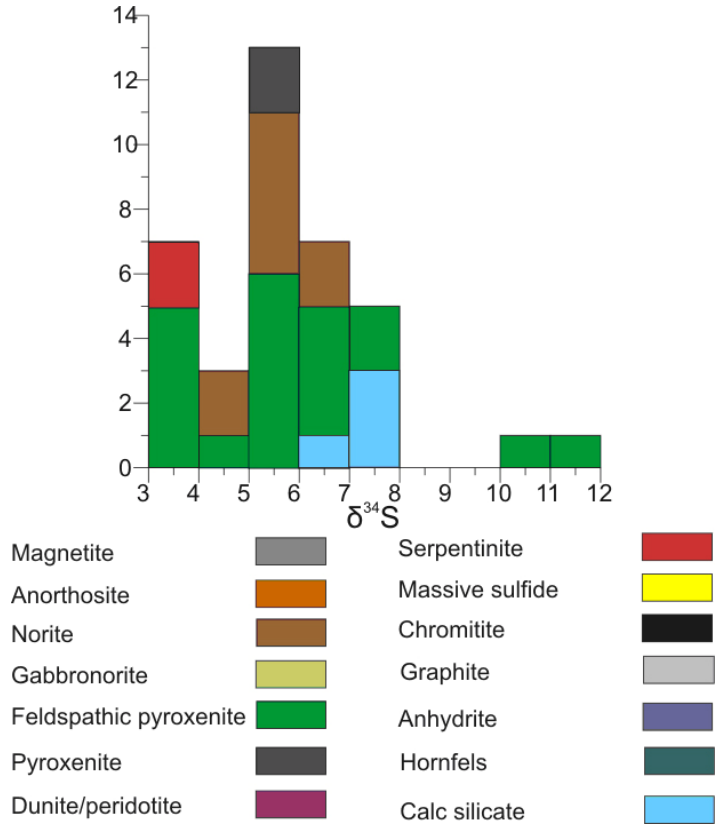

Figure 4.7: Histograms showing sulphur isotopes for the northern sector of the Platreef on Farm Drenthe. Note: graphite and magnetite refer to the dominant mineralogy of the host rock rather than actual minerals analysed.

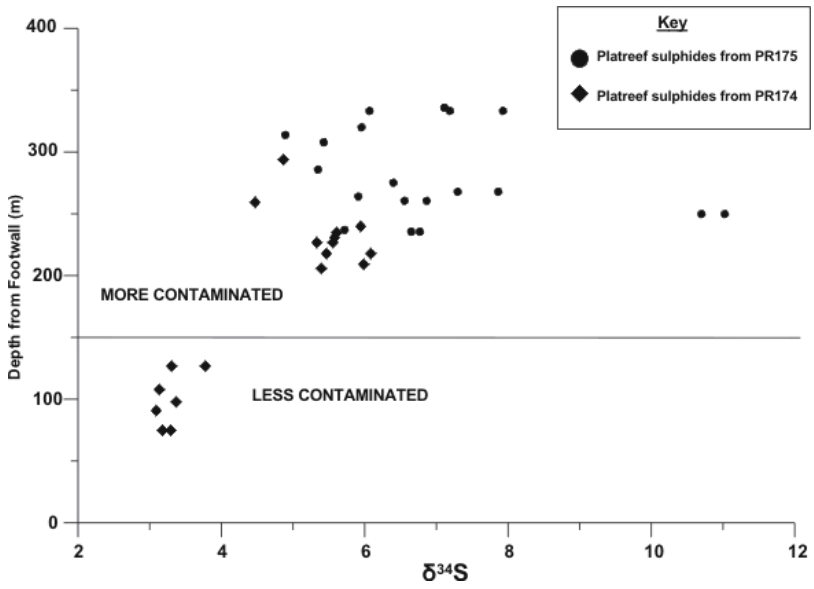

Figure 4.8: Diagram showing variation of $\delta^{34}S$ values with depth and increasing distance from the footwall in the northern sector of the Platreef on Farm Drenthe. 'Less Contaminated' refers to those samples which have $\delta^{34}S$ values close to accepted mantle values, 'More Contaminated' refers to those samples whose $\delta^{34}S$ values indicate to a sulphur contribution from an external source.

Sedimentary Material:

Sulphides from sedimentary material taken from Farm Duitschland that represent unmetamorphosed footwall gave varying sulphur isotope values. Bornite from dolomite at the top of the Duitschland sequence yielded $\delta^{34}S$ values of +1.5‰, and pyrite from the shales towards the base of the sequence gave $\delta^{34}S$ values of +8.2‰ (Table 4.4) (Figure 4.9).

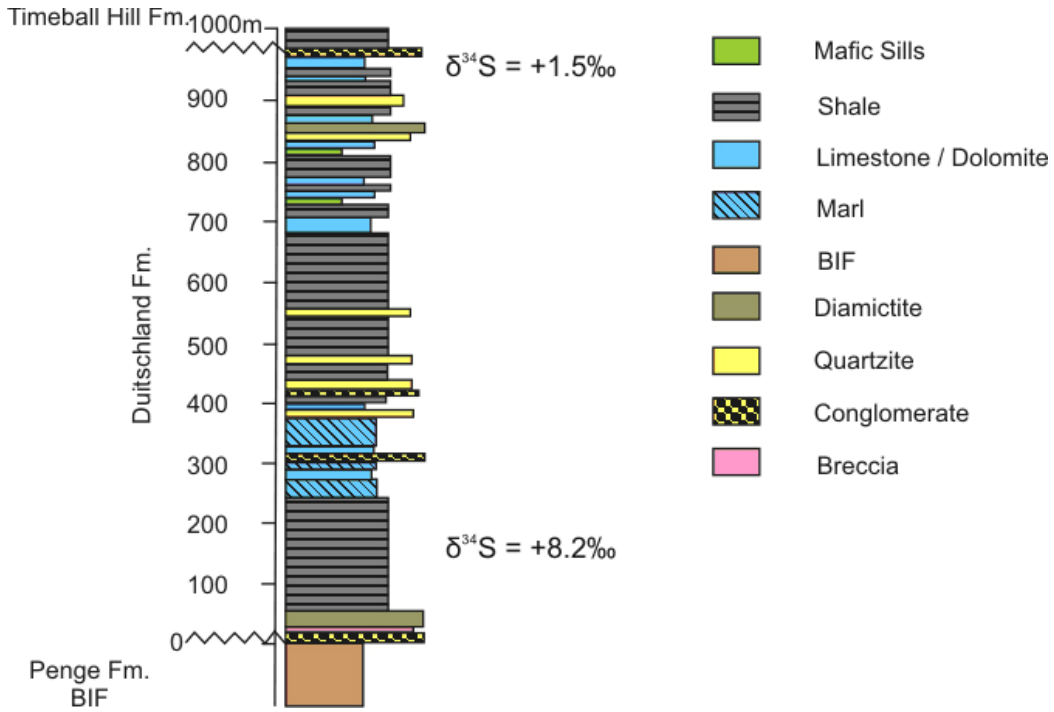

Figure 4.9: Stratigraphy of the Duitschland Formation showing measured sulphur isotope values.

Vein Material:

Anhydrite veins from the central sector of the Platreef gave $\delta^{34}S$ values of between +19.8‰ and +20.2‰, and galena associated with these anhydrites yielded a $\delta^{34}S$ value of -3.1‰ (Table 4.4). Chalcopyrite formed along crystal planes in a calcite vein gave a $\delta^{34}S$ value of +4.3‰. Sphalerite and chalcopyrite from a quartz – calcite vein (PRS17) yielded similar $\delta^{34}S$ values of +5.6‰ and +5.2‰ respectively, with galena from the same vein having a $\delta^{34}S$ value of +1.1‰ (Table 4.4).

Table 4.4: Sulphur isotope data for the footwall and vein material associated with the Platreef. Samples labelled DL are from Farm Duitschland, TN from Farm Tweefontein North, VK from Farm Vaalkop, and ZN from Farm Zwartfontein.

Sample Number	Rock Type	Mineral	Sulphide/Sulphate Texture	$\delta^{34}S$‰ CDT
DL1	Dolomite	Bornite	Alteration vein	1.5
DL2	Shale	Pyrite	Medium grained nodules along bedding planes	8.2
TN75	Anhydrite	Anhydrite	Vein	20.2
VK75-305	Anhydrite	Anhydrite	Vein	19.8
ZN 396-214.4	Anhydrite	Galena	Crystalline	-3.1
Calcite Vein	Calcite	Chalcopyrite	Crystalline, along calcite crystal planes	4.3
PRS17	Quartz - Calcite Vein	Sphalerite	Crystalline	5.6
PRS17	Quartz - Calcite Vein	Chalcopyrite	Crystalline	5.2
PRS17	Quartz - Calcite Vein	Galena	Crystalline	1.1

Discussion of Results

The Kaapvaal Craton underlies the Bushveld Complex and the surrounding sedimentary successions including the Transvaal Supergroup. Sulphur isotope analyses of sulphides from eclogites and associated kimberlites on the Kaapvaal Craton yield $\delta^{34}S$ values of +0.2 to +2.1 ‰ (Tsai, 1979). This provides a viable range of $\delta^{34}S$ values for magmatic sulphides as they occur beneath the Kaapvaal Craton. In this study, sulphides with values within this range were obtained from the top of cores in the upper part of the Platreef on farms Macalacaskop and Turfspruit. Therefore the group of $\delta^{34}S$ values that have an average of +1.4‰ is suggested to be of magmatic origin and hence help to constrain a magmatic end member for the Platreef.

In the southern sector of the Platreef with increasing proximity towards the footwall contact these values increase from +1.4‰ to +5.2‰, which is seen clearly in Figure 4.5 where data are plotted against height above footwall contact. The only elevated $\delta^{34}S$ values more that 175m above the footwall contact are related to a hornfels raft. It is suggested that this increased $\delta^{34}S$ value towards the footwall contact reflects an increasing crustal contribution of sulphur close to the floor. In the southern sector the most likely source of crustal sulphur is from a Duitschland Formation footwall which has positive sulphur isotope values (this

study, Baker, 2005), whereas $\delta^{34}S$ values for other lithologies within the Transvaal Supergroup are generally negative (Cameron, 1982). This contamination probably occurred through the release of sulphur- and other volatile- and trace element-enriched fluids from the pyrite-rich shale during metamorphism to cordierite spinel hornfels which occurs as rafts in the southern sector of the Platreef.

In comparison to the southern sector of the Platreef, the sulphur isotope data from the northern sector is slightly different, with increased $\delta^{34}S$ values (average +6.4‰) being concentrated in the top half of the package rather than towards the footwall (Figure 4.8). In the 175 m closest to the footwall, there is a lower sulphur isotope contamination signature (average +3.3‰) which reflects the near-to-magmatic values that would characterize any sulphur that may have come from the granite footwall. As granites are typically low in sulphur, and there is little to no sulphur present in the lower half of the Platreef in PR-174 and PR-175 it is logical that very little crustal contamination is recorded in this part of the sequence.

In contrast, the increased sulphur isotope values towards the top of the Platreef appear to coincide with the presence of altered dolomite rafts in the upper Platreef in the area sampled, as well as the increased presence of sulphides. These dolomites are therefore the most likely source of crustal sulphur in this area of the Platreef, and this is supported by the $\delta^{34}S$ values obtained from calc-silicates which are similar to the higher $\delta^{34}S$ values from the more contaminated area of the package. It should be noted that although there is a presence of dolomite within core PR-175, there is none that is directly recorded in core PR-174. This is reflected in the slight difference in $\delta^{34}S$ values of the two cores. Core PR-174, which does not contain any dolomite, has slightly lower $\delta^{34}S$ values in the upper part of the Platreef ranging from +4.47 to +6.07‰. Core PR-175, which does contain altered dolomite xenoliths, shows a greater degree of crustal contamination within the upper part of the Platreef with $\delta^{34}S$ values ranging from +4.89 to 11.03‰.

When combined with data from previous work, Buchanan et al. (1981), Buchanan and Rouse (1984), Hulbert (1983), Liebenberg (1968), and Manyeruke (2003) the data from this study indicates a variation of contaminated $\delta^{34}S$ values for the Platreef along strike according to footwall composition (Figure 4.10). Where the footwall comprises quartzite, sulphur isotope values are approximately +3‰, whereas with a footwall of Duitschland Formation dolomites $\delta^{34}S$ values are approximately +5‰. In the central sector where the footwall is Malmani dolomites, sulphides have sulphur isotope values of +3‰ to +6‰. In the northern sector, where the footwall is granite, there is little evidence for contamination from the direct footwall in the lower part of the Platreef pyroxenites where $\delta^{34}S$ values are approximately +3‰. However in the upper portion of the Platreef on Farm Drenthe where dolomite rafts occur they have contributed crustal sulphur to the system, increasing sulphur isotope values to approximately +6‰. These dolomite rafts are believed to represent roof rocks from the Malmani Subgroup of the Transvaal Supergroup.

Sulphur isotope geothermometry conducted on a sulphide-bearing quartz-calcite vein (PRS-17) using coexisting sphalerite and galena yielded a temperature of formation of 403°C. This temperature is similar to temperatures obtained from the same sample through fluid inclusion studies (L. Zhitova, pers. comm). This vein material may represent a remnant of volatile-rich fluids that passed through the Platreef after its emplacement.

It is suggested that during metamorphism of sedimentary footwall and xenoliths by magma, volatiles, including sulphur, are released into the magma. These volatiles travel through the system, causing sulphur saturation and the formation of an immiscible sulphide liquid which re-crystallised any pre-existing magmatic sulphides. This external contribution of sulphur to the system is especially linked to the presence of xenoliths both in the north and south, and greater concentrations of sulphide mineralisation occur around these xenoliths. The magmatic sulphides which occur at the top of the core in the southern sector of the Platreef have not

been affected by these volatiles, unless they are close to a xenolith (core ATS-046) and hence retain their primary sulphur isotope signature. Equally the uncontaminated sulphides at the base of Platreef in the northern sector have not been affected by sulphur-carrying fluids, whereas the sulphides at the top of the package have. In order to further clarify whether pyritic shales or dolomites or both lithologies from the Duitschland Formation are the source of external sulphur within the southern sector of the Platreef multiple-sulphur isotope analysis was conducted on samples.

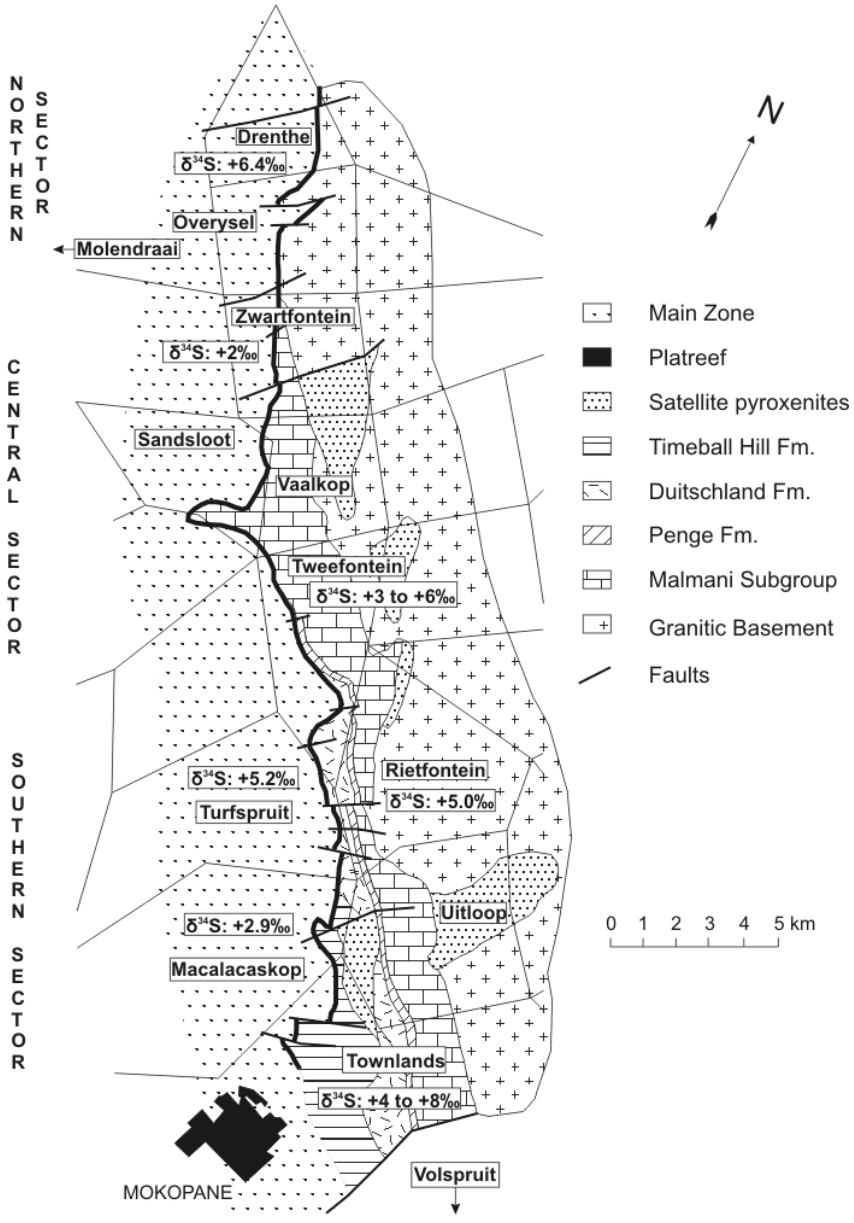

Figure 4.10: Geological map of the Platreef showing non-magmatic sulphur isotope data for Platreef. Data from Buchanan et al. (1981), Buchanan and Rouse (1984), Hulbert (1983), Liebenberg (1968), Manyeruke (2003) and this study.

CHAPTER FIVE
MULTIPLE SULPHUR ISOTOPE ANALYSES

Introduction

In order to confirm the initial observations of conventional sulphur isotope analyses, multiple sulphur isotope analyses were undertaken on samples from cores ATS-046, ATS-057, and ARF-08 from farms Turfspruit and Rietfontein. All of these cores are from the southern sector of the Platreef, and have a footwall comprising Duitschland Formation dolomites, and contain xenoliths of metamorphosed Duitschland Formation shales. Analyses were conducted on sulphide separates at the University of Maryland, United States of America.

Multiple Sulphur Isotope Theory and Concepts

An important aspect of sulphur isotope analysis is the study of mass-independent fractionation of sulphur. This process can be quantified by examining $\Delta^{33}S$ and $\Delta^{36}S$ which are defined as follows:

$$\Delta^{33}S = \delta^{33}S - 1000\,(\{1+\delta^{34}S/1000\}^{0.515} - 1)$$
$$\Delta^{36}S = \delta^{36}S - 1000\,(\{1+\delta^{36}S/1000\}^{1.91} - 1).$$

For the last 2 billion years, since the existence of a well oxygenated atmosphere, the behaviour of ^{33}S and ^{36}S has occurred dependent on mass, which would produce $\Delta^{33}S$ and $\Delta^{36}S$ values of close to zero (Figure 5.1). The earth's history is divided into three stages using $\Delta^{33}S$ signatures (Figure 5.1) (Farquhar & Wing, 2003). Stage I extends from before 3.8 Ga to 2.45 Ga and shows highly variable $\Delta^{33}S$. In Stage II, which extends from 2.45 to 2 Ga, there is a more subdued variation in $\Delta^{33}S$. Stage III has a very low variation (less than ±0.2‰) in $\Delta^{33}S$, and extends from 2 Ga to the present. The transition from Stage I to Stage II is thought to be due to a change in the Earth's atmospheric chemistry (Farquhar & Wing, 2003). Before 2 billion years ago, mass-independent fractionation of sulphur was believed to occur due to ultraviolet photolysis of sulphur in the Archaean atmosphere (Farquhar & Wing, 2003). The lack of oxygen, and hence ozone, in this time period allowed for ultraviolet rays to penetrate through to the Earth's atmosphere, causing mass independent fractionation.

Sulphur which has a magmatic source will not have undergone mass-independent fractionation, as it has not been exposed to any atmospheric processes (Farquhar & Wing, 2003).

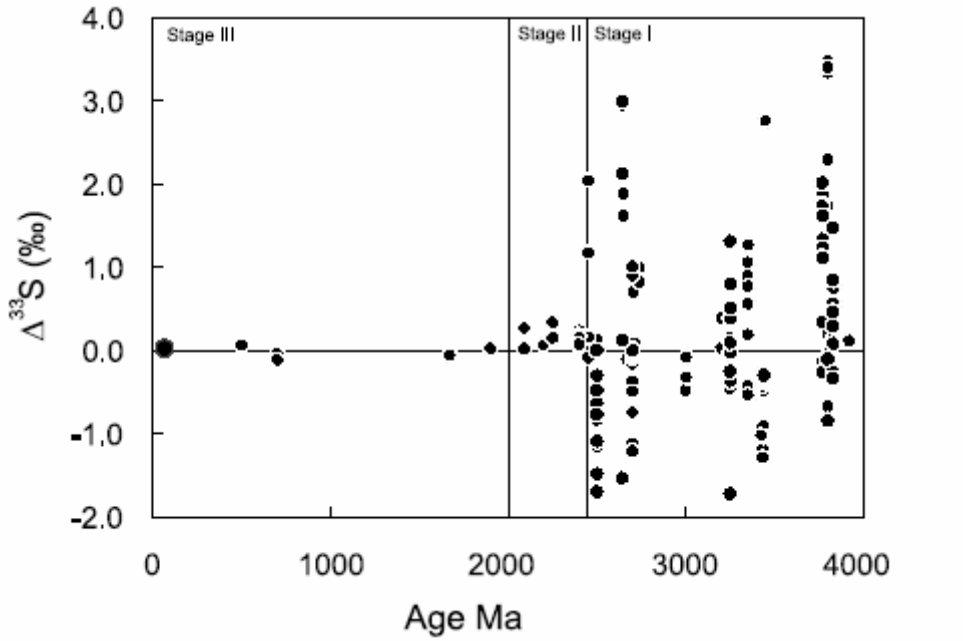

Figure 5.1: Plot of $\Delta^{33}S$ vs. age for terrestrial rocks containing atmospheric sulphur (Farquhar and Wing, 2003) showing highly variable $\Delta^{33}S$ in Stage I pre-2.45 Ga, Stage II showing slightly less $\Delta^{33}S$ variation, and Stage III, from 2 Ga onwards, showing no variation.

Previous Work

A detailed multiple sulphur isotope study has been conducted on the part of the Transvaal Supergroup covering the top of the Malmani Dolomites, the Penge and Duitschland Formations, and the bottom of the Timeball Hill Formation in the area of Farm Duitschland (Figure 5.2) (Baker, 2006). The Malmani dolomites are characterised by relatively high $\delta^{34}S$ (10 – 15‰) and high $\Delta^{33}S$ (1.0 – 2.8‰) (Figure 5.2), and the Penge Formation has relatively low $\delta^{34}S$ (5 - 6‰) and $\Delta^{33}S$ (0.1 – 0.2‰) values. There is a major break in both $\delta^{34}S$ and $\Delta^{33}S$ that has been identified between the Lower and Upper Duitschland Formations, with the Lower Duitschland having slightly raised $\delta^{34}S$ (3 - 10‰) and $\Delta^{33}S$ (0.5 – 1.5‰) values (Figure 5.2). In contrast the Upper Duitschland has high $\delta^{34}S$ values of approximately 15 - 40‰, but low $\Delta^{33}S$ values of 0 – 0.3‰. This indicates a major change in the Earth's atmosphere between the deposition of the Lower and Upper Duitschland Formations. It is unclear at this

stage if this change marks the shift between Stages II and III as proposed by Farquhar and Wing (2003), or is a localised shift that preceded the global atmospheric change. The Timeball Hill Formation has very negative $\delta^{34}S$ values of approximately -27 to -30‰, and low $\Delta^{33}S$ values of 0 – 0.2‰ (Baker, 2006).

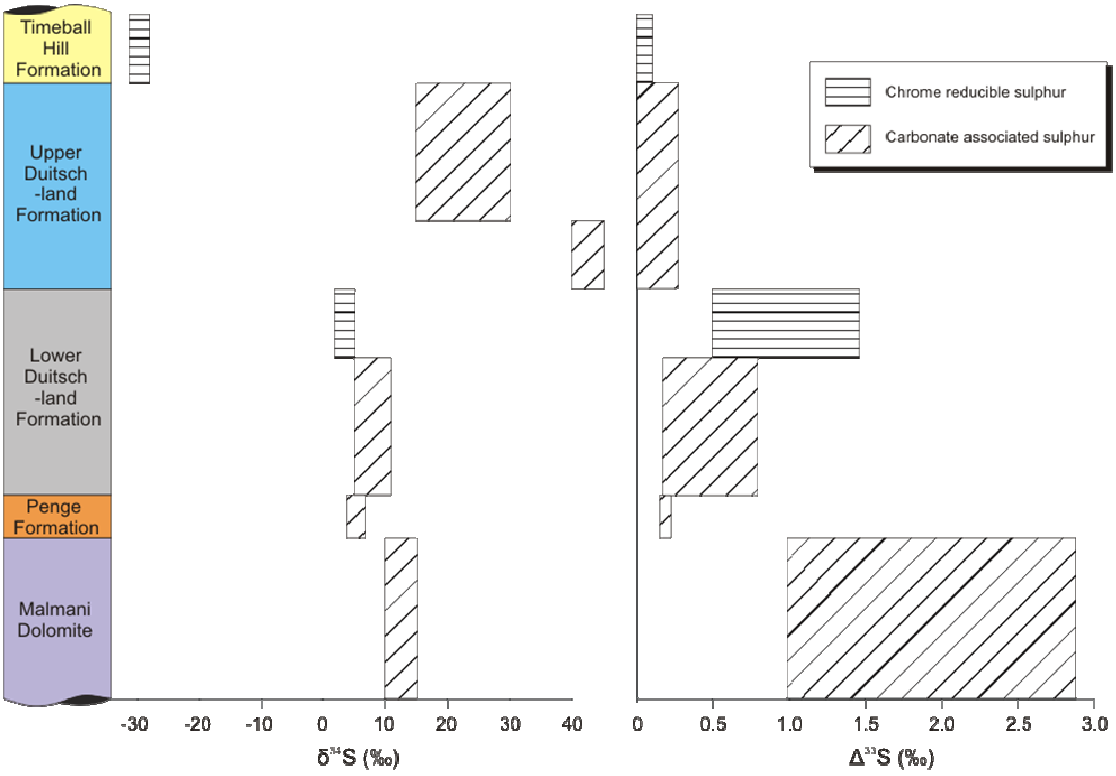

Figure 5.2: Diagram showing multiple sulphur isotope data for the Transvaal Supergroup against a simplified stratigraphic column, data from Baker (2006). 'Chrome reducible sulphur' refers to sulphur extracted from pure sulphide minerals, 'carbonate associated sulphur' refers to sulphur that is chemically extracted from carbonates before analysis.

Methodology

Sulphide mineral separates (pyrrhotite and chalcopyrite) were analysed from cores ATS-046, ATS-057 and ARF-08, all of which have a footwall of Duitschland Formation. Analyses were conducted at the University of Maryland in order to examine their $\Delta^{33}S$ and $\delta^{34}S$ values. Sulphur multiple isotope analyses followed the methods of Hu et al. (2003). Sulphides were converted to SF_6 by laser heating of separated sulphides in an F_2 atmosphere. The resulting SF_6 was purified first cryogenically and then with a gas chromatograph. Purified SF_6 was introduced to a ThermoFinnigan MAT 253 dual-inlet gas-source mass spectrometer where sulphur

isotope abundances were measured by monitoring the $^{32}SF_5^+$, $^{33}SF_5^+$, $^{34}SF_5^+$ ion beams at mass to charge ratio of m/z = 127, 128, and 129, respectively. All sulphur isotope data is reported relative to Cañon Diablo Troilite (CDT). The analytical precision is estimated to be ±0.12 ‰ for $\delta^{34}S$, and ±0.008‰ for $\Delta^{33}S$ based on the long term standard deviation between duplicates of an in-house pyrite standard (P1).

Results

The samples that were analysed for this study can be divided into three separate groups. Group I has low $\Delta^{33}S$ and $\delta^{34}S$ values (0.17 – 0.19‰ and 1.25 – 2.03‰ respectively), whereas Group II is characterised by relatively high $\delta^{34}S$ (4.84 - 6.43‰) and $\Delta^{33}S$ (0.41 - 0.57‰) values (Table 5.1, Figure 5.3). In contrast Group III has very low $\Delta^{33}S$ values (0.07 – 0.17‰) but very high $\delta^{34}S$ values (20.62 – 28.72‰) (Table 5.1, Figure 5.2).

Table 5.1: Multiple Sulphur Isotope Analyses on sulphides from three cores.

Sample Number	Rock Type	Mineral	Sulphide Texture	$\delta^{34}S$ (‰ CDT)	$\Delta^{33}S$ (‰ CDT)
ARF 08/49.26	Norite	Pyrrhotite	Fine grained disseminated	4.84	0.45
ARF 08/124.64	Massive Sulphide	Pyrrhotite	Massive Sulphide	5.17	0.46
ARF 08/124.64	Massive Sulphide	Pyrrhotite	Massive Sulphide	6.43	0.53
ARF 08/129.78	Norite	Pyrrhotite	Medium to coarse grained blebs	5.30	0.47
ATS 46/60.34	Pegmatoidal Norite	Chalcopyrite	Coarse grained bleb	2.03	0.19
ATS 46/461.21	Feldspathic Pyroxenite	Pyrrhotite	Medium-grained interstitial	5.22	0.41
ATS 57/72.48	Pyroxenite	Pyrrhotite	Coarse grained bleb	1.25	0.17
ATS 57/219.26	Pyroxenite	Pyrrhotite	Net-textured	5.30	0.47
ATS 57/221.39	Massive Sulphide / Pyroxenite	Chalcopyrite	Massive Sulphide	6.32	0.57
ATS 57/221.39	Massive Sulphide / Pyroxenite	Pyrrhotite	Massive Sulphide	5.49	0.56
ATS 57/325.25	Calc-Silicate	Pyrrhotite	Coarse grained bleb	28.72	0.07
ATS 57/335.07	Calc-Silicate	Pyrite	Fine grained disseminated	20.62	0.17

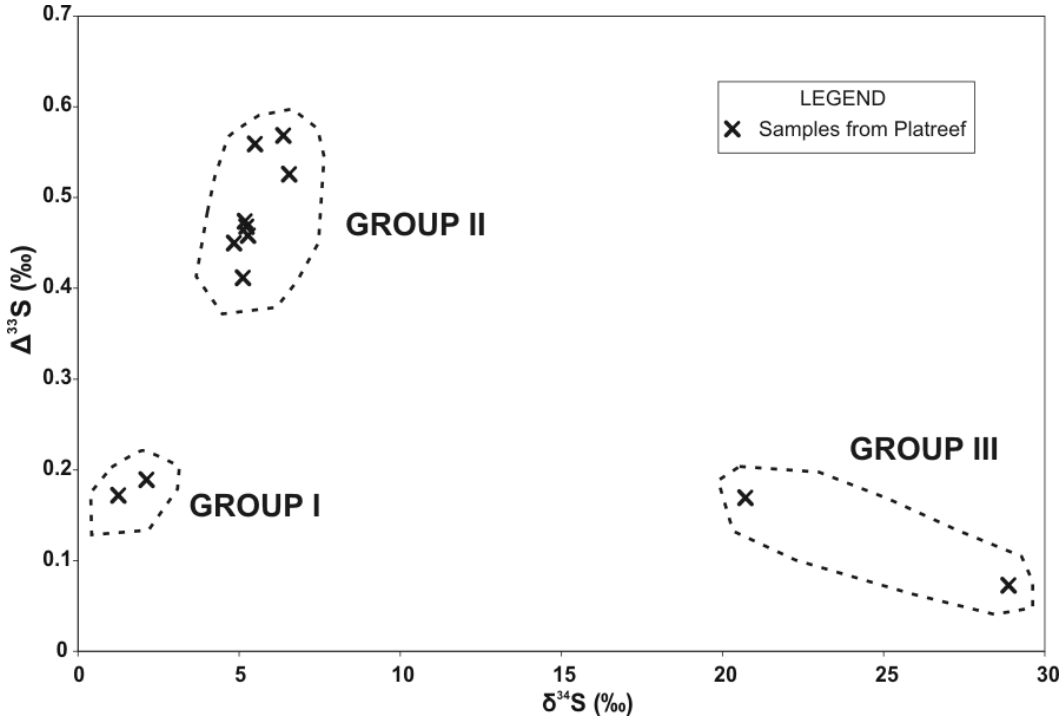

Figure 5.3: Diagram showing multiple sulphur isotope data from this study, as well as the grouping of the data.

Discussion of Results

Analysis of the mass-independent fraction of sulphur isotopes supports the interpretation of the sulphur isotope data that external sulphur has been added to the Platreef from sedimentary floor rocks and xenoliths. The low $\delta^{34}S$ and $\Delta^{33}S$ values of Group I are indicative of a close-to-magmatic source for the sulphur that formed these sulphide minerals. The samples which comprise this group are all taken from the Platreef more than 175m from the footwall. Non-zero $\Delta^{33}S$ values in Group II indicate that the sulphur within these sulphides does not have a wholly mantle origin. The measured $\Delta^{33}S$ values are all greater than 0.4‰, and when both $\Delta^{33}S$ and $\delta^{34}S$ values are compared to those of the Duitschland Formation (Figure 5.2), the source of the crustal sulphur is consistent with a source from the Lower Duitschland Formation (Figure 5.4). The most likely source of this sulphur was probably originally pyrite in organic-rich shales. It is proposed that this sulphur would have originally started out in elemental sulphur aerosols, and would have ended up in the pyrites after being reduced to H_2S (aq), either abiotically or by bacteria that metabolised elemental sulphur (Farquhar et al., 2000). When plotted with data from the Duitschland Formation of Baker (2006) (Figure 5.2), the Group III sulphides appear to have a

major sulphur contribution from the Upper Duitschland Formation (Figure 5.4). These sulphides were sampled from calc-silicates which comprise the direct metamorphosed footwall of the Platreef in the relevant cores.

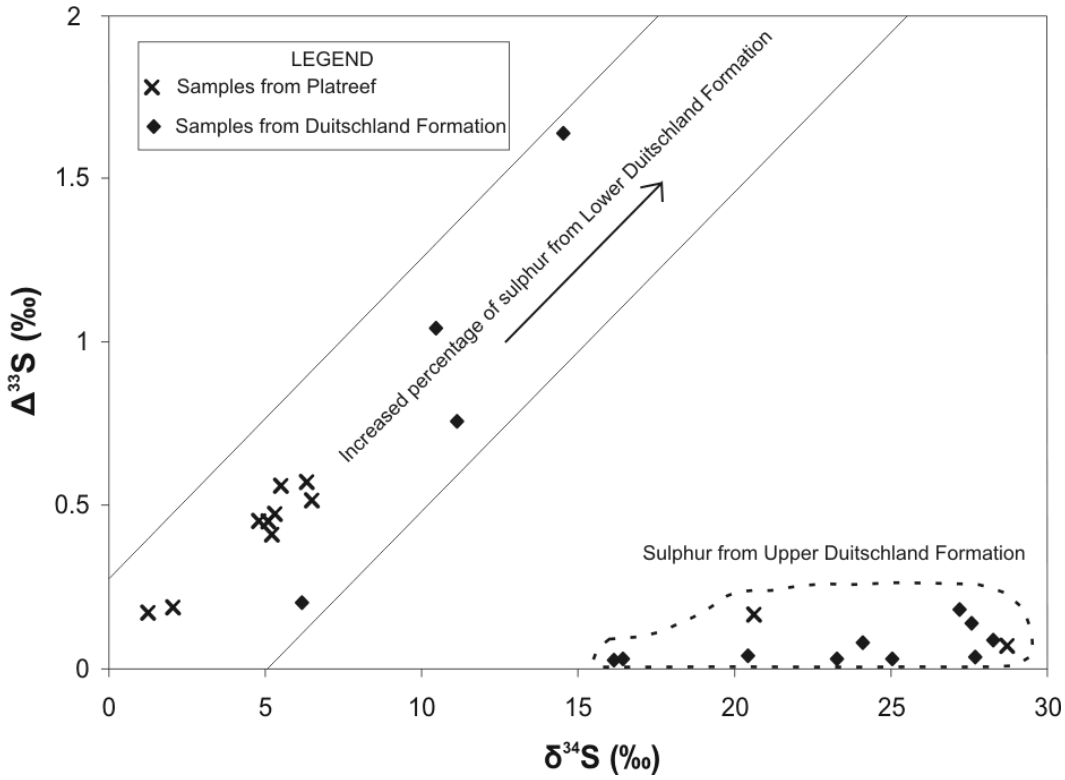

Figure 5.4: Diagram plotting $\delta^{34}S$ vs. $\Delta^{33}S$ for both the Platreef (this study), and the Upper and Lower Duitschland Formations (Baker, 2006).

When combined, this data indicates that the contamination in the southern Platreef has come from pyritic shales of the Lower Duitschland Formation, and as is indicated by conventional sulphur isotope analyses, decreases away from the footwall. However, the remnant footwall in this area is predominantly Upper Duitschland Formation dolomites, not Lower Duitschland Formation as implied from $\delta^{34}S$ isotope data.

In order to investigate further the local variation of contamination within the Platreef depending on changing footwall and sedimentary xenoliths another isotope system was used. Oxygen isotope analysis is based on similar principles to those for sulphur isotope analysis and also allows for the extent of crustal contamination within a magmatic system to be assessed. Samples from the southern sector were therefore examined using this method, and data was compared to that of previous studies (Harris and Chaumba, 2001; Pronost, 2005).

CHAPTER SIX
OXYGEN ISOTOPE ANALYSES

Introduction

Oxygen isotopes provide another geochemical method of tracing possible crustal contamination within igneous systems, with similar basic principles to those of sulphur isotope analyses. They were also conducted to compare oxygen isotope data from the southern sector of the Platreef with pre-existing data from the central sector of the Platreef (Harris and Chaumba, 2001). Silicate separates were extracted from three cores (AMK021 from Farm Macalacaskop, and ATS046 and ITS033 from Farm Turfspruit) in order to compare $\delta^{18}O$ values with depth through the Platreef as well as possible variations with different footwalls. Samples were chosen on the same basis as that of the samples chosen for sulphur isotope analyses, in that samples from core ITS033 with a Duitschland Formation footwall were selected as possibly having no crustal contamination. Samples from core AMK021 were chosen for analysis to reflect a footwall of Timeball Hill Formation, and core ATS046 was sampled as it has a footwall of Duitschland Formation. Silicate separates that were analysed were plagioclase, pyroxene, cordierite, and calc-silicate, and they were analysed at the University of Cape Town, South Africa.

Oxygen Isotope Theory and Concepts

There are three stable isotopes of oxygen, ^{16}O, ^{17}O, and ^{18}O, of which ^{16}O is the most abundant (99.763%), followed by ^{18}O (0.1995%), with ^{17}O being the least abundant (0.0375%). Due to this, the $^{18}O/^{16}O$ ratio is used in isotopic studies, and expressed as $\delta^{18}O$ in percent per mil, which is represented by the following formula:

$$\delta^{18}O‰ = [(^{18}O/^{16}O_{(sample)} - {}^{18}O/^{16}O_{(standard)})/ {}^{18}O/^{16}O_{(standard)}] \times 1000.$$

The standard which is used in this study is the Standard Mean Ocean Water (SMOW), which is distributed by the Atomic Energy Agency in Vienna.

In nature, $\delta^{18}O$ varies greatly depending on the processes involved, with most variation occurring in meteoric water. Chondrite meteorites and the mantle have $\delta^{18}O$ values close to +5.7 ‰, whereas granites, metamorphic rocks, and sediments are isotopically enriched in $\delta^{18}O$ compared to the mantle (Rollinson, 1993).

One of the most common uses of oxygen isotope data in co-existing mineral pairs is that of geothermometry. This is determined using the equation:

$$1000 \ln \alpha_{\text{mineral 1 – mineral 2}} = A(10^6/T^2) + B$$

whereby A and B are experimentally determined for particular mineral pairs, and where B usually equals zero. Another useful relationship is that the difference of $\delta^{18}O$ between minerals (expressed as $\Delta_{\text{mineral 1 – mineral 2}} = \delta^{18}O_{\text{mineral 1}} - \delta^{18}O_{\text{mineral 2}}$) is approximately equal to $1000 \ln \alpha_{\text{mineral 1 – mineral 2}}$ (Note: this is only applicable for δ values less than 10). Therefore the temperature of formation of co-existing mineral pairs can be determined using their $\delta^{18}O$ values.

Previous Work

Oxygen isotope work has been conducted both on the Platreef (Harris and Chaumba, 2001) and the main Bushveld (Schiffries and Rye, 1989; Reid et al., 1993; Harris et al., 2005). Schiffries and Rye (1989) analysed mineral separates taken from the eastern limb of the Bushveld Complex and sampled from each of the zones within the Rustenburg Layered Suite (RLS). Average $\delta^{18}O$ values showed little variation either laterally through the intrusion or with depth. The authors recorded that $\delta^{18}O$ values from mineral separates within the Bushveld are "heavier" than the values expected for a basaltic magma of +5.7‰ (Rollinson, 1993), with $\delta^{18}O$ values for plagioclase varying from +6.8 to +7.7‰, and for orthopyroxenes varying from +6.1 to +7.0‰. The differences between $\delta^{18}O_{plag}$ and $\delta^{18}O_{opx}$ ($\Delta^{18}O_{plag\text{-}opx}$) however are generally small (~0.5), and are typical of magmatic systems. Sedimentary rock samples taken from the Transvaal Supergroup showed a variety of $\delta^{18}O$ values, with 9 to 11‰ for quartzites, 11 to 15‰ for pelites, and 19 to 21‰ for carbonates (Schiffries and Rye, 1989). This

data suggests that the magmas which formed the Bushveld Complex were contaminated before emplacement, and that the magma was well mixed. The slightly elevated $\delta^{18}O$ values could be attributed to the assimilation of Transvaal Supergroup rocks into the magma with 10 – 29% contamination.

Reid et al. (1993) examined samples taken from boreholes that intersected a pothole formed in the Merensky Reef of the Western Limb of the Bushveld Complex. They found that their $\delta^{18}O$ data agreed well with those of Schiffries and Rye (1989), with $\delta^{18}O_{plag}$ values of approximately +7.1‰, and $\delta^{18}O_{opx}$ values of approximately +6.6‰ and no variation with depth observed. They also recorded a $\Delta^{18}O_{plag\text{-}opx} = 0.5$, which is also in agreement with Schiffries and Rye (1989).

These observations were supported by Harris et al. (2005) who also found slightly elevated $\delta^{18}O$ values within the RLS of the Bushveld Complex, and no stratigraphic variation. This is thought to indicate that Bushveld Complex magmas were contaminated before emplacement, supporting the staging chamber hypothesis. However, the most likely contaminant is suggested to be the middle to lower crust, and not Transvaal Supergroup rocks as previously proposed. This is also supported by a Sr-Nd isotope study conducted by Maier et al. (2000).

Harris and Chaumba (2001) conducted stable isotope studies on mineral separates taken from the Sandsloot Mine in the Northern Limb. Pyroxene and plagioclase from the Main and Upper Zones of the Northern Limb both showed little variation of $\delta^{18}O$, with plagioclase having values of +7.0 to +8.3‰ (from 18 samples), and pyroxene having values of +6.1 to +7.6‰. The authors also noted a slight decrease of $\delta^{18}O$ values with increased stratigraphic height, which is probably a function of changing mineralogy.

However according to Harris and Chaumba (2001), samples from the Platreef itself show considerable variation in plagioclase and pyroxene $\delta^{18}O$ values. The plagioclase and pyroxene from the Platreef have higher $\delta^{18}O$ values than those

from the Upper and Main Zone which the authors attribute to crustal contamination. Another feature is that many of the samples are not in oxygen isotope equilibrium at magmatic temperatures which is attributed to water-rock interaction. Carbonate samples from the Platreef show a wide range of $\delta^{18}O$ values with samples varying from +6.9 to +25.5‰, which can be caused by decarbonation during metamorphism. However, samples from footwall dolomites have $\delta^{18}O$ values of 19-24‰ (Harris and Chaumba, 2001).

From this data the authors conclude that a degree of assimilation (up to 18%) of Transvaal rocks had occurred as indicated by the high $\delta^{18}O$ values recorded. These high $\delta^{18}O$ values have been attributed to the assimilation of Malmani dolomites which comprise the footwall of the Platreef on Farm Sandsloot. The possibility of lower crustal material causing the contamination is dismissed by the authors as published $\delta^{18}O$ values for the lower crust on the Kaapvaal Craton as exposed by the Vredefort impact structure are approximately 8.7‰ (La Grange et al, 2000). This would mean that 44% contamination would have to occur to cause the increased $\delta^{18}O$ values seen in the Platreef, which is highly unlikely. It is noted that this contamination is only observed within the Platreef, and is not seen in any of the other units that comprise the Northern Limb of the Bushveld Complex, or in the Bushveld as a whole. The authors also note that due to the lack of variation in the $\delta^{18}O$ values for the Bushveld as a whole, and the Northern Limb itself, that contamination probably occurred in a staging chamber, and when it intruded it was well mixed.

Methodology

Samples were chosen for oxygen isotope analysis from different depths and lithologies within the cores from the southern sector of the Platreef, in order to examine both variations with depth, and with different footwalls and proximity to hornfels rafts. Samples were crushed and sieved and the +125 μm fraction was then washed and dried. From this fraction, silicate separates were hand picked,

pyroxene and plagioclase in the case of most samples, cordierite from the hornfels, and calc-silicates from the footwall of AMK-021 and ATS-046.

These silicate separates were then crushed to a fine powder, and placed in an oven at approximately 50°C to dry. Once dry, the sample was weighed out (~10 mg) and placed in a nickel reaction vessel (inside diameter ~ 12 mm) which is over pressurised above atmosphere by dry nitrogen (Vennemann and Smith, 1990). The extraction line consisted of ten reaction vessels, of which eight were used for samples, and two for standards (Harris and Erlank, 1992). The silicates were then degassed under a vacuum on conventional silicate lines at 200°C for a minimum of two hours (Harris et al. 2005). After degassing, the minerals were reacted with seven times the stoichiometric amount of CIF_3 at a temperature of 550°C. The resultant O_2 was converted to CO_2 using a hot platinised carbon rod. The pressure of the sample is then measured with a manometer in order to approximate the yield of CO_2 from the original sample. Finally the gas is collected and sealed into a glass tube in preparation for analyses in the Mass Spectrometer.

The stable isotope ratios are then measured using a Finnigan MAT252 Mass Spectrometer and reported as $\delta^{18}O$. An internal standard of Murchison Line Quartz (MQ) was used, and the average value of MQ was used to normalise the raw data to the SMOW scale (Harris et al, 2005).

Results

In the Platreef, some small variations of oxygen isotope data occur according to height above the footwall (Figure 6.1). Recorded $\delta^{18}O$ values varying from +6‰ to +9‰ for plagioclase, and +6.5‰ to +8.5‰ for pyroxene (Table 6.1). Cordierite from hornfels rafts showed slightly higher $\delta^{18}O$ values with a maximum of +11.5‰ (AMK021/393.33, ATS046/207.25), whereas a calc-silicate from the direct footwall (ATS046/496.25) had a similar $\delta^{18}O$ to the Platreef itself (+8‰). The $\Delta_{plag\text{-}opx}$ values recorded by this study show a large variation from -1.48 to +2.41 (Table 6.1).

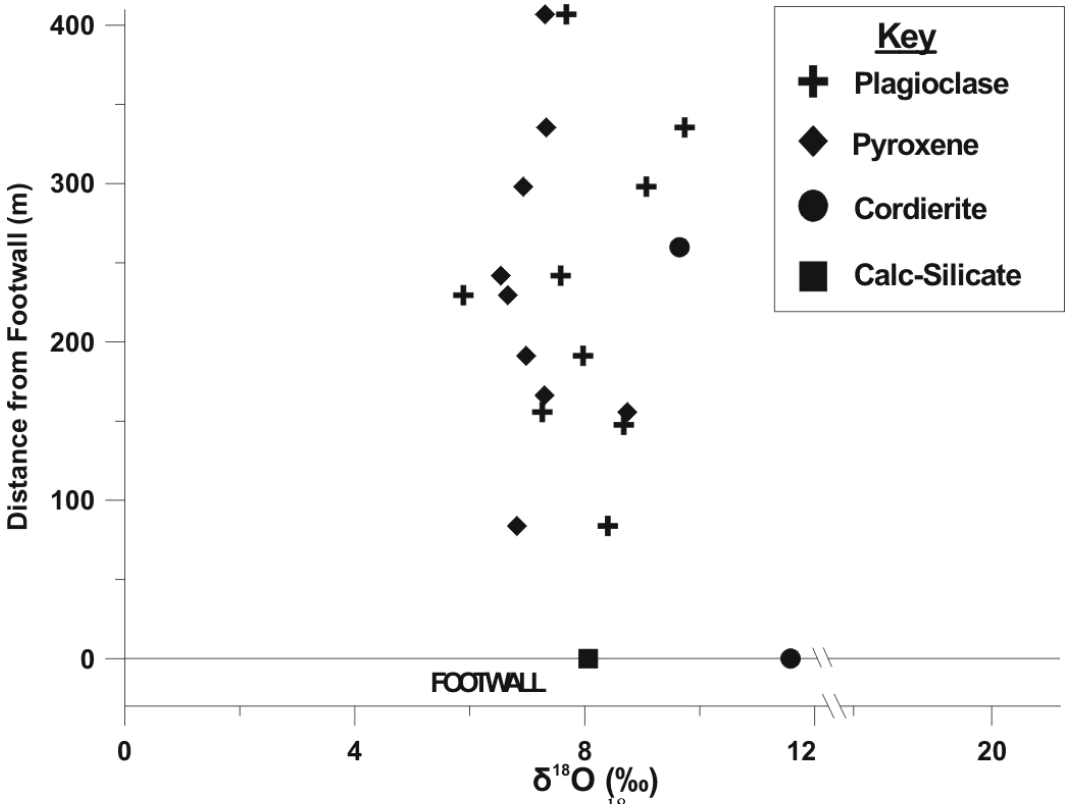

Figure 6.1: Diagram showing variation of $\delta^{18}O$ with depth and distance from footwall, as well as $\delta^{18}O$ values for footwall material that was analysed.

Table 6.1: Details of all oxygen isotope analyses for this study (‰, V-SMOW), as well as the difference between $\delta^{18}O_{plag}$ and $\delta^{18}O_{opx}$ analyses ($\Delta_{plag\text{-}opx}$). (Note: plag = plagioclase, opx = orthopyroxene, cord = cordierite, calc-sil. = calc-silicate.)

Sample No.	Rock Type	$\delta^{18}O_{plag.}$	$\delta^{18}O_{opx.}$	$\delta^{18}O_{cord.}$	$\delta^{18}O_{calc\text{-}sil.}$	$\Delta^{18}O_{plag\text{-}opx}$
AMK021/90.25	Spotted Anorthosite	9.1	6.9			2.2
AMK021/222.06	Serpentinite		7.3			
AMK021/232.62	Pyroxenite	7.3	8.7			-1.4
AMK021/240.62	Pyroxenite	8.7				
AMK021/393.33	Metamorphosed Quartzite			11.6		
ATS046/60.19	Norite - Leuconorite	7.7	7.3			0.4
ATS046/131.64	Feldspathic Pyroxenite	9.7	7.3			2.4
ATS046/207.25	Hornfels			9.7		
ATS046/275.80	Olivine. Feldspathic Pyroxenite	8.0	7.0			1.0
ATS046/383.23	Feldspathic Pyroxenite - Pyroxenite	8.4	6.8			1.6
ATS046/496.25	Calc Silicate				8.1	
ITS033/241.16	Feldspathic Pyroxenite	7.6	6.5			1.1
ITS033/253.44	Pyroxenite	5.9	6.7			-0.8

Oxygen isotope geothermometry was calculated using the oxygen isotopes of plagioclase – pyroxene pairs. The crystallisation temperature of the silicates varied from 629°C to 867°C (Table 6.2), with the higher temperatures being recorded in samples with low or negative $\Delta^{18}O_{plag\text{-}px}$ values.

Table 6.2: Results of Oxygen Isotope Geothermometry on samples with plagioclase – pyroxene pairs.

Sample Number	$\delta^{18}O_{plag.}$	$\delta^{18}O_{opx.}$	T (K)	T (°C)
AMK021/90.25	9.07	6.93	908	635
AMK021/232.62	7.26	8.74	1140	867
ATS046/60.19	7.68	7.31	1014	741
ATS046/131.64	9.74	7.33	902	629
ATS046/275.80	7.97	6.98	973	700
ATS046/383.23	8.4	6.82	936	663
ITS033/241.16	7.58	6.54	965	692
ITS033/253.44	5.89	6.66	1105	832

Discussion of Results

The $\delta^{18}O$ data from this study agrees in general with that of previous studies (Harris and Chaumba, 2001, Harris et al., 2005, Reid et al., 1993, Schiffries and Rye, 1989). These data sets vary from a typical mantle value of +5.7‰. This might suggest the presence of crustal oxygen within the northern limb. However, in contrast to the sulphur isotope data, there is little variation with depth through the entire sequence, especially. This might be expected however as oxygen is a major element, and sulphur is a trace element. A small amount of influx of sulphur from a sedimentary source will be noticeable, but 5‰ contamination of a magma with a $\delta^{18}O$ of 7‰ by a hornfels with a $\delta^{18}O$ of 10‰ will not make a noticeable difference. It is however important to note that the Platreef pyroxenites in contact with shale/quartzite have slightly higher $\delta^{18}O$ values than the RLS in general, and are also different to those recorded at Sandsloot (Harris and Chaumba, 2001; Pronost, 2005) (Figure 6.2). This data indicates that either a greater degree of crustal contamination at Sandsloot, or that the contaminants at Sandsloot have higher $\delta^{18}O$ values. Here, it is suggested that the latter of these two possibilities is the more likely, because $\delta^{18}O$ values for the Malmani dolomite

footwall at Sandsloot are much higher than the $\delta^{18}O$ values for hornfels xenoliths and quartzite footwall in the southern sector of the Platreef.

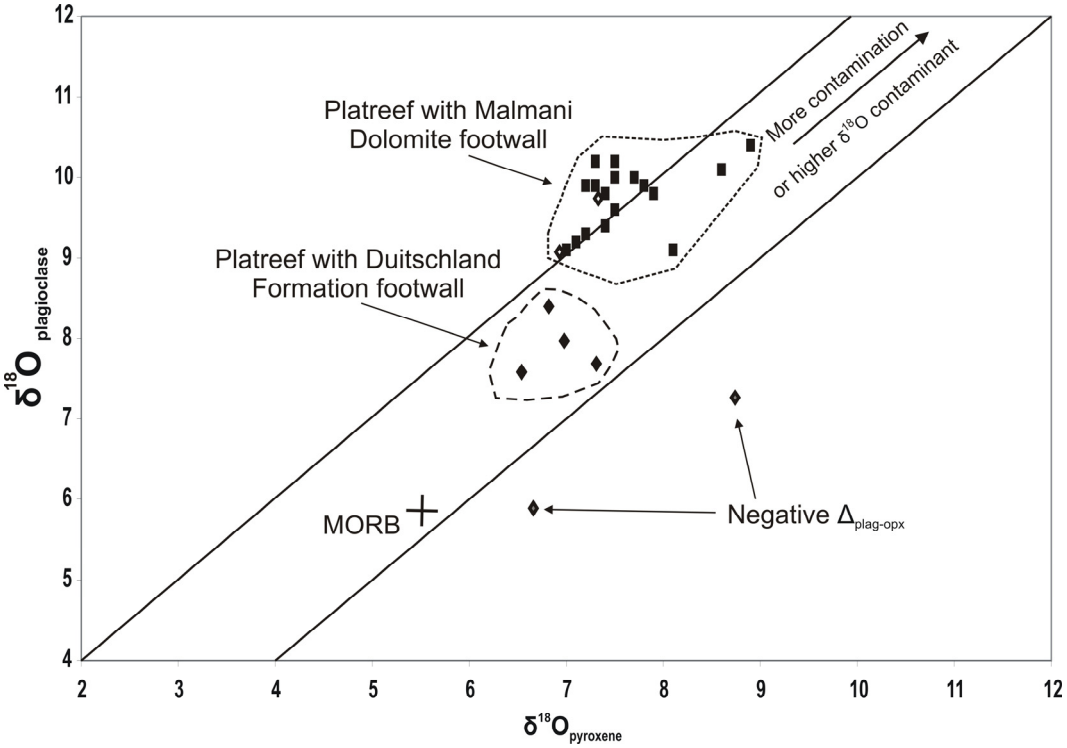

Figure 6.2: Diagram showing different oxygen isotope data for different sectors of the Platreef. Data for Platreef with Malmani dolomite footwall from Harris and Chaumba (2003) and Pronost (2005).

Previous authors (Schiffries and Rye, 1989; Reid et al. 1993) have recorded $\Delta^{18}O_{plag\text{-}px}$ values of approximately +0.5‰; indicating that silicate minerals from the Bushveld Complex formed through magmatic processes. These authors suggest that these $\Delta^{18}O_{plag\text{-}px}$ values coupled with non-mantle $\delta^{18}O$ values indicate that contamination of the magma occurred pre-intrusion, probably in a staging chamber. However, the $\Delta^{18}O_{plag\text{-}opx}$ values recorded in this study do not completely support the interpretation that the silicate minerals in the Platreef were formed purely through magmatic processes. Data presented in this study suggests that some sub-solidus re-equilibration has occurred. This may be due to deuteric fluids moving through the northern limb in the final stages of its formation and possibly causing the re-crystallisation of certain silicate minerals. For example this may be the result of a granitic component flushing through the system, which is now represented in the Platreef as quartzo-feldspathic veins (Hutchinson and

Kinnaird, 2005). This fluid is probably related to the volatile-rich fluid that assisted in the formation of the sulphides within the Platreef. This interpretation is supported by oxygen isotope geothermometry with the temperature range of 629 - 867°C being general too low for silicates to have been formed entirely through normal magmatic crystallization.

CHAPTER SEVEN
DISCUSSION AND CONCLUSIONS

Introduction

The main aim of this study was to determine the method of formation of sulphide minerals within the Platreef, of the Northern Limb of the Bushveld Complex. If it was determined that there was an external source of sulphur which led to the formation of these sulphide minerals, this source was also to be located. For this purpose the main evidence for external sources of sulphur compared to a magmatic source of sulphur should be presented before discussing the results of this study.

Discussion

There are three main lines of evidence which can indicate that an external source of sulphur is involved in the formation of sulphide mineral deposits (Naldrett, 2004):

The first, and most conclusive, line of evidence is the non-mantle isotopic composition of sulphur. As discussed in Chapter Four, sulphur that has its origin within the mantle will have $\delta^{34}S$ values of approximately zero (-2 to +2‰). However if sulphur from an external source has been added to the system the $\delta^{34}S$ values will be more positive or negative than this mantle, or magmatic range.

The second line of evidence is the association of sulphides within a magmatic intrusion with inclusions or xenoliths of country rock: specifically if the country rock is rich in sulphur, for example evaporites, sulphur-rich dolomites, or pyritic shales. This provides a viable source for the external sulphur.

The third line of evidence is based on experimental data which indicates that magmas are able to dissolve more sulphur as they rise to the surface (Figure 7.1).

Therefore unless the magma acquires sulphur from the rocks that it passes through it will move further away from the point of sulphur saturation as the pressure decreases. With this evidence in mind, the results from this study can be examined to determine how the sulphide minerals of the Platreef formed.

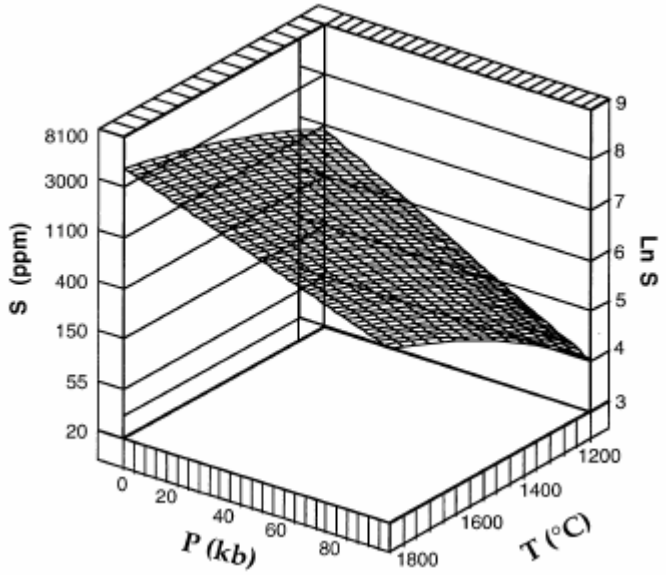

Figure 7.1: Sulphur contents at sulphide saturation in synthetic basalt vs. pressure and temperature (Mavrogenes and O'Neill, 1999).

The different components of this study, when synthesised present a clear picture with regards to the formation of sulphide mineralisation within the Platreef, and the importance of the varying footwall in this area of the Bushveld Complex. An initial comparison of the southern and northern sectors based on their sulphide mineralogy indicates very different processes. In the southern sector the sulphide mineralisation is generally concentrated in the base of the Platreef, whereas in the northern sector it is focussed in the top half of the cores sampled. However, there is a close correlation between the occurrences of sulphide mineralisation and the occurrence of metasedimentary xenoliths.

Southern Sector of the Platreef

In the southern sector of the Platreef, the footwall is predominantly comprised of sedimentary rocks from the Duitschland Formation. These have been

metamorphosed during the emplacement of the Platreef, and the Platreef itself contains altered xenoliths of these footwall lithologies. Importantly however, the xenoliths which generally occur within the lower part of the Platreef are dominantly cordierite-spinel hornfels, which are probably metamorphosed shales, whereas the footwall in the same core comprises calc-silicate skarns which have a dolomite protolith.

The occurrences of sulphide mineralisation within the southern sector of the Platreef also appear to be focussed in the lower half of the package, although in core ATS-046 there is a concentration of sulphides within the top portion of the core related to the presence of a hornfels raft (Figure 7.2). It is therefore apparent that the occurrence of sulphides is intimately linked to the presence of metasedimentary material, whether in proximity to xenoliths, or close to the basal contact with the footwall.

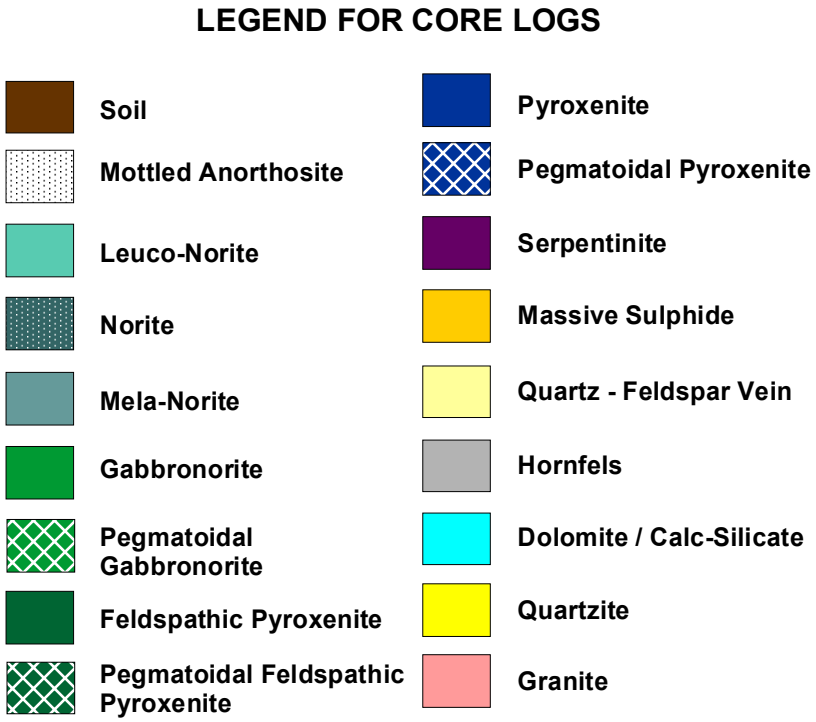

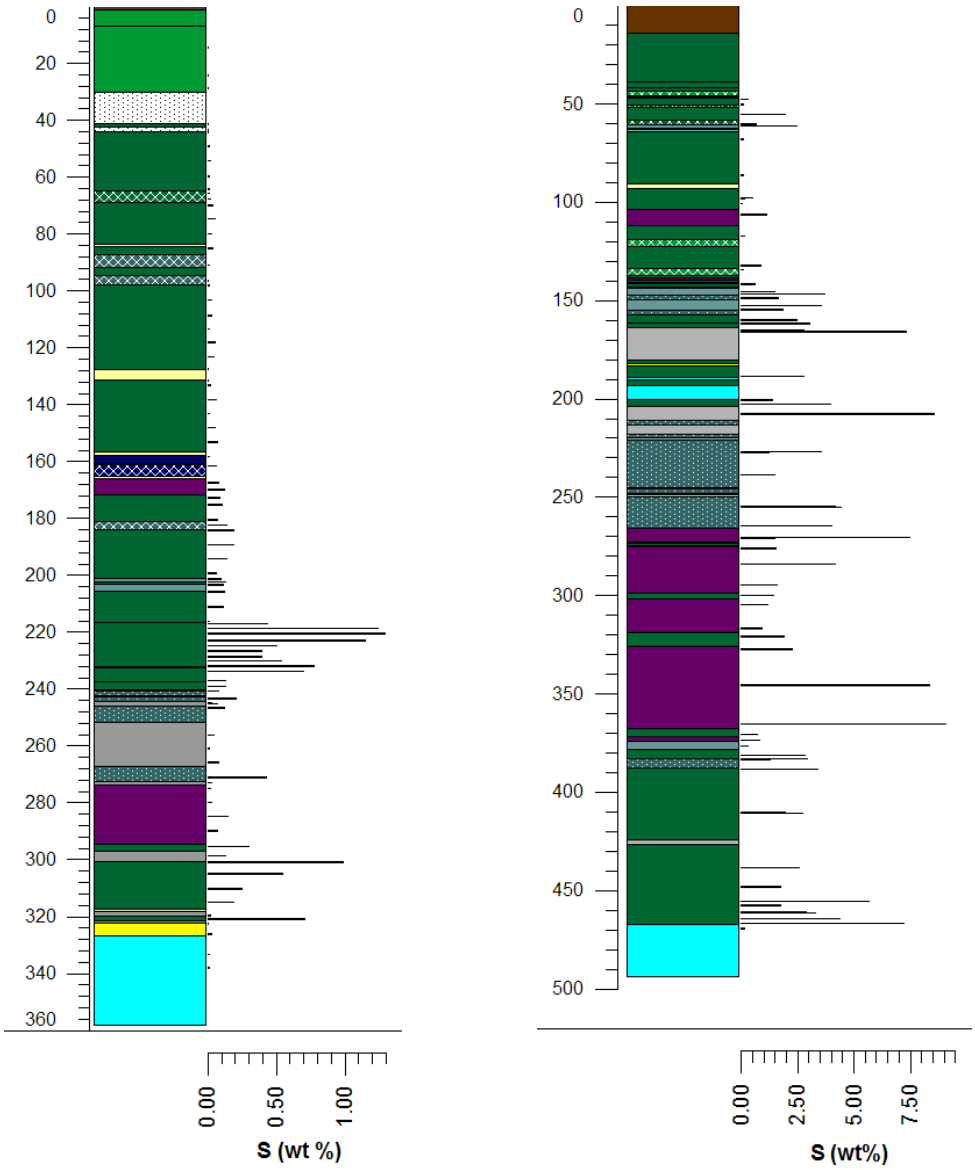

Figure 7.2: Core logs and sulphur concentration (wt%) of cores ATS-57 and ATS-46 respectively.

This observation of a close relationship between sulphide abundance and metasedimentary lithology occurrence is further supported by the sulphur isotope data. The sulphur isotope analyses from the southern sector where the footwall is Duitschland Formation can be divided into two groups, one of which has $\delta^{34}S$ values which are close to magmatic (average of +1.4‰), and another which has $\delta^{34}S$ values which indicate contamination by an external source (average of +5.1‰) (Figure 7.3). This 'contaminated' section of the Platreef is focussed in the bottom 175m of the package, again associated with the presence of footwall material. It is also important to note that some increased $\delta^{34}S$ values are seen in

core ATS-046 higher up in the package. These are found in the sulphides associated with a hornfels raft at ~180 m depth (Figure 7.3). The more magmatic sulphur isotopes occur at the top of the package away from any footwall material. Sulphides analysed from footwall lithologies have a variation in sulphur isotope values. Pyritic-bearing hornfels rafts from within the Platreef have $\delta^{34}S$ values of between +5.2 and +9.7‰. Footwall calc-silicates have heavier sulphur isotope values of approximately +16‰, although they can have $\delta^{34}S$ values of up to +29‰ (Figure 7.3).

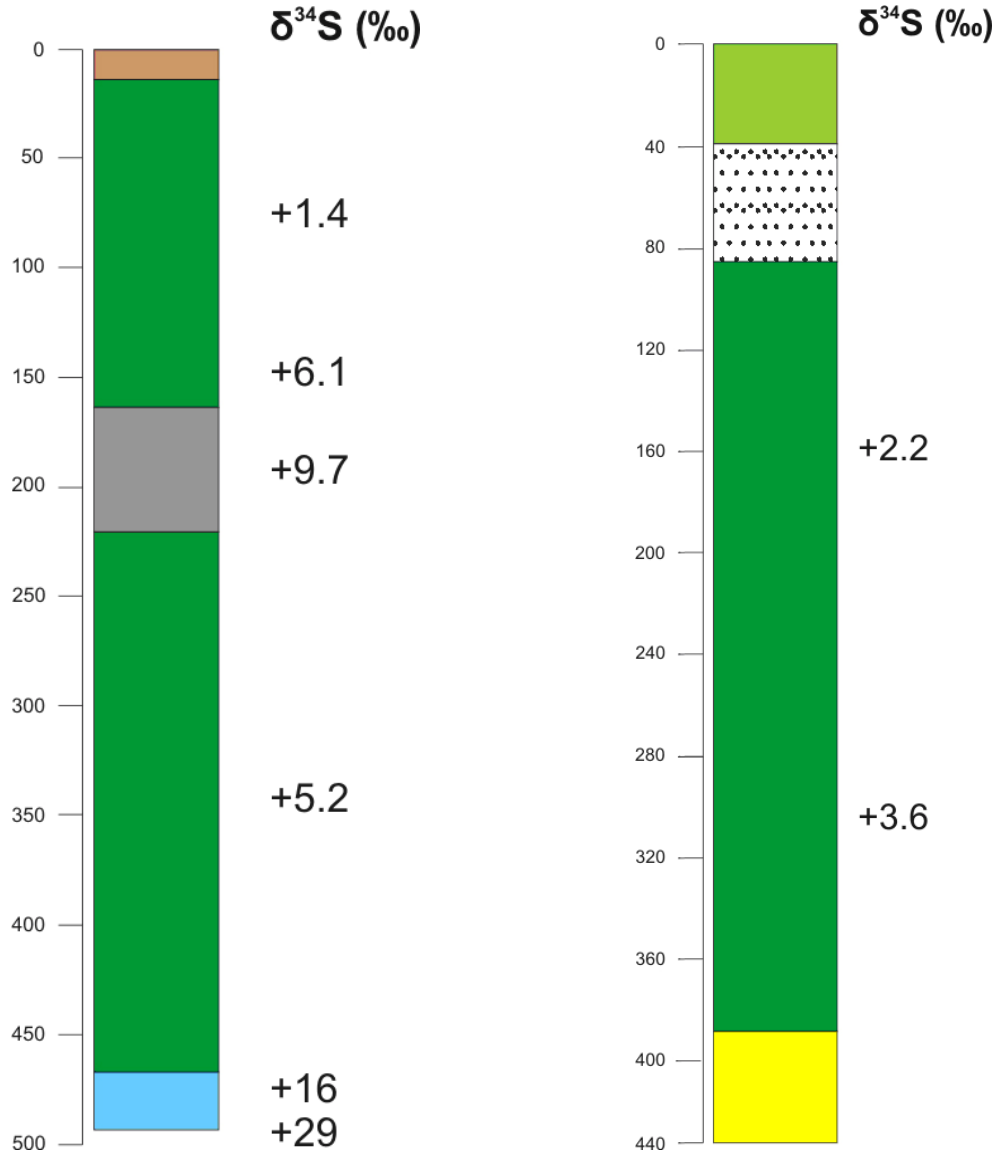

Figure 7.3: Generalised core logs for the southern sector of the Platreef with an Upper Duitschland Formation and Timeball Hill Formation (respectively) showing average sulphur isotope values for different parts of the Platreef package.

In core AMK-021 from Farm Macalacaskop, where the footwall lithology is Timeball Hill Formation quartzites, the extent of the contamination from footwall material is not as pronounced with $\delta^{34}S$ values averaging +2.9‰. It should be noted that a slight decrease from +3.6‰ to +2.2‰ is observed with increasing height above the footwall (Figure 7.3). Sulphide concentrations are again associated with the presence of footwall material and sulphur isotope values for these sulphides show a greater contribution of sulphur from an external source. This indicates the importance of the presence of footwall in the formation of sulphide mineralisation, supporting the observations made in cores where the footwall is Duitschland Formation.

When multiple sulphur isotopes are examined in conjunction with these observations the source of the crustal sulphur within the Platreef can be constrained further. Analyses of samples from core with a footwall of Duitschland Formation can be divided into three separate groups. Group I has low $\Delta^{33}S$ and $\delta^{34}S$ values (0.17 – 0.19‰ and 1.25 – 2.03‰ respectively), whereas Group II is characterised by relatively high $\delta^{34}S$ (4.84 - 6.43‰) and $\Delta^{33}S$ (0.41 - 0.57‰) values. In contrast Group III has very low $\Delta^{33}S$ values (0.07 – 0.17‰) but very high $\delta^{34}S$ values (20.62 – 28.72‰). Each of these groups coincides with specific parts of the Platreef package (Figure 7.4). Group I comprises samples from the top of the Platreef package, which are suggested to be close to magmatic based on $\delta^{34}S$ values alone. The multiple-sulphur isotope analyses support this observation with $\Delta^{33}S$ values being close to zero and therefore close to magmatic. Group II samples come from the bottom 175 m of the package, and are associated with hornfels rafts. The $\Delta^{33}S$ values for this group are relatively high and indicate that sulphur from a sedimentary source is present. The samples from Group III are of sulphides from within the calc-silicate footwall of the Platreef.

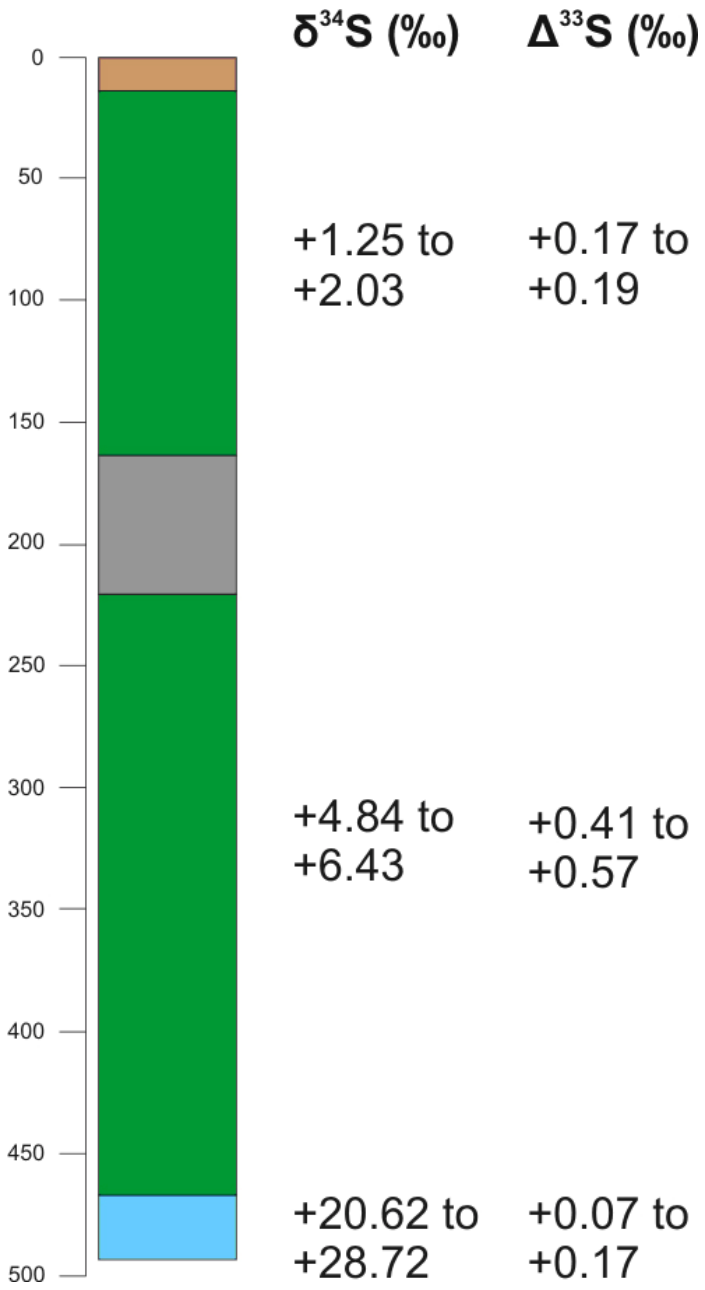

Figure 7.4: Simplified core log of the Platreef where the footwall comprises Upper Duitschland Formation with multiple-sulphur isotope data for different sectors of the Platreef.

When these Groups are plotted with multiple-sulphur isotopes from the Duitschland Formation a trend can be recognized (Figure 7.5). Groups I and II form a mixing line between magmatic values and Lower Duitschland Formation sulphides, with the more contaminated Group II sulphides falling closer to the sedimentary samples. Group III sulphides all appear to have originated from the Upper Duitschland Formation. This implies that all of the sedimentary sulphur

component that is observed within the Platreef itself is from pyritic shales of the Lower Duitschland, whereas the direct footwall comprises metamorphosed dolomites of the Upper Duitschland Formation.

The subsequent metamorphism of Lower Duitschland xenoliths released sulphur-rich volatiles into the lower portion of the Platreef package, causing the formation of an immiscible sulphide liquid. This immiscible sulphide liquid formed sulphide minerals that retained the crustal multiple-sulphur isotope signature. Mixing calculations indicate that up to 70% of the sulphur within these sulphides came from the Lower Duitschland. With increasing distance from the source of this crustal signature the crustal contribution of sulphur decreases until any sulphide minerals that have formed have close to magmatic $\delta^{34}S$ values.

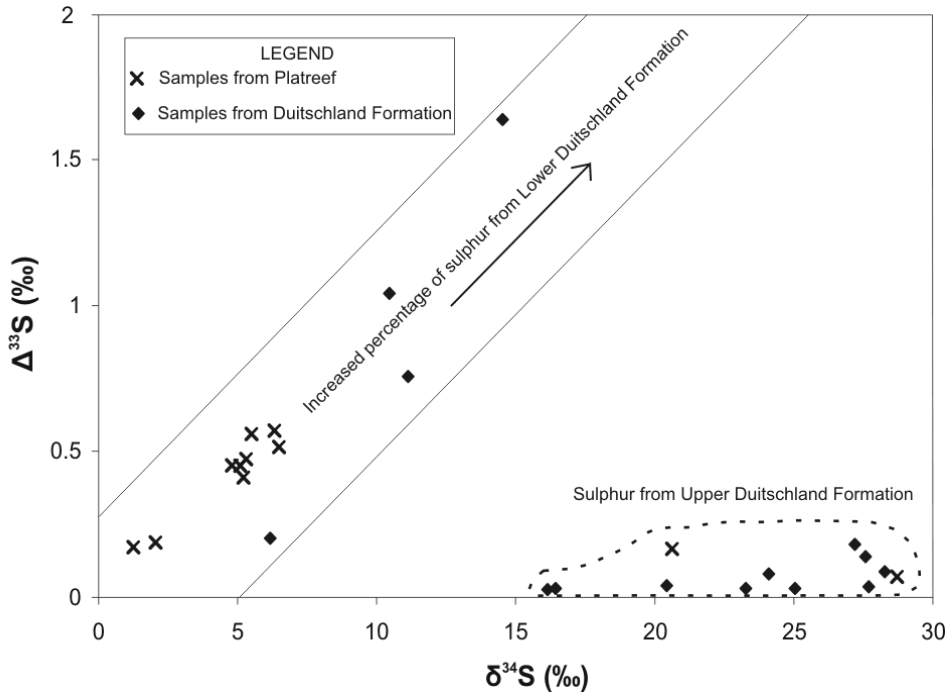

Figure 7.5: Diagram plotting $\delta^{34}S$ vs. $\Delta^{33}S$ for both the Platreef (this study), and the Upper and Lower Duitschland Formations (Baker, 2006).

In the Transvaal Supergroup, the Upper Duitschland Formation occurs stratigraphically above the Lower Duitschland, so it would be anticipated that rafts of Upper Duitschland Formation might occur within the Platreef, where the footwall is of Lower Duitschland. However isotope analyses clearly indicate that this is not the case. Several possibilities can be proposed as to why this occurs:

1. Faulted blocks may have juxtaposed Lower and Upper Duitschland in parts of southern sector of the Platreef.
2. Thrusting has superimposed Lower Duitschland on top of Upper Duitschland in places.
3. There is more isotopic variation within the Upper Duitschland than has been indicated with the current sampling density undertaken.

It is beyond the scope of this thesis to favour any particular model, and further research is required to resolve this question. It is suggested that a more comprehensive study is required in the southern sector of the Platreef to resolve the structure of the footwall in that area and identify any possible faulted blocks or thrusts that may have superimposed the Lower Duitschland over the Upper Duitschland in that area. Also more detailed sampling should be undertaken within the Upper Duitschland Formation to resolve the possibility of more isotopic variation occurring than is currently identified.

Oxygen isotope studies for this sector of the Platreef also support the presence of local crustal contamination in the system. Elevated $\delta^{18}O$ values (+6 to +9‰ for plagioclase, and +6.5 to +8.5‰ for pyroxene) in cores with a footwall of Duitschland Formation indicate a crustal oxygen component within the Platreef package. The increased $\Delta^{18}O_{plag\text{-}px}$ values also suggest that some sub-solidus re-equilibration has occurred, probably due to the movement through the system of volatiles released from the metamorphosed footwall and xenoliths. This is supported by the relatively low subsolidus temperatures recorded for the samples analysed.

Northern Sector of the Platreef

Within the northern sector of the Platreef, sulphur isotope data also indicates that there has been a contribution to the sulphides of sulphur from an external source which has aided in the formation of sulphide minerals. However, in contrast to

the southern sector, the sulphide mineralisation in the northern sector occurs in the top half of the Platreef package (Figure 7.6) which is again linked to the presence of altered sulphur-bearing dolomite xenoliths which in the northern sector occur towards the hanging wall. The main concentrations of sulphide minerals are associated with these xenoliths with much lower concentrations occurring in the lower portion of the Platreef (Figure 7.6), where the footwall is sulphur-poor granites.

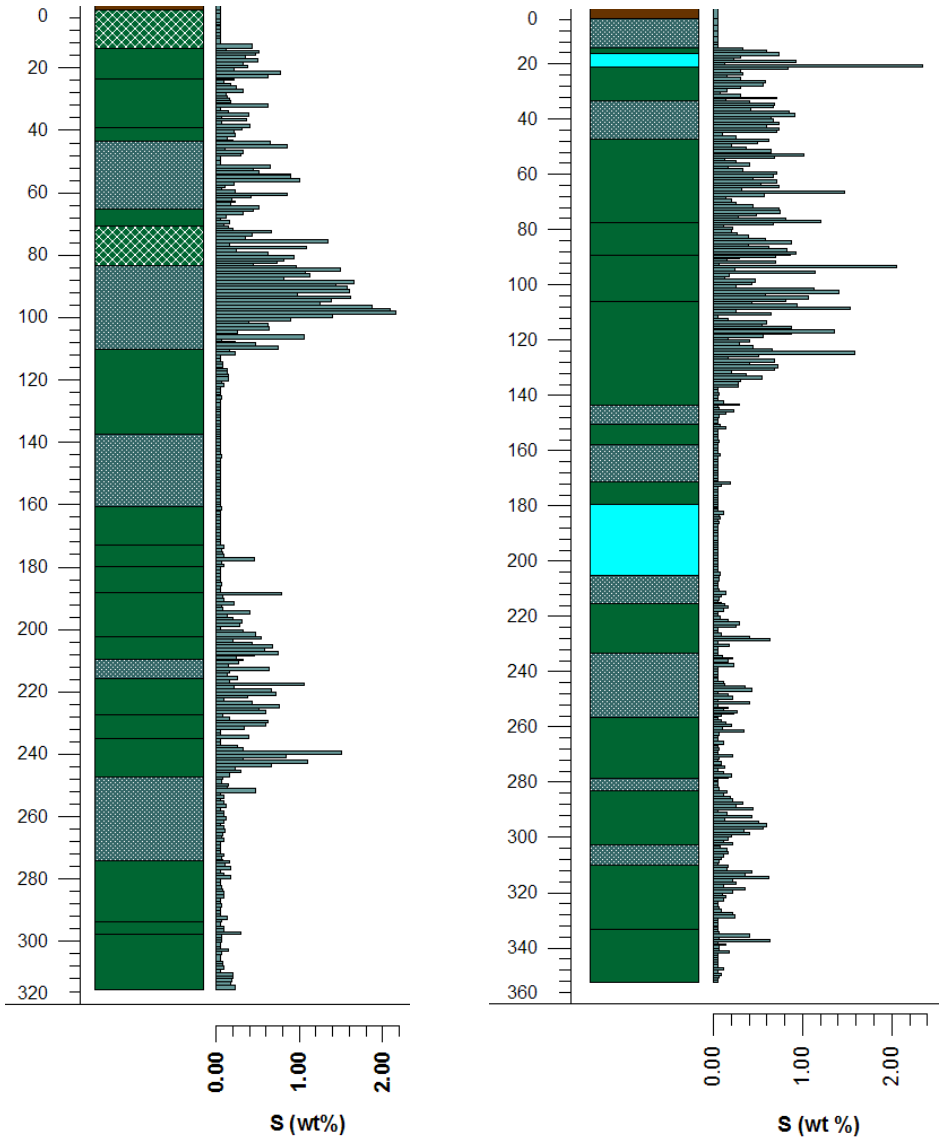

Figure 7.6: Core logs with sulphur concentration (wt%) for cores PR-174 and PR-174 respectively.

Sulphur isotopes in this sector again fall into two groups similar to that of the southern sector, with a close-to-magmatic group with an average $\delta^{34}S$ value of +3.3‰, and a contaminated group with an average $\delta^{34}S$ value of +6.4‰ (Figure 7.7). As in the southern sector the samples from the contaminated group are associated with sedimentary xenoliths and the lower, more magmatic $\delta^{34}S$ values occur away from any sedimentary material.

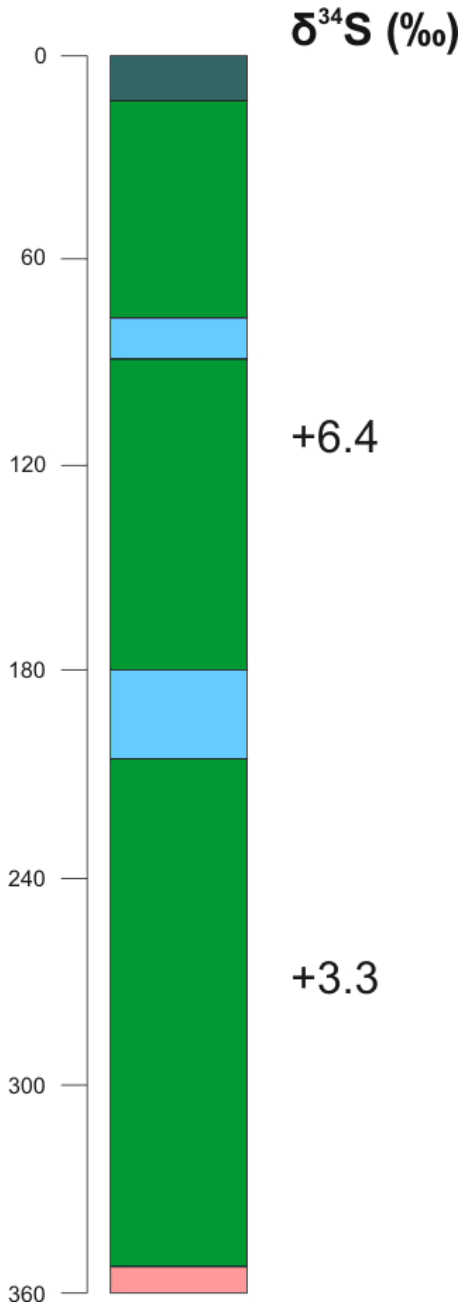

Figure 7.7: Generalised core of the Platreef package on Farm Drenthe showing average sulphur isotope values for different parts of the Platreef.

It can therefore be suggested that sulphur was released with other volatiles from dolomite xenoliths, leading to the formation of sulphide minerals in the upper part of the package. Again the source of these dolomite rafts must be considered, as the footwall in this sector of the Platreef is Archaean granite. It is suggested that the most likely source of these rafts, given their location at the top of the package, is from the roof, which when the Platreef was intruded most likely comprised Malmani dolomites.

When the observations from both the southern and northern sectors of the Platreef are compared and combined with pre-existing data for the central sector, several general observations can be made.

1. The entire length of the Platreef has been affected by contamination from crustal sulphur sources to some degree. This contamination is suggested to be from volatile-rich fluids which were released from metasedimentary crustal xenoliths and footwall during metamorphism. It is unlikely that the sulphur was incorporated by whole rock assimilation of xenolithic metasedimentary material as there is no geochemical evidence for major and trace element contamination close to xenoliths (Kinnaird, 2005).
2. The proximity between sulphide enrichment and sulphur-bearing sediments (as footwall or xenoliths) is important and indicates the source of the sulphur which led to sulphide formation.
3. Contamination occurred on a localised scale, depending on the composition of the sedimentary lithologies and the proximity of the contaminant to the magma. In the southern sector of the Platreef the source of the sulphur is almost certainly pyritic shales of the Lower Duitschland Formation. In the central sector, sulphur has most likely come from sulphur-rich dolomites and evaporites from the Malmani dolomites. In the northern sector, sulphur-rich fluids were released from Malmani dolomite rafts that collapsed from the roof into the magma during the emplacement of the Platreef. The Archaean footwall in this

area has had little or no control on the formation of the sulphides within the Platreef.

This model is slightly different from that previously proposed by authors who have presented sulphur isotope analyses from the Platreef. Buchanan et al. (1981) and Buchanan and Rouse (1984) proposed that crustal sulphur contributed to the formation of sulphide within the Platreef but suggested that this sulphur came only from anhydrites within the Malmani Subgroup. Manyeruke et al. (2005) concluded that crustal sulphur had contributed to the formation of sulphides on the Farm Townlands in the southern sector of the Platreef but did not propose a source. In contrast Liebenberg (1968) and Hulbert (1983) both concluded that no crustal sulphur had been added to the Platreef system and that formation of sulphides was a purely magmatic process.

Holwell et al. (2005) and Holwell and McDonald (2006) proposed that in the northern sector of the Platreef on Farm Overysel there has been no crustal sulphur contribution to the formation of sulphides, although they do note the presence of slightly heavy $\delta^{34}S$ values within the footwall of the cores studied. This study however indicates that this is not strictly the case in the northern sector, with the presence of calc-silicate xenoliths contributing crustal sulphur to the system and playing an important role in the formation of sulphides.

Hutchinson and Kinnaird (2005) noted the importance of metasedimentary material in the formation of PGE mineralisation within the southern sector of the Platreef. In the upper part of the Platreef the PGMs occur as relatively primary ores such as sperrylite and are associated with sulphides. Lower in the Platreef package the PGMs become more varied and occur as bismuthides, arsenides and tellurides and no longer occur within sulphides. The authors commented that volatile-rich fluids moving through the system were responsible for the re-mobilisation of PGMs, as well as the more varied mineralogy observed in the lower part of the Platreef. This is supported by the model presented in this study,

with these volatile-rich fluids not only re-mobilising PGMs but also leading to the formation and concentration of sulphides.

Several authors have proposed that the Platreef was intruded in a series of magmatic events rather than as one intrusion (Kinnaird, 2005; Mothetha, 2006). This study cannot particularly comment on the validity of this model, as the contribution of crustal sulphur to the system occurred post-emplacement. It is however clear that the presence of metasedimentary material creates isotopically different packages in the Platreef system which could be due to several magmatic events.

Similar Global Deposits

There are several similar deposits globally which also exhibit a dependence on proximity to sulphur-bearing crustal material to aid in the formation of sulphide minerals. These include Noril'sk (Siberia), the Duluth Complex (North America), Voisey's Bay (Canada), Pechenga (Russia), Kambalda (Australia) and Raglan (Canada). A comparison between some of these deposits and the Platreef is therefore appropriate with specific focus on the formation of sulphide mineralisation.

Noril'sk, Siberia

The Noril'sk Ni-Cu sulphide deposits comprise part of an extensive ultramafic-mafic intrusive sequence which formed in conjunction with the Permian-Triassic flood basalts in Siberia (Figure 7.8). These magmas were intruded into a sequence of Palaeozoic sediments that mark repeated marine transgressions and regressions (Figure 7.8). These sediments comprise dolomite, limestone, argillite, calcareous and dolomitic marl, and sulphur-rich evaporites which are overlain by coal. This sedimentary sequence is overlain by flood basalts. In many areas the ultramafic - mafic intrusives have caused the formation of breccias, which contain 'hornfelsed and metasomatised' sandstones, argillites, basalts and coal (Naldrett, 2004). The sulphide mineralisation at Noril'sk is generally focused in a massive

sulphide body at the base of the intrusion; with some mineralisation disseminated above this.

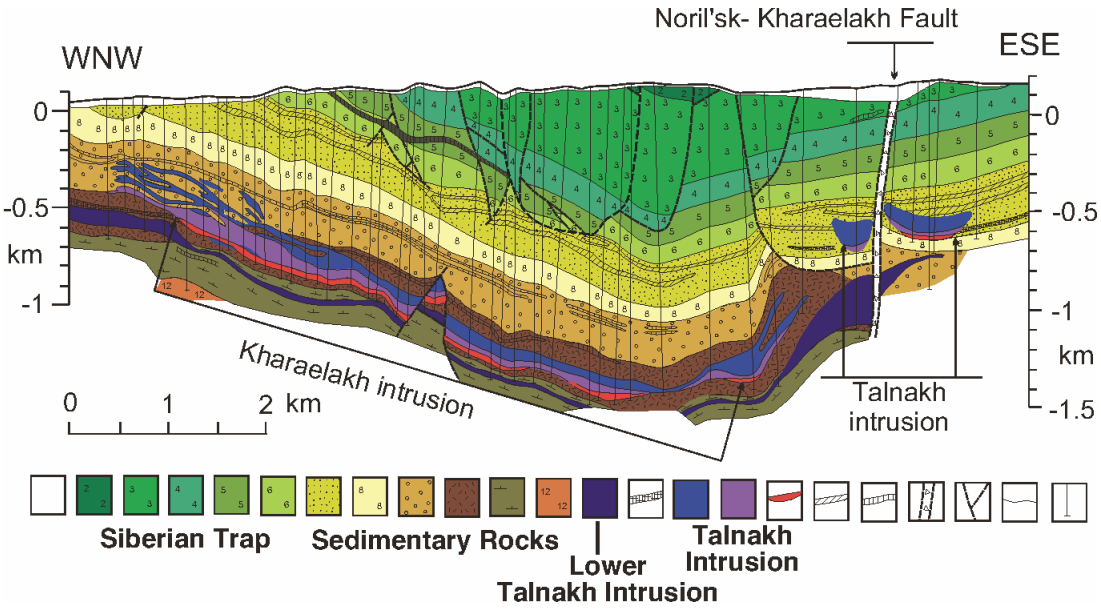

Figure 7.8: Geological cross-section of part of the Noril'sk deposits, after Naldrett et al. 1992.

Sulphur isotope analyses conducted by Godlevsky and Grinenko (1963), Gorbachev and Grinenko (1973), Grinenko (1985a,b) and Li et al. (2003) indicate that there is a crustal sulphur component within the Noril'sk deposits, with $\delta^{34}S$ values ranging from +5 to +15‰. These authors also noted that there was little difference between the various deposits or different ore types. Analysis of a sulphide-poor gabbrodolerite in the area yielded sulphur isotope values of -1.3 and +3.6‰ (Li et al, 2003) which is similar to values for unmineralised intrusions in the area (Grinenko, 1985a). Authors agree that the sulphur which contributed to the formation of these sulphide deposits was most likely derived from sulphur-rich evaporites within the footwall sediments, and suggest that the presence of coal may have aided in the assimilation of the sulphur by the magma. The sulphur isotope analyses support the conclusions that sulphur was added to the system by an external source, similar to the evidence seen in the Platreef.

Duluth Complex, North America

The Duluth Complex is a 240 km long, north-east striking intrusion, which on its western margin discordantly overlies the Animikie sediments, cutting into lower strata from south to north (Naldrett, 2004) (Figure 7.9). The mineralised zones of this deposit are characterised by numerous xenoliths of country rock of the Virginian and Biwabik Formations. These inclusions include hornfelsed slate, which occurs even where the footwall is granite. In the 'Local Boy' area of the intrusion these xenoliths are surrounded by an alteration halo of norite and sulphides.

Sulphur isotope analyses have been conducted on various sedimentary footwall lithologies of the Duluth Complex by Mainwaring and Naldrett (1977), and yielded $\delta^{34}S$ values of between +11 and +18‰. Ripley (1981) examined sulphur isotopes for the Dunka Road deposit within the complex, which yielded values of +0.2 to +15.3‰, which he noted to be similar to the range of $\delta^{34}S$ values found for pyrrhotites within the Virginia Formation sedimentary sequence. Ripley (1986) concluded that the sulphur within the sulphide deposits of the Duluth Complex came from country rock, and that this contamination occurred in situ, with no widespread equilibrium. It was also noted that this sulphur was most likely introduced as a volatile phase rather than being the result of whole-rock assimilation.

The parallels of the Duluth Complex and the Platreef are striking. Both deposits transgress their footwall lithologies, and contain xenoliths of country rock material, which are associated with enrichment of sulphide mineralisation. The sulphur isotope analyses reinforce the interpretation that the source of the sulphur is of local derivation from the country rock and that this contamination of sulphur occurs on a very local scale, and occurred as the addition of a volatile-rich phase.

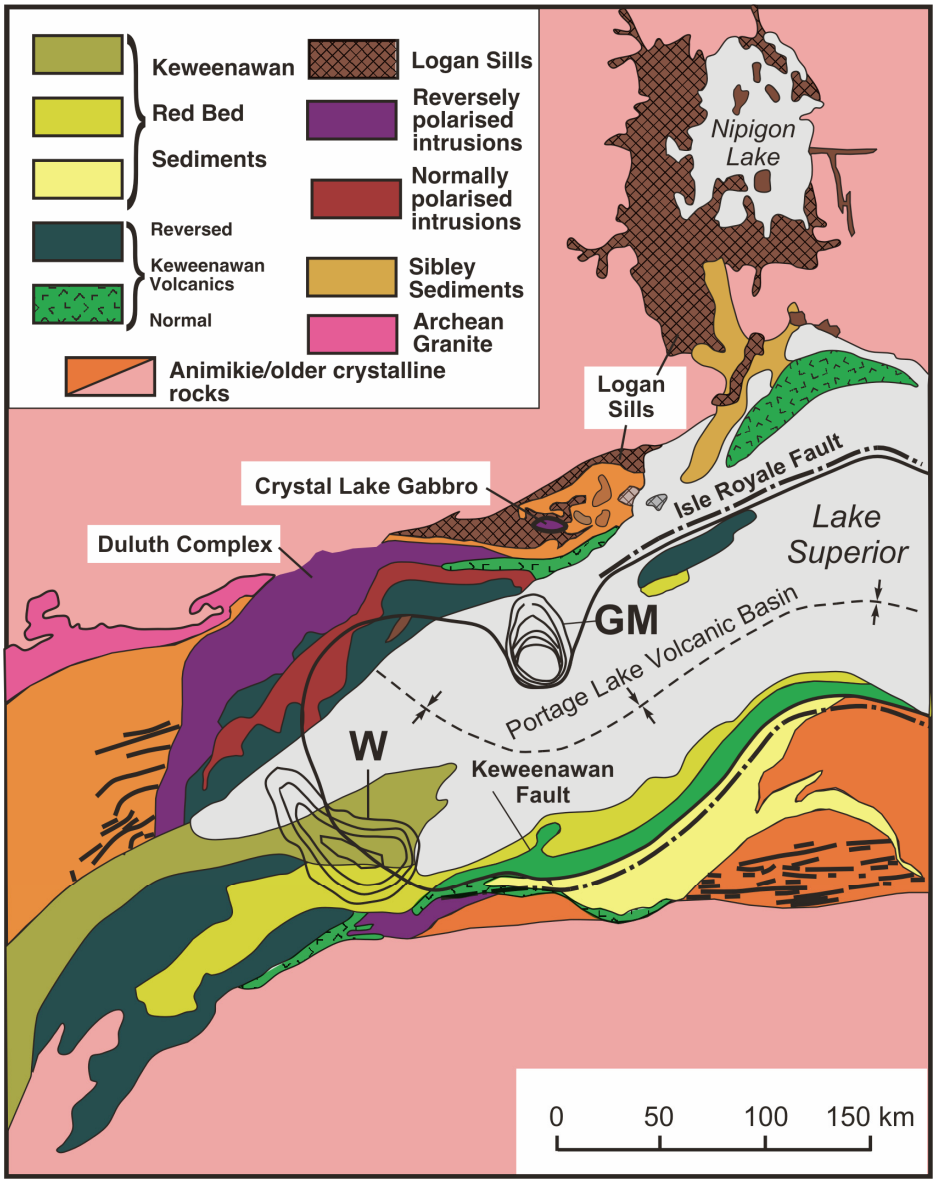

Figure 7.9: Geological map of the Duluth Complex, from Naldrett, 2004, W and GM indicate basement highs.

Voisey's Bay, Canada

The Voisey's Bay deposit in Canada transects the Proterozoic Churchill Province, which comprises reworked Archaean rocks and Proterozoic interbanded garnet-sillimanite and sulphide- and graphite-bearing quartzo-feldspathic paragneisses; and the Archaean Nain Province which comprises interbanded granitic, intermediate and mafic orthogneisses (Naldrett, 2004) (Figure 7.10). The deposit itself comprises two troctolitic intrusions. The sulphides within this deposit are often associated with the Basal Breccia Sequence (BBS) which contains

inclusions of both country rock ultramafics and gneisses. Li and Naldrett (2000) noted that these inclusions have reacted extensively with the magma which formed the deposit.

Ripley et al. (1999) examined the sulphur isotope values of a variety of ores that make up the Voisey's Bay deposit. The disseminated ores of the Eastern Deeps had $\delta^{34}S$ values of -2.0 to +2.7‰, the massive ore of the Ovoid and Mini-Ovoid had sulphur isotope values of -2.1 to 0‰, and disseminated mineralisation from the Reid Brook Zone was found to have $\delta^{34}S$ values of -4.1 to +1.4‰. Pyrrhotite from the Tasivyak gneiss from the Churchill Province had $\delta^{34}S$ values of -17.0 to -0.9‰, whereas the Nain gneiss had sulphur isotope values from +0.2 to +3.3‰. It was determined that there was a general decrease in sulphur isotopes within the deposit to the west, and therefore more sulphur was derived from the Tasivyak gneiss in the western part of the deposit than in the east.

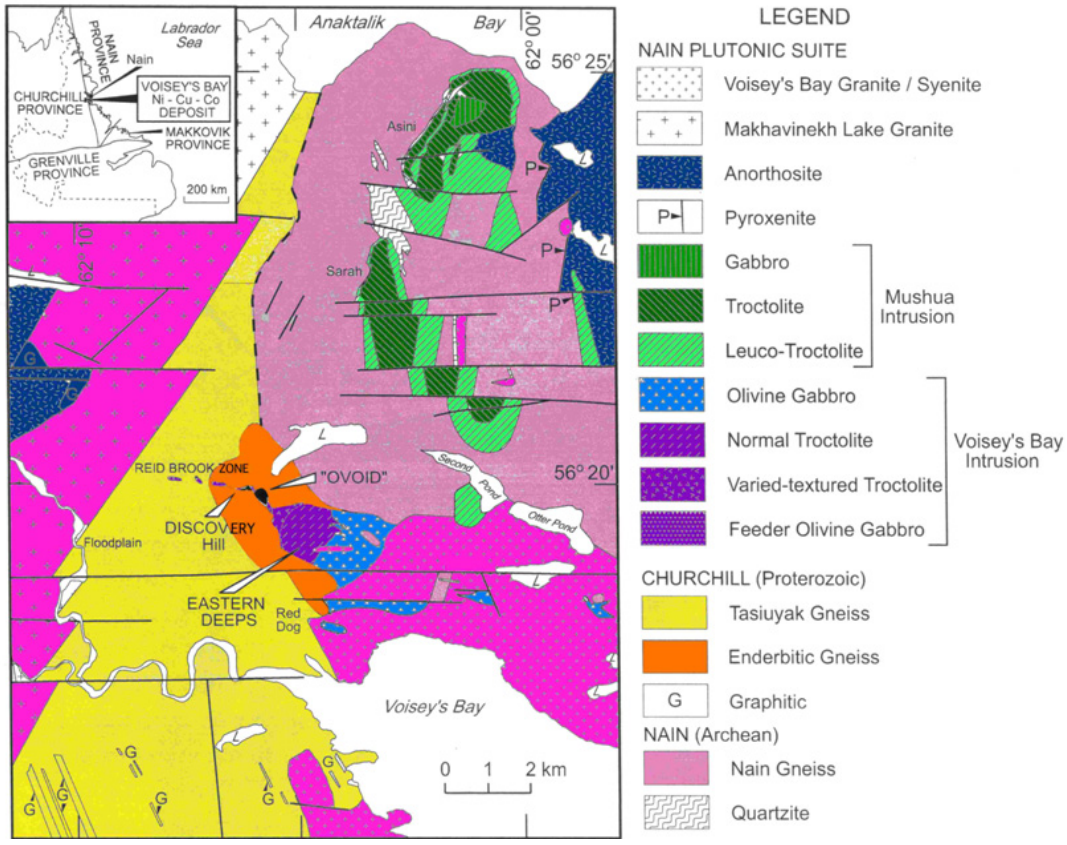

Figure 7.10: Geological map of the area of the Voisey's Bay Deposit (from Li and Naldrett, 1999).

Again this deposit indicates the importance of the association of sulphide mineralisation with country rock material, and the role sulphur isotopes play in determining the source of sulphur.

Conclusions

This study has positively identified pyritic shales from the Lower Duitschland Formation of the Transvaal Supergroup as the main source of crustal sulphur within sulphide mineralisation in the southern sector of the Platreef. In contrast the northern sector of the Platreef concentrations of sulphide mineralisation can be attributed to crustal sulphur that has been added to the system from sulphur-rich dolomites most likely from the Malmani Subgroup in the roof of the Platreef.

The sulphur most likely enters the system within a volatile rich fluid that formed during the metamorphism of crustal metasedimentary material with the result that sulphide mineralisation was concentrated in areas where sulphur-bearing sedimentary rocks were present. This oxygen-, sulphur-, and other volatile-rich fluid also causes the sub-solidus recrystallisation of silicate minerals, as well as the re-mobilisation of PGEs (Hutchinson and Kinnaird, 2005).

The evidence that supports the importance of an external source of sulphur in aiding the formation of sulphides within the Platreef that has been presented by this study can also been seen in a variety of other sulphide deposits globally. The use of sulphur isotopes has been successfully applied to such deposits as the Duluth Complex and Noril'sk. The association of sulphur-bearing country rock, as footwall and xenoliths, with magmatic sulphides has been observed at Voisey's Bay, Noril'sk, Duluth, Pechenga, Kambalda, and Raglan. Equally important is the frequent observation that these external sources are more localised than regional, which concurs with the data for the Platreef. This conclusion is in contrast to the regional contamination proposed by previous authors (Buchanan et al, 1981; Buchanan and Rouse, 1984).

Data from multiple-sulphur isotope analysis has played a pivotal role in allowing the full understanding of the dynamics involved in the formation of sulphides within the Platreef. Thus this relatively new tool, which has never before been applied to the understanding of such an ore deposit, will become indispensable in the interpretation of Archaean to early Proterozoic sulphide deposits in the future.

The understanding of the formation of the Platreef is an ongoing work, with the understanding of the formation of sulphides within the Platreef playing an important part towards this understanding. The extent that the role of contamination played in the formation of this deposits has yet to be fully understood, and will be an ongoing research topic for the future.

REFERENCES

Armitage, P.E.B., McDonald, I., Edwards, S.J., and Manby, G.M. (2002). Platinum-group element mineralisation in the Platreef and calc-silicate footwall at Sandsloot, Potgietersrus District, South Africa. *Transactions of the Institution of Mining and Metallurgy*, **111**, B36 – B45.

Ashwal, L.D., Webb, S.J, and Knoper, M.W. (2005). Physical and mineralogical properties of Bushveld rocks: Magnetic susceptibility, density and mineral chemistry profiles in the 2950 m Bellevue drillcore, Northern Lobe. *South African Journal of Geology*, **108**, 199 – 232.

Baker, M., (2006). Stable isotopic evidence for the rise of oxygen and the reorganization of the sulphur cycle from the 2.3 – 2.4 Ga Duitschland Formation, South Africa. *Unpublished MSc Thesis, University of Maryland, United States of America.*

Bekker, A., Kaufman, A.J., Karhu, J.A., Beukes, N.J., Swart, Q.D., Coetzee, L.L., Eriksson, K.A. (2001). Chemostratigraphy of the Paleoproterozoic Duitschland Formation, South Africa: Implications for Coupled Climate Change and Carbon Cycling. *American Journal of Science*, **301**, 261 - 285.

Buchanan, D.L., Nolan, J., Suddaby, P., Rouse, J.E., Viljoen, M.J., and Davenport, J.W.J. (1981). The Genesis of Sulfide Mineralization in a Portion of the Potgietersrus Limb of the Bushveld Complex. *Economic Geology*, **76**, 568 – 579.

Buchanan, D.L. and Rouse, J.E. (1984). Role of contamination in the precipitation of sulphides in the Platreef of the Bushveld Complex. *In:* Buchanan, D.L. and Jones, M.J. (Editors) *Sulphide Deposits in Mafic and Ultramafic Rocks, Proceedings of IGCP Projects 161 and 91, Third Nickel Sulphide Field Conference, Perth, Western Austarlia, 23-25 May, 1982, Institute of Mining and Metallurgy*, 141 – 146.

Buick, I.S., Maas, R. and Gibson, R. (2001). Precise U-Pb titanite age constraints on the emplacement of the Bushveld Complex, South Africa. *Journal of the Geological Society*, **158**, 3 – 6.

Cameron E.M., (1982). Sulphate and sulphate reduction in early Precambrian oceans. *Nature*, **296**, 145 – 148.

Catuneanu, O., and Eriksson, P.G. (1999). The sequence stratigraphic concept and the Precambrian rock record: an example from the 2.7 – 2.1 Ga Transvaal Supergroup, Kaapvaal Craton. *Precambrian Research,* **97**, 215 – 251.

Coetzee, L.L. (2001). Genetic Stratigraphy of the Paleoproterozoic Pretoria Group in the Western Transvaal. *Unpublished M.Sc. Thesis, Rand Afrikaans University, Johannesburg, South Africa*, 212 pp.

Eales, H.V. and Cawthorn, R.G. (1996). The Bushveld Complex, *In:* Cawthorn, R.G. (Editor) *Layered Intrusions*. Elsevier Science, Amsterdam, The Netherlands, 181 – 221.

Eriksson P.G., Altermann, W., Catuneanu, O., van der Merwe, R., and Bumby, A.J. (2001). Major influences on the evolution of the 2.67 – 2.1 Ga Transvaal basin, Kaapvaal craton. *Sedimentary Geology*, **141-142**, 205 - 231

Farquhar, J. and Wing, B.A. (2003). Multiple sulphur isotopes and the evolution of the atmosphere. *Earth and Planetary Science Letters,* **213**, 1-13.

Farquhar, J., Bao, H.M., Thiemens, M. (2000). Atmospheric influence of earth's earliest sulfur cycle. *Science*, **289**, 756-758.

Gain, S.B., and Mostert, A.B. (1982). The Geological Setting of the Platinoid and Base Metal Sulfide Mineralization in the Platreef of the Bushveld Igneous Complex in Drenthe, North of Potgietersus. *Economic Geology*, **77**, 1395 – 1404.

Gill, R. (1999). *Modern Analytical Geochemistry: An Introduction to quantitative chemical analysis for earth, environmental and materials scientists*. Longman Group, Harlow, England, 329 pp.

Godlevsky, M.N. and Grinenko, L.N. (1963). Some data on sulfur isotope compositions from sulfides of the Noril'sk deposits. *Geokhimiya*, **1**, 35 – 40 (In Russian).

Gorbachev, N.S. and Grinenko, L.N. (1973). Sulfur isotope compositions from sulfides and sulfates of the Oktyabrsky nickel-copper deposit (Noril'sk region) and some aspects of their genesis. *Geokhimiya*, **8**, 1127 – 1136 (In Russian).

Grassineau, N.V., Mattey, D.P. and Lowry, D. (2001). Sulfur Isotope Analysis of Sulfide and Sulfate Minerals by Continuous Flow-Isotope Ratio Mass Spectrometry. *Analytical Chemistry*, **73**, 220 – 225.

Grinenko, L.N. (1985a). Sources of sulfur of the nickeliferous and barren gabbrodolerite intrusions of the north-west Siberian platform. *International Geological Review*, **27**, 695 – 708.

Grinenko, L.N. (1985b). Sulfur sources of nickel-bearing and barren gabbrodolerite intrusions in the north-west part of the Siberian Platform. *Geologiya rudnykh mestorozhdeniy*, **1**, 3 – 15 (In Russian).

Harris, C., and Chaumba, J.B. (2001). Crustal Contamination and Fluid-Rock Interaction during the Formation of the Platreef, Northern Limb of the Bushveld Complex, South Africa. *Journal of Petrology*, **12**, 1321 – 1347.

Harris C. and Erlank A.J. (1992). The production of large-volume low-δ18O rhyolites during the rifting of Africa and Antarctica: the Lebombo Monocline, southern Africa. *Geochimica et Cosmochimica Acta*, **56**, 3561 - 3570.

Harris C., Pronost, J.J.M., Ashwal, L.D., and Cawthorn, R.G. (2005). Oxygen and Hydrogen Isotope Stratigraphy of the Rustenburg Layered Suite, Bushveld Complex: Constraints on Crustal Contamination. *Journal of Petrology*, **40**, 579-601.

Horstmann U.E. and Malinga O. (2003). Sulphur isotope analysis on a PDZ ANCA / GEO 20-20 continuous flow isotope ratio mass-spectrometer. Part I – Hardware. *Report Stable Isotope Lab 2003–06* (South Africa, Council for Geosciences)

Holwell, D.A., Armitage, P. E. B. and McDonald, I. (2005). Observations on the relationship between the Platreef and its hangingwall. *Applied Earth Science (Transactions of the Institute of Mining and Metallurgy B)*, **114**, B199 – B207.

Holwell, D.A. and McDonald, I. (2006). Petrology, geochemistry and the mechanisms determining the distribution of platinum-group element and base metal sulphide mineralisation in the Platreef at Overysel, northern Bushveld Complex, South Africa. *Mineralium Deposita*, **41**, 575 – 598.

Hu, G., Rumble, D., and Wang, P. (2003). An ultraviolet laser microprobe for the in situ analysis of multisulfur isotopes and its use in measuring Archean sulfur isotope mass-independent anomalies. *Geochimica et Cosmochimica Acta*. **67**, 3101–3117.

Hulbert L.J. (1983). A petrological investigation of the Rustenburg Layered Suite and associated mineralization south of Potgietersrus. *Unpublished DSc. Thesis, University of Pretoria, South Africa.*

Hutchinson, D., Kinnaird, J.A. and Schürmann, L.W. (2004). Complex Multi-Stage Mineralisation History in the Southern Sector of the Platreef, Bushveld Complex, RSA. In: *Geoscience Africa 2004, Abstract Volume*, (Johannesburg, University of the Witwatersrand, 293 – 294.

Hutchinson, D. and Kinnaird, J.A. (2005). Complex multistage genesis for the Ni–Cu–PGE mineralisation in the southern region of the Platreef, Bushveld Complex, South Africa. *Applied Earth Science (Transactions of the Institute of Mining and Metallurgy B)*, **114**, B208 – B224.

Kinnaird, J.K. (2004). An Overview of the Platreef. *Geoscience Africa 2004, Abstract Volume, University of the Witwatersrand, Johannesburg, South Africa,* 345 – 346.

Kinnaird, J.A. (2005). Geochemical evidence for multiphase emplacement in the southern Platreef. *Applied Earth Science (Transactions of the Institute of Mining and Metallurgy B)*, **114**, B225 – B242.

Kinnaird, J.A., Hutchinson, D., Schürmann, L.W., Nex, P. and De Lange, R. (2005). Petrology and mineralisation of the southern Platreef: northern limb of the Bushveld Complex, South Africa. *Mineralium Deposita*, **40**, 576-597.

Kinnaird, J.A. and McDonald, I. (2005). An introduction to mineralisation in the northern limb of the Bushveld Complex. *Applied Earth Science (Transactions of the Institute of Mining and Metallurgy B)*, **114**, B194 – B198.

Kruger, F.J. (1990). The stratigraphy of the Bushveld Complex: a reappraisal and the relocation of Main Zone boundaries. *South African Journal of Geology*, **93**, 376 – 381.

Kruger, F.J. (2005). Thoughts on the Platreef – A Critical Zone or Main Zone Phenomenon? *2nd Platreef Workshop 2005, Abstract Volume, Mokopane, South Africa*.

La Grange, M.S., Stevens, G., and Harris, C. (2000). Metamorphism of Witwatersrand rocks in the collar of the Vredefort structure: a petrographic and O isotope study. *Journal of African Earth Sciences*, **31**, 39 – 40.

Li, C. and Naldrett, A.J. (1999). Geology and petrology of the Voisey's Bay intrusion: reaction of olivine with sulfide and silicate liquids. *Lithos*, **47**, 1-31.

Li, C. and Naldrett, A.J. (2000). Melting reactions of gneissic inclusions with enclosing magma at Voisey's Bay: Implications with respect to ore genesis. *Economic Geology*, **95**, 801 – 814.

Li, C., Ripley, E.M., Maier, W.D., and Gomwe, T.E.S. (2002). Olivine and sulphur isotopic compositions of the Uitkomst Ni-Cu sulfide ore-bearing complex, South Africa: evidence for sulfur contamination and multiple magma emplacements. *Chemical Geology*, **188**, 149 – 159.

Li, C., Ripley, E.M. and Naldrett, A.J. (2003). Compositional variations of olivine and sulfur isotopes in the Noril'sk and Talnakh intrustions Siberia: Implications for ore-forming processes in dynamic magma conduits. *Economic Geology*, **98**, 69 – 86.

Liebenberg L. (1968). The Sulphides in the Layered Sequence of the Bushveld Igneous Complex. *Unpublished DSc. Thesis, University of Pretoria, South Africa*.

Mainwaring, P.R. and Naldrett, A.J. (1977). Country-rock assimilation and the genesis of copper-nickel sulfides in the Waterhen intrusion Duluth Complex Minnesota. *Economic Geology*, **72**, 1269 – 1284.

Maier, W. D., Arndt, N. T. and Curl, E. A. (2000). Progressive crustal contamination of the Bushveld Complex: evidence from Nd isotopic analyses of the cumulate rocks. *Contributions to Mineralogy and Petrology*, **140**, 316–27.

Manyeruke T.D. (2003). The petrography and geochemistry of the Platreef on the farm Townlands, near Potgietersrus, northern Bushveld Complex. *Unpublished MSc. Thesis, University of Pretoria, South Africa*.

Manyeruke, T.D., Maier, W.D. and Barnes S-J (2005). Major and trace element geochemistry of the Platreef on the farm Townlands, northern Bushveld Complex. *South African Journal of Geology*, **108**, 381 – 396.

Martini, J.E.J. (1979). A copper-bearing bed in the Pretoria group in northeastern Transvaal. *Geocongress 77: Geological Society of South Africa Special Publication*. **6**, 65 – 72.

Mavrogenes, J.A. and O'Neill, H.S. (1999). The relative effects of pressure, temperature and oxygen fugacity on the solubility of sulfide in mafic magmas. *Geochimica et Cosmochimica Acta*, **63**, 1173–1180.

Mothetha, M.V. (2006). Petrology and Geochemistry of the Southern Sector of the Platreef, Bushveld Complex. *Unpublished MSc. Thesis, University of the Witwatersrand, South Africa*.

Naldrett, A.J. (2004). Magmatic Sulfide Deposits Geology, Geochemisty and Exploration. Springer, 727 pp.

Naldrett, A.J., Lightfoot, P.C., Fedorenko, V.A., Gorbachev, N.S. and Doherty, W. (1992). Geology and geochemistry of intrusions and flood basalts of the Noril'sk region USSR with implications for the origin of the nickel-copper ores. *Economic Geology*, **87**, 975 – 1004.

Pronost J. (2005). Effects de la contamination continentale des interactions fluids-roches sur le Platreef, complexe igne du Bushveld, Afrique du Sud. *Unpublished PhD Thesis, University Clermont Ferrand, France*.

Reczko, B.F.F. (1994). The geochemistry of the sedimentary rocks of the Pretoria Group, Traansvaal Sequence. *Volume One, Unpublished Ph.D. Thesis, University of Pretoria, South Africa,* 385 pp.

Reid, D.L., Cawthorn, R. G., Kruger, F. J. and Tredoux, M. (1993). Isotope and trace-element patterns below the Merensky Reef, Bushveld Complex, South Africa: Evidence for fluids? *Chemical Geology*, **106**, 171 – 186.

Ripley, E.M. (1981). Sulfur isotopic abundances of the Dunka Road copper-nickel deposit Duluth Complex Minnesota. *Economic Geology*, **76**, 619 – 620.

Ripley, E.M. (1986). Applications of stable isotope studies to problems of magmatic sulfide ore genesis with special reference to the Duluth Complex Minnesota. *In:* Friedrich, G.H., Genkin, A.D., Naldrett, A.J., Ridge, J.D., Sillitoe, R.H., and Vokes, F.M. (Editors) *Geology and Metallogeny of Copper Deposits,* Society for Geology Applied to Ore Deposits Special Publication **4**, Springer-Verlag, Berlin-Heidelberg, 25 – 42.

Ripley, E.M., Park, Y-R, Li, C. and Naldrett, A.J. (1999). Sulfur and oxygen isotopic evidence of country rock contamination in the Voisey's Bay Ni-Cu-Co deposit Labrador Canada. *Lithos*, **47**, 53 – 68.

Rollinson, H.R. (1993). *Using Geochemical Data: Evaluation, Presentation, Interpretation*. Longman Group, Harlow, England, 352 pp.

S.A.C.S. (1980). South African Council of Stratigraphy.

Schiffries, C.M. and Rye D.M. (1989). Stable Isotopic Systematics of the Bushveld Complex: I. Constraints of Magmatic Processes in Layered Intrusions. *American Journal of Science*, **289**, 841 – 873.

Sharman-Harris, E.R. (2004). Petrographic, Mineralogical and Isotopic Studies of the Southern Platreef, Bushveld Igneous Complex. *Unpublished Honours Project, University of the Witwatersrand, South Africa*, 68 pp.

Tsai, H. (1979). Mineral inclusions in diamond: Premier, Jagersfontein and Finsch kimberlites, South Africa, and Williamson Mine, Tanzania. In: Boyd, F.R., Meyer, H.O.A. (Eds) *Kimberlites, diatremes and diamonds: their geology, petrology and geochemistry* (American Geophysical Union), 16-26.

Van der Merwe, M.J. (1976). The Layered Sequence of the Potgietersrus Limb of the Bushveld Complex. *Economic Geology*, **71**, 1337 – 1351.

Van der Merwe, M.J. (1978). The Geology of the Basic and Ultramafic Rocks of the Potgietersrus Limb of the Bushveld Complex. *Unpublished Ph.D. Thesis, University of the Witwatersrand, South Africa,* 176 pp.

Vennemann, T.W. and Smith, H.S. (1990). The rate and temperature of reaction of ClF_3 with silicate minerals, and their relevance to oxygen isotope analysis. *Chemical Geology*, **86**, 83 – 88.

Wagner, P.A. (1929). *The platinum deposits and mines of South Africa.* (London, Struik), 338pp.

White, J.A. (1994). The Potgietersrus Prospect – Geology and Exploration History. *XVth CMMI Congress, Johannesburg, SAIMM*, **3**, 173 – 181.

White, W.M. (2001). *Geochemistry*. Unpublished work, obtained from L. Ashwal (2002).

APPENDIX 1
Sample Descriptions for core ATS-057

Sample No.	From	To	Sample Description	Sulphides	Thin Sections
ATS-57/57.58	57.46	57.70	Grey-green, medium to coarse grained (4-8mm), crystaline, pred. pyroxene w/ minor plagioclase, PYROXENITE.	5%, disseminated, inter-granular, 1-3 mm, 80% pyrh/pent. 20% chalc. A few grains seem to have minor associated biotite.	A3196
ATS-57/72.48	72.39	72.56	Grey for most of core, coarse-grained to pegmatitic (5mm-3cm), crystalline pyroxene w/ interstitial plagioclase and pyroxene. Bottom 6 cm predominately white/cream plag. with interstitial pyroxene. PYROXENITE	15%, two different phases, mainly disseminated, inter-granular, 1mm - 3cm, 90% chalc., 10% pyrh/pent. Chalcopyrite occurs as both a brassy/tarnished colour, and a more yellow colour. In bottom 6cm of sample one interstitial bleb occurs (2cm), 85% chalc., 15% pent/pyrh. Immiscible textures seen in bleb, with chalc. surrounding smaller pyrh/pent blebs.	A3197
ATS-57/102.79	102.69	102.89	Light grey, coarse grained (5-8 mm), appears to have both cumulus pyroxene and plagioclase, but also interstitial pyroxene and plag. Some minor biotite. Sample becomes more rich in plagioclase in bottom 5 cm of sample, with large (1-3 cm) tabular crystals occuring with interstitial biotite. FELDSPATHIC PYROXENITE	5%, disseminated, inter-granular, 1-3 mm, 90% pyrh/pent. 10% chalc. A few grains are surrounded by a silver-coloured, metallic mineral (magnetite)	A3198
ATS-57/118.78	118.70	118.86	Dark green-grey, medium to coarse grained (3-15 mm), larger crystalline pyroxenes with interstitial plagioclase and pyroxene, some minor biotite. Has random-orientated fractures running through the sample, filled with a dark very fine grained material. PYROXENITE.	5%, disseminated, inter-granular, 1-5 mm, 80% pyrh/pent, 20% chalc. A few grains seem to have associated biotite.	A3199

ATS-57/140.14	140.07	140.20	Mottled white and grey, medium to coarse grained (3-5 mm), approx. 50/50 plagioclase/ pyroxene, becomes more coarse-grained and pyroxene-rich with depth, and pyroxene becomes more crystalline. There is also approximatly 15% graphite in the sample, as well as minor biotite. PARAPYROXENITE	3%, disseminated, inter-granular, 1-3 mm, 95% pyrh/pent, 5% chalc. Larger (2 cm) sulphide at base of sample, interstitial.	A3200
ATS-57/151.40	151.31	151.49	Dark grey, pegmatitic (1-4 cm), interlocking crystalline pyroxenes with minor interstitial plagioclase. PYROXENITE	5%, disseminated, intergranular, 1-5 mm, 80% pent/pyrh, 20% chalc.	A3201
ATS-57/180.64	180.59	180.69	Mottled white and grey-green, fine to coarse grained (1-5mm), inhomogenous, cumulate pyroxene, with interstitial plagioclase and pyroxene, modal percentage varies through sample. FELDSPATHIC PYROXENITE	5%, disseminated, intergranular, 1-5 mm, 90% pent/pyrh, 10% chalc.	A3202
ATS-57/218.39	218.26	218.51	Dark grey, predominantly fine grained (1-2 mm) with some coarser grains (3-8 mm) at top of sample, probably pyroxene and plagioclase, too fine grained to tell proportions. PYROXENITE	25%, sulphides concentrated at either end of the sample, and occur as large (3-5 cm) intergranular blebs, and are "net-textured". The sulphides form a 60-70% matrix, with silicate minerals as clasts within this matrix, the silicates appear to have been partially rounded, probably by the sulphide liquid as the rock formed. Bleb at top of sample has less chalc. (10% chalc., 90% pyrh/pent) than bleb at bottom of sample (75% pyrh/pent, 25% chalc.). Sulphides occur as disseminated intergranular blebs (1-10 mm) throught the sample and are 80% pent/pyrh, 20% chalc.	A3203

ATS-57/221.39	221.33	221.45	Dark grey-green silicates within a sulphide matrix, fine-grained (1-2 mm), euhedral to sub-euhedral, pyroxene and perhaps some plagioclase. MASSIVE SULPHIDE / PYROXENITE	60%, sulphides are "net-texured", forming a inter-granular matrix which contains silicate clasts, which are euhedral to sub-euhedral. Percantage of sulphide to silicate varies through the sample, 20% chalc, 80% pent/pyrh.	A3204
ATS-57/268.15	268.07	268.23	Dark grey, fine-grained (1-2 mm), pyroxene and plag, too fine grained to identify textures. Approximatly 3cm zone which is coarser grained (1 - 5 mm) with a larger (1.5 cm) rounded silicate occurs towards bottom of core. FELDSPATHIC PYROXENITE	10%, mostly very fine-grained (<1mm) and disseminated through the sample. Concetration increases in coarser grained zone. 90% pyrh/pent, 10% chalc.	A3205
ATS-57/290.41	290.35	290.47	Mottled dark green/black - light green/white, medium to coarse grained (2-5 mm), cumulus pyroxene and plagioclase, has been serpentinised (~20%). SERPENTINITE / PYROXENITE	10%, interstitial, fine to medium grained (1-3 mm), 50% pent/pyrh, 50% chalc.	A3206
ATS-57/304.59	304.46	304.72	Light grey, fine-grained (1-2 mm), some larger (2 mm) cumulus plagioclase grains with intestitial pyroxene. FELDSPATHIC PYROXENITE	30%, very fine grained (<1 mm), disseminated, interstitial, 90% pyrh/pent, 10% chalc.	A3207
ATS-57/325.32	325.25	325.38	Light grey - white with darker patches, massive, non-crystalline, inhomogeneous, sedimentary origin. QUARTZITE	30%, massive sulphide at top of sample, has "flow" textures, all pyrh/pent, very minor chalc. along bottom boundary of sulphide. Also some minor, very fine-grained (1 mm), sulphide associated with a dark patch, prob. pyrh/pent.	A3208
ATS-57/335.07	334.95	335.19	Grey, white, green and black, very fine grained, inhomogeneous, remanant bedding visible, predominately calc-silicate mineralogy. CALC-SILICATE / DOLOMITE	20%, sulphides occur along remenant bedding planes, discrete grains can be seen, many are euhedral, probably pyrite.	A3209

APPENDIX 2
Thin section descritptions for core ATS-057

Sample No.	Rock Type	Start Depth	End Depth	Thin Section No.	Transmitted Light	Reflected Light
ATS-57/57.58	Pyroxenite	57.46	57.70	A3196	Opx dominated, with associated cpx. Interstitial plagioclase, minor interstitial biotite.	Fine grained interstitial sulphides ~1mm (are either 100% pyrrhotite, 100% chalcopyrite, or ~60% pyrrh/40% chalc), some very fine grained chalcopyrite occurs in the rims of altered silicates.
ATS-57/72.48	Pyroxenite	72.39	72.56	A3197A	Highly altered plag and opx, calcite rims around sulphide is mineral.	Large interstitial sulphide bleb (2cm), with minor associated fine grained sulphide blebs along the grain boundary. Dominated by chalcopyrite (90%) with some minor pyrrhotite (10%) usually occurring along the rims.
ATS-57/72.48	Pyroxenite	72.39	72.56	A3197B	Sample is mostly highly altered (sericitised) pyroxenes and plagioclase, may be some coarse grained laths of biotite.	Fine grained interstitial sulphides (1-3mm) vary in composition but are usually chalcopyrite dominated, pyrrhotite <50%.
ATS-57/102.79	Feldspathic Pyroxenite	102.69	102.89	A3198	Altered (sericitised) plagioclase and pyroxene with minor associated biotite.	Fine grained sulphide (1-2mm) bleb. Appears to have primary pyrrhotite dominating it (70%) with chalcopyrite (15%) and pentlandite (15%) occuring as a later stage rim.
ATS-57/118.78	Pyroxenite	118.70	118.86	A3199	Cumulus opx and cpx with interstitial plagioclase and minor biotite. Some minor sericitisation.	Sulphides are fine grained (1-2mm) and interstitial. One area of grains is 99% pyrrhotite with some very minor chalcopyrite (1%), another area of grains is 75% pyrrhotite with 25% chalcopyrite occuring on the rim of the grains.

APPENDIX 3
Sample Descriptions for core AMK-021

Sample No.	From	To	Sample Description	Sulphides
AMK021/109.09	108.93	109.25	Medium grey with minor white patches, medium grained (~3-4 mm), composed of interlocking cumulus pyroxene crystals (80%) with interstital plagioclase (15%). FELDSPATHIC PYROXENITE	5%, all interstitial sulphides (1-5 mm), composed primarily of pyrrhotite with minor chalcopyrite.
AMK-021/125.76	125.62	125.90	Medium grained, with cumulus pyroxenes and plagioclase, also interstitial plag. Some serpentinisation is present. GABBRONORITE	3%, blebby, fine to medium grained (1 - 4 mm). Dominated by pyrrhotite, too fine grained to see detailed mineralogy.
AMK021/218.40	218.24	218.55	Medium grey to black, medium grained (~4 mm), composed primarily of pyroxene (95%) with minor biotite (3%). PYROXENITE	2%, blebby sulphides (2-4 mm), primarily pyrrhotite.
AMK-021/222.06	221.88	222.24	Fine to coarse grained, with cumulus pyroxenes and minor interstitial plagioclase. Large percentage of serpentinisation, with the re-crystallisation of pyroxenes also occuring. FELDSPATHIC PYROXENITE	3%, fine grained (1 - 2mm), interstitial sulphides. Too fine-grained to determine sulphide mineral percentages.
AMK021/227.15	227.07	227.23	Dark grey to black with white interstital sectors, medium grained (~4 mm), consisting of cumulus pyroxene (70%) with interstitial plagioclase (15%). Sectors of the core are composed of fine-grained serpentinite. FELDSPATHIC PYROXENITE	15%, blebby and interstitial sulphides (1-5 mm), composed primarily of pyrrhotite (90%) with trace chalcopyrite (10%).
AMK-021/232.62	232.49	232.75	Coarse to very coarse grained, with cumulus pyroxenes and minor interstitial plagioclase. Pyroxenes have been slightly altered. PYROXENITE	5%, blebby sulphides, fine to medium grained (1 - 3 mm). Too fine-grained to determine mineralogy.

AMK-021/235.31	235.23	235.38	Coarse to very coarse grained, with cumulus pyroxenes and interstitial plagioclase. Appears to be altered, with serpentinisation occuring in places. FELDSPATHIC PYROXENITE	10%, coarse to very coarse grained blebs. Smaller blebs are pyrrhotite dominated, with chalcopyrite and pentlandite occuring on the rims. Very coarse grained blebs are 75% chalcopyrite, with 25% pentlandite occuring as cross-cutting veins.
AMK021/236.68	236.54	236.82	Medium grey , fine-grained (1-2 mm), shows small recrystallized plagioclase crystals (50%) bound by interstitial pyroxene (40%), moderately serpentinised, salt and pepper texture. NORITE	10%, fine-grained (1 mm), occuring as disseminated crystals and stringers in discreet fine-grained pyroxene patches (recrystallized xenoliths?).
AMK-021/240.62	240.37	240.86	Pale grey, massive, possibly altered pyroxenes with serpentinite. Also some plagioclase. FELDSPATHIC PYROXENITE	5%, Fine to coarse grained blebby sulphides (1 - 10 mm). 80% pyrrh/pent, 20% chalcopyrite occuring around the rims of blebs.
AMK021/343.14	342.97	343.30	Dark grey - black, medium grained (2-4 mm), massive and homogeneous, composed entirely of interlocking pyroxene crystals (95%) with minor biotite (4%) and rare sulphides. PYROXENITE	1%, occuring as disseminated sulphide blebs (~1 mm), primarily pyrrhotite.

ATS-57/140.14	Parapyroxenite	140.07	140.20	A3200	Cumulus opx and cpx with interstitial plagioclase and minor biotite associated with graphite veins. Minor sericitisation.	Sulphides are associated with veins of graphite. Dominantly pyrrhotite (90%) with some minor chalcopyrite.
ATS-57/151.40	Pyroxenite	151.31	151.49	A3201A	Pegmatoidal, dominated by opx, some cpx. Plagioclase is interstitial, some minor biotite occurs. There are some zones of sericitisation.	Sulphides occur as fine interstitial grains (<1mm) and have appear to have been partially dissolved by fluids which also caused the sericitisation. Compostion of grains varies - 50% pyrrhotite, 50% pentlandite / 60% pyrrhotite, 40% chalcopyrite / 90% pentlandite, 10% pyrrhotite (occuring as flame lamellae).
ATS-57/151.40	Pyroxenite	151.31	151.49	A3201B	Pegmatoidal, dominated by opx, some cpx. Plagioclase is interstitial, some minor biotite occurs. There are some zones of sericitisation.	Sulphides are fine grained (1-2mm) and interstitial. They appear to have been partially dissolved by sericitisation. These sulphides are either 100% pentlandite or 100% chalcopyrite. Sulphides also occur as veinlets with pyroxenes - these are 90% chalcopyrite with 10% pentlandite occuring on the edges of the veinlets.
ATS-57/180.64	Feldspathic Pyroxenite	180.59	180.69	A3202	Fine grained, cumulus opx, cpx with interstitial plagioclase, minor biotite. Some sericitisation has occurred.	Sulphides occur as fine grained (1-2mm) interstitial blebs with varying composition. Dominated by pyrrhotite (80 - 95%) with minor chalcopyrite (0 - 15%) and pentlandite (1 - 10%).
ATS-57/218.39	Pyroxenite	218.26	218.51	A3203A	Predominantly opx, with minor plagioclase and biotite. Grains have been partially dissolved by sulphides, giving them a rounded apperance.	Sulphides are 'net-textured' occuring as a 'matrix' for the silicates. Dominantly pyrrhotite (80%), with chalcopyrite (10%) and pentlandite (10%) occurring together in patches and veinlets through the pyrrhotite.

ATS-57/218.39	Pyroxenite	218.26	218.51	A3203B	Fine to medium grained cumulus opx and cpx with interstitial plagioclase. Some medium grained biotite lathes.	Sulphides are fine-grained (<1mm) and interstitial. They are dominantly chalcopyrite (90%) with some minor pentlandite (10%) occurring on the rims of the grains.
ATS-57/218.39	Pyroxenite	218.26	218.51	A3203C	Opx, cpx and plag occur as coarse-grained rounded clasts that have been sericitised. They contain inclusions of chlorite and biotite.	Sulphides are 'net-textured' occuring as a 'matrix' for the silicates. Dominantly pyrrhotite (90%), with chalcopyrite (7%) and pentlandite (3%) occuring together in patches and veinlets through the pyrrhotite.
ATS-57/221.39	Massive Sulphide / Pyroxenite	221.33	221.45	A3204A1	Fine to medium grained cumulus ortho- and clinopyroxene that have been highly sericitised, and have associated biotite. They have been rounded.	Sulphides are 'net-textured' occuring as a 'matrix' for the silicates. Dominantly pyrrhotite (80%), with chalcopyrite (15%) and pentlandite (5%) occuring together in patches and veinlets through the pyrrhotite. Some sulphides occur within with the rounded silicates and are dominantly chalcopyrite.
ATS-57/221.39	Massive Sulphide / Pyroxenite	221.33	221.45	A3204A2	Fine to medium grained cumulus ortho- and clinopyroxene that have been highly sericitised, and have associated biotite. Sulphides have partially dissolved the silicates giving them a rounded apperance.	Sulphides are 'net-textured' occuring as a 'matrix' for the silicates. Dominantly pyrrhotite (80%), with chalcopyrite (15%) and pentlandite (5%) occuring together in patches and veinlets through the pyrrhotite. Some sulphides occur within the rounded silicates and have varying compositions although are usually chalcopyrite dominated with associated pyrrhotite.
ATS-57/221.39	Massive Sulphide / Pyroxenite	221.33	221.45	A3204B	Silicates are fine to coarse grained, have been partially dissolved by sulphides giving them a rounded apperance, and are partially sericitised. Dominantly opx, with some cpx and plag.	Sulphides are 'net-textured' occurring as a 'matrix' for the silicates. Dominantly pyrrhotite (70%), with chalcopyrite (20%) and pentlandite (10%) occurring together in patches and veinlets through the pyrrhotite.

ATS-57/268.15	Feldspathic Pyroxenite	268.07	268.23	A3205A	Fine grained cumulus orthopyroxene and clinopyroxene with interstitial plagioclase. Very minor biotite.	Fine grained (<1mm) interstitial sulphides. Grains vary in composition - 100% pentlandite / 100% pyrrhotite / 60% pyrrhotite, 20% pentlandite, 20% chalcopyrite.
ATS-57/268.15	Feldspathic Pyroxenite	268.07	268.23	A3205B	Irregular grains of plagioclase, orthopyroxene and clinopyroxene with minor biotite. Silicates are all sericitised in varying degrees and have been partly dissolved by the sulphide fluid.	Sulphides are interstitial/net textured in general they appear to be pyrrhotite dominated (70%) with accessory chalcopyrite (20%) and pentlandite (10%) although there are zones which are chalcopyrite dominated (85%) with accessory pentlandite (15%).
ATS-57/290.41	Serpentinite / Pyroxenite	290.35	290.47	A3206	Highly serpentinised pyroxenite with cumulus pyroxenes now predominatly occuring as secondary olivine. Plagioclase and biotite occur as interstitial phases.	Sulphides are medium grained (1-3mm) and interstitial. Have varying compositions but are dominated by pyrrhotite (70%) with associated pentlandite (10%), chalcopyrite (10%) and bornite (10%).
ATS-57/304.59	Feldspathic Pyroxenite	304.46	304.72	A3207	Fine to medium grained cumulus opx and cpx with interstitial plagioclase and biotite.	Fine to medium grained (<1 - 3mm) interstitial sulphides dominantly pyrrhotite (80%) with minor associated chalcopyrite (10%) and pentlandite (10%).
ATS-57/325.32	Quartzite	325.25	325.38	A3208A	Fine to very fine grained quartz, zone of alteration (sericitisation) occurs on edge of sulphide bleb.	Sulphide occurs as massive bleb which is 99% pyrrhotite, with some very minor chalcopyrite occuring on the rim of the bleb.
ATS-57/325.32	Quartzite	325.25	325.38	A3208B	Fine to very fine grained quartz. There is a vein of anhydrite (?) running through the sample.	Some very small patches of very fine grained interstitial sulphides - 100% pyrrhotite.
ATS-57/335.07	Calc - Silicate / Dolomite	334.95	335.19	A3209	Fine grained calcite/dolomite	Sulphides occur in zones of fine to medium grained pyrite, with occasional replacement pyrrhotite.
ATS-57/335.07	Calc - Silicate / Dolomite	334.95	335.19	A3209A	Fine grained calcite/dolomite	Sulphides occur in zones of fine to medium grained pyrite, with occasional replacement pyrrhotite.

ATS-57/335.07	Calc - Silicate / Dolomite	334.95	335.19	A3209B	Fine grained calcite/dolomite	Sulphides occur as fine grains discretely distributed through the sample, possibly along remnant bedding planes. Sulphides are dominantly bornite with some pyrite.

APPENDIX 4
Polished block descriptions for cores AMK-021, ATS-057 and ATS-046

Sample Number	Sulphide Descriptions
AMK21-10 (108.93 - 109.25)	Fine grained interstitial sulphides generally <1mm. Seems to be mainly pyrrhotite (60%) and pentlandite (35%). Minor chalcopyrite. Sulphides are generally messy/moth-eaten.
AMK21-11A (125.62 - 125.90)	One large sulphide bleb (1cm wide, 1.5cm long) and two other minor sulphides (1mm). Smaller blebs are 75% pyrrhotite with 25% chalcopyrite along rim. Large bleb is all pyrrhotite, although there are two phases, one of which may be recrystallisation.
AMK21-11B (125.62 - 125.90)	Massive sulphide bleb, almost completely pyrrhotite, but again 2 different phases. Chalcopyrite occurs on the rims as very fine grains, although there is one larger chalcopyrite grain (5mm) on the edge of the large grain.
AMK21-1 (218.24 - 218.55)	Medium grained (1-2mm) disseminated sulphide blebs. Pyrrhotite and chalcopyrite occur in same blebs, with % varying from 30 - 60% chalcopyrite. Chalcopyrite also occurs as very thin stringers and very fine-grained disseminated blebs with silicates.
AMK21-2 (221.88 - 222.24)	Fine grained (<1mm) highly disseminated blebs. Blebs are very complex with at least 3 different minerals: definatly chalcopyrite, pentlandite, and probably magnetite. Magnetite is usually the dominating phase - has probably been reacted with the olivines in sample. Also some bornite observed.
AMK21-3 (227.07 - 227.23)	Interstitial sulphides ranging from 1mm to 5mm, occuring on the rims of the silicates. Usually dominated by pyrhhotite (50-70%) with associated chalcopyrite and pentlandite. Do get entire zones that are chalcopyrite/pentlandite, with little pyrrhotite.
AMK21-4 (232.49 - 232.75)	Interstitial sulphides (2-5mm). Dominated by pyrrhotite (65-80%), then pentlandite. Generally minor chalcopyrite on rims, although two of the smaller grains are dominated by chalcopyrite (50-80%).
AMK21-5 (235.23 - 235.38)	One large sulphide bleb (1cm wide, 2cm long) which is dominantly chalcopyrite (80%) with a linear vein of pyrhhotite (1.5 mm in width) cross cutting the vein. Also some other minor pyrrhotite blebs, possibly some very minor pentlandite. Some fine grained satellite sulphides are observed, 100% chalcopyrite.
AMK21-6A (236.54 - 236.82)	Fine grained (<2mm) disseminated interstitial sulphides. Occur as blebs and as very small veinlets along the edges of silicates. Grains are either chalcopyrite with very very minor pentlandite and pyrrhotite, or pyrrhotite with minor pentlandite along the rims.
AMK21-6B (236.54 - 236.82)	Fine grained (<1mm) highly disseminated blebs. Generally pyrrhotite with pentlandite and chalcopyrite ocuuring predominantly on the rims. Some of the smaller grains are pure chalcopyrite, and some are pyrrhotite with minor pentlandite

AMK21-7 (240.37 - 240.86)	Fine to very fine grained highly disseminated sulphides. Compositions vary, and are either 95% chalcopyrite, or 40% pentalandite, 40% pyrrhotite, 20% chalcopyrite.
AMK21-12 (342.97 - 343.30)	Fine grained disseminated blebs (<1mm). Usually about 60% pyrrhotite. Can contain pentlandite, and pentlandite+chalcopyrite usually around the rims of the pyrrhotite.

ATS57-57.58	Medium grained (1-2mm) interstitial blebby sulphides, with very thin veinlets around the edges of some of silicates. Blebs are 60-80% pyrrhotite, with the remainder usually being pentlandite. Some flame textures seen. Some blebs have ~5% chalcopyrite on rim. All the thin veinlets are chalocpyrite, appear to be later than blebs.
ATS57-72.48A	Very coarse grained sulphide bleb (1.5cm x 2cm), 80% chalcopyrite, pyrhhotite or pentlandite occurs mainly on the rims, with some small grains within the chalcopyrite, and accessory sphalerite
ATS57-72.48B	2 large sulphide blebs (0.5 - 1.2cm), which may be interstitial, with several smaller satellite grains (1-2mm). Dominated by chalcopyrite (85%), with mainly pyrhhotite around the rims, with some pentlandite.
ATS57-102.79	Very fine grained (<1mm),very disseminated sulphides. Think they are all pentlandite.
ATS57-118.78	Fine to coarse grained (1-12 mm) interstitial sulphides. Dominantly pyrrhotite (60-80%) with small grains of chalcopyrite and pentlandite on the rims of the grains.
ATS57-140.14	Fine to coarse grained (1-12 mm) interstitial sulphides, as well as thin veinlets surrounding some silicates. Blebs are 80% pyrrhotite with pentlandite and chalcopyrite grains around the rims, the veinlets are all chalcopyrite.
ATS57-151.40	One interstitial sulphide grain (2x4mm). I think it is completely pentlandite. Some stringers of something that might be magnetite.
ATS57-180.64	Disseminated blebby sulphides (<1mm to 5mm). Think they are 80% pentlandite with chalcopyrite grains around the rims.
ATS57-218.39A1	Massive and net textured sulphides, silicates are highly altered. Sulphide look 'moth-eaten'. Very complex mineralogy, 60-80% pyrrhotite, with zones of pentlandite and chalcopyrite, not only on rim but also within pyrrhotite.
ATS57-218.39A2	Massive sulphide with net-texture. Silicate grains are 1-3mm and occur as 'clasts' within a sulphide 'matrix'. Again a very complex mineralogy, 60-80% pyrrhotite, with zones of pentlandite and chalcopyrite, not only on rim but also within pyrrhotite.
ATS57-218.39C1	Fine grained (1-2mm) interstitial sulphides, surrounding serpentinised silicates. Generally 75% pyrrhotite, with chalcopyrite usually on rims. One grain appears to be pentlandite and chalcopyrite.
ATS57-218.39C2	Massive sulphide, with large (1mm - 1cm) rounded silicate clasts. 70-80% pyrhhotite, with zones of chalcopyrite and pentlandite.

ATS57-218.39C3	Massive sulphide, with large (1mm - 1cm) rounded silicate clasts, also some interstitial sulphide occuring as veinlets around silicate grains. 70-80% pyrhhotite, with zones of chalcopyrite and pentlandite. Sulphides may have corroded silicates.
ATS57-221.39B1	Massive sulphide with silicate clasts, 'net-textured' in places. Again sulphides seem to have corroded silicates in places. Again, 70-80% pyrrhotite with zones of chalcopyrite and pentlandite. There are also patches of chalcopyrite by itself.
ATS57-221.39B2	Massive sulphide with two zones of 'net-texture'. Appears that chalcopyrite/pentlandite zones are related to the silicates. Massive is 99% pyrrhotite, although there are flame exsolution textures of pentlandite associated to small silicate veins and clasts. In net-textured zone the sulphides are mixture of pyrrhotite, chalcopyrite and pentlandite and (usually chalcopyrite) has corroded the silicates.
ATS57-268.15A	Very fine grained (<1mm) disseminated sulphides. 70-80% pyrrhotite, with chalcopyrite and pentlandite blebs usually on the rims.
ATS57-268.15B1	Medium grained (1-2mm) disseminated sulphides. 70-80% pyrrhotite, with chalcopyrite and pentlandite blebs usually on the rims.
ATS57-268.15B2	Fine grained net-textured sulphides, with one large (1.5cm) rounded silicate clast. Concentration of sulphide increases on the rims of this silicate. 50-80% pyrrhotite, with zones of intermixed chalcopyrite and pentlandite which are more prevelent close to large silicate grain. Some corrosion of silicates has occured.
ATS57-290.41	Medium grained (1-2mm) disseminated sulphides. 50-70% pyrrhotite, with chalcopyrite. Large percentage of magnetite, not only in sulphides but also in silicates.
ATS57-325.32A	Massive sulphide bleb with associated smaller blebs (almost looks like a flow texture). Almost all of it is pyrrhotite, with some minor chalcopyrite in the finer grains on the edges.
ATS57-335.07	Fine-grained disseminated sulphides, varying in size from <1mm to 3mm. I think it is pyrite.
ATS57-335.07A	Fine-grained disseminated sulphides, varying in size from <1mm to 3mm, although larger grains may be an amalgamation of smaller grains. Probably pyrite.
ATS57-335.07B	Fine-grained disseminated sulphides, varying in size from <1mm to 3mm, although larger grains may be an amalgamation of smaller grains. Probably pyrite.

ATS46b (61.05 - 61.19)	One large >20mm sulphide bleb composed of pyrrhotite (75%), pentlandite (5%) and chalcopyrite (20%). The three phases are seperate, with the pentlandite occuring as a vein between the chalcopyrite and pyrrhotite.
ATS46ah (106.25 - 106.53)	Sulphide total approx. 2% (mode) of 3mm disseminated intercumulus composite pyrrhotite (80%), pentlandite and chalcopyrite (10-20%)

ATS46e1 (146.53 - 146.88)	Sulphide total approx. 13-18% (mode) of <6mm disseminated intercumulus blebs of pyrrhotite (93-97%), pentlandite (1-2) and chalcopyrite (2-3%).
ATS46ap*a* (154.55 - 154.79)	Sub-horizontal vein of sulphide-rich net-textured pyrrhotite.
ATS46g (165.73 - 165.91)	Sulphide total approx. 7-8% (mode) of <5mm disseminated intercumulus pyrrhotite (85%) pentlandite (5%) and chalcopyrite (10%), and sub-net textured pyrrhotite (97-98%), pentlandite (2-3%) & chalcopyrite (1-2%).
ATS46i1 (207.25 - 207.74)	Sulphides total 6% (mode) of large 10mm sized blebs composed of composite pyrrhotite (85%), chalcopyrite (12%0 and pentlandite (3%).
ATS46i2 (207.25 - 207.74)	Small 8mm wide net-textured veinlet composed of pyrrhotite and minor pentlandite (92-94%) and chalcopyrite (6-8%).
ATS46j (227.07 - 227.33)	Sulphides total approx. 7-25% (mode), average 13% of <7mm disseminated intercumulus pyrrhotite & (97-98%), chalcopyrite (2-3%).
ATS46aw (254.87 - 255.11)	Sulphide total approx. 4-5% (mode) of 2mm disseminated intercumulus to net-textured pyrrhotite (92-96%), pentlandite and chalcopyrite (4-8%)
ATS46m2 (275.80 - 276.20)	Sulphide total approx. 8% (mode) of <5mm disseminated intercumulus to patchy sub-net textured pyrrhotite (88-90%), pentlandite (0-2%) and chalcopyrite (10-12%).
ATS46bd (316.41 - 316.83)	Sulphide total approx. 6-8% (mode) of 4mm disseminated intercumulus to patchs of sub-net textured pyrrhotite (99%), pentlandite and chalcopyrite (1%).
ATS46bg (345.50 - 345.69)	Sulphide in dunitic unit total approx. 35-40% (mode) of 7mm net textured pyrrhotite (95-98%), pentlandite and chalcopyrite (2-5%).
ATS46bi (370.33 - 370.63)	Sulphide total approx. 10-13% (mode) of 9mm disseminated intercumulus blebs of pyrrhotite (85-95%), pentlandite, and chalcopyrite and bornite (5-15%).
ATS46bp*a* (438.15 - 438.31)	Sulphide total approx. 4-7% (mode) of 4mm disseminated intercumulus to patches of sub massive textured pyrrhotite (85-90%), pentlandite and chalcopyrite (10-15%).
ATS46w (469.25 - 496.50)	Sulphides total 56% (mode) in green serpentine clot, of small <1mm finely disseminated mono-mineralic pyrrhotite (100%).

APPENDIX 5a

Description of sulphide mineralisation intervals for core PR-174

Sulphide Interval			Host Rock	Sulphide Description
From (m)	To (m)	Length (m)		
13	23	10	Feldspathic Pyroxenite	Very fine grained, disseminated interstitial sulphides
55	56	1	Norite	Blebby sulphides (1-2 cm), 80% pent/pyrr. 20% chalc. Occur just below slightly serpentinised zone. Some sulphides associated to pegmatitic zone.
73	76	3	Serpentinised Pyroxenite	Blebby interstitial sulphides (1-5 mm), generally associated to serpentinised zones. Grains are either pent/pyrr OR chalc, you do not see both phases together.
76	77	1	Pegmatoidal Feldspathic Pyroxenite	Fine-grained interstitial sulphides, predominantly pent/pyrr. Associated to very fine-grained pale grey/green raft, and pegmatitic raft.
80	81	1	Serpentinite	Large (1-2 cm) bleeby, interstitial sulphides, also some finer grained material (<3 mm). Generally 80% pent/pyrr, 20% chalc, however % of chalc varies.
82	83.36	1.36	Very coarse grained/pegmatoidal pyroxenite, dominated by opx.	Sulphides occur as 1-2 cm blebs, which are either pent/pyrr OR chalc, no mixed grains.
83	105	22	Norite	Fine-grained (1-3 mm) interstitial sulphides. 90% pent/pyrr, 10% chalc.
105.52	106.74	1.22	Serpentinised Pyroxenite	Sulphides have variable grain size (1mm - 1 cm), ~90% pent/pyrr, ~10% chalc.
108	111	3	Feldspathic Pyroxenite	Texture changes from above, fewer sulphides, and finer grained
188	189	1	Feldspathic Pyroxenite	3cm thick zone of 50% sulphides with 'cumulus' silicates (net-textured). Sulphides are pent/pyrr.
204	229	25	Blocks of gabbro-norite with pyroxenite (Granofels).	Sulphides are associated to serpentinised zones, usually interstitial, with same grain size as host rock. 80% pent/pyrr, 20% chalc.
229	230	1	Feldspathic Pyroxenite	Large sulphide bleb (4 cm) with other associated smaller blebs (1 - 6 mm). Generally pent/pyrr, with chalc found on rims.
230	231	1	Feldspathic Pyroxenite	Smaller (1-2 mm) interstitial sulphides, dominantly pent/pyrr.
240	245	5	Highly serpentinised zone of pyroxenite.	Sulphides occur as blebs of varying size (2 mm - 3 cm). Dominantly pent/pyrr with chalc. occuring on the rims.

APPENDIX 5b

Description of sulphide mineralisation intervals for core PR-175

Sulphide Interval			Host Rock	Sulphide Description
From (m)	To (m)	Length (m)		
0	34	34	Feldspathic Pyroxentie / Norite	Fine-grained interstitial, disseminated sulphides. 75% pent/pyrr, 25% chalc. Grain size of blebs varies with change in silicate grain size.
35	51	16	Gabbro-type rock	Sulphides are larger and more blebby and do not always correlate with silicate grain size. Not as magmatic? 80% pent/pyrr, 20% chalc.
59	89	30	Variable norite/gabbro (depends on change in % px.)	Sulphide grain sizes vary with silicate grain size, are generally intergranular. Dominated by pent/pyrr, but more chalc. Is seen in feldspathic zones.
91	92	1	Feldspathic zone	Sulphides occur as large blebs (2mm - 2cm), and are sometimes intergranular but not always. Show pent/pyrr - chalc immiscibility
98	106	8	Very coarse grained pyroxenite.	Sulphides are fine-grained, disseminated and intergranular, some larger sulphides occur (~1 cm), but not as blebs. Dominated by pent/pyrr.
113	116	3	Slightly feldspathic pyroxenite	Sulphides are blebby and intergranular, they are dominated by pent/pyrr.
			DOLOMITE ZONE	
128	134	6	Varying percentage of pyroxene to plagioclase, slightly more feldspathic.	Sulphides are blebby and have a larger grain size than associated silicates. They are dominantly pent/pyrr.
			Spotted anorthosite, followed by a dolomite raft. Large alteration halo seen.	Generally no sulphides, although some very fine-grained, very disseminated sulphides seen, usually associated with pyroxenite blocks.
227	228	1	Pyroxenite just above feldpathic block.	Fine-grained (1-2 mm) intergranular sulphides dominated by pent/pyrr.
245	250	5	Generally pyroxenite with some alteration zones	Sulphides usually fine-grained and disseminated, although some larger (1 2 cm) intergranular blebs occur. 90% pent/pyrr, 10% chalc.
257	258	1	Pyroxenite	Several pent/pyrr blebs (~5 mm grain size)

287	289	2	Medium-grained pyroxenite	Sulphide blebs (1-5 mm) associated to feldspathic zones, 90% pent/pyrr, 10% chalc.
296	296		Feldspathic Pyroxenite	Large (1cm wide, 6cm long) pent/pyrr bleb.
297	298	1	Pyroxenite/ Feldspathic Pyroxenite	A few intergranular pent/pyrr blebs
303	305	2	Feldspathic - gabbro/norite	Blebby sulphides which vary in size (2 mm - 2 cm), 70% pent/pyrr, 30% chalc.
312	313	1	Feldspathic Pyroxenite	Large sulphide blebs up to 4 cm in size. 70% pent/pyrr, 30 % chalc, with chalc generally occuring on rims.
318	320	2	Pyroxenite	Fine grained interstitial sulphides, disseminated, seem to be dominated by pent/pyrr.
332	336	4	Fine-grained pyroxenite	Fine-grained interstitial sulphides, some slightly larger blebs, generally dominated by pent/pyrr.

APPENDIX SIX

PUBLICATIONS

A new look at sulphide mineralisation of the northern limb, Bushveld Complex: a stable isotope study

E. R. Sharman-Harris, J. A. Kinnaird, C. Harris and U. E. Horstmann

The Platreef is the main platinum-group element (PGE)-bearing horizon in the northern limb of the Bushveld Complex, South Africa. It is considered to be richer in sulphides than other similar horizons within the Bushveld Complex, in particular the Merensky Reef. Previous work has indicated that assimilation of dolomite may be a mechanism to add sulphur to the magma from which the Platreef formed. Sulphur isotope data presented in this study indicates an additional sulphur source contributing to the Platreef. In the southern Platreef, the Duitschland Formation of the Transvaal Supergroup forms part of the direct footwall. Within this sequence are pyrite-rich shales, which we suggest contributed to the sulphur budget of the Platreef. Local variations in sulphur isotopes, as well as a decrease in crustal sulphur in the Platreef further away from the footwall, also indicate local rather than regional contamination processes. Platreef samples have $\delta^{18}O$ values that are higher than expected in a mantle-derived magma, but there is no apparent systematic variation in $\delta^{18}O$ with distance from the footwall. This may possibly indicate contamination of the Bushveld magma pre-intrusion, probably in a staging chamber. However, when compared to data from the central sector of the Platreef itself, analysis from this study have lower $\delta^{18}O$ values indicating changes in the degree of contamination with varying footwall lithology. Also, differences between plagioclase and pyroxene $\delta^{18}O$ values indicate exchange with fluids. It is possible that late-stage deuteric fluids may have caused this exchange.

E. R. Sharman-Harris (E-mail: sharmane@science.pg.wits.ac.za) and J. A. Kinnaird (for correspondence E-mail: kinnairdj@geosciences.wits.ac.za) are in the School of Geosciences, University of the Witwatersrand, Private Bag 3, Wits, 2050, South Africa; C. Harris (E-mail: charris@geology.uct.ac.za) is in the Department of Geological Sciences, University of Cape Town, Rondebosch 7700, South Africa; and U. E. Horstmann (E-mail: horstmann@src.wits.ac.za) is at iThemba Labs Gauteng, Private Bag 11, Wits, 2050, South Africa.

 Manuscript received 9 July 2005; accepted in final form 4 November 2005.

Keywords: Bushveld Complex, sulphide mineralisation, S/O isotopes, $\delta^{18}O$ values, $\delta^{34}S$ values

INTRODUCTION

The Platreef is the main platinum-group element (PGE) bearing lithology of the northern limb of the Bushveld Complex. It has been the site of platinum prospecting and mining since the 1920s. The term Platreef as used in this paper refers to a series of pyroxenites and norites, containing xenoliths/rafts of footwall rock. The Platreef is irregularly mineralised with PGE, Cu and Ni, and a greater modal percentage of sulphides is present than in the Merensky Reef. There is an extremely varied PGE mineralogy, occurring mainly as tellurides, bismuthotellurides, antimonides and arsenides of Pd, Pt, and Rh.[1,20] The main base-metal sulphides within the Platreef are pyrrhotite, pyrite, pentlandite, and chalcopyrite.

In this paper, we aim to examine sulphur and oxygen isotope data from the southern sector of the Platreef to gain a better understanding of the role that contamination played and in order to compare these data to those from earlier work conducted in the central and northern sectors of the Platreef. We conducted a detailed isotopic study through 400 m of the Platreef and also investigated isotopic variations in different metasedimentary footwall lithologies of the Platreef itself as well as from unaltered sedimentary lithologies of the Duitschland Formation.

REGIONAL GEOGRAPHY

Transvaal Supergroup

The Palaeoproterozoic Transvaal Supergroup (Fig. 1) was deposited between 2·67 and 2·07 Ga[8,10] in the Transvaal and the Griqualand West Basins which are separated by the Vryburg Rise.[3] The Supergroup attains a maximum thickness of 12 km within the Transvaal Basin.[10] The basement rocks of the Transvaal Supergroup are predominantly Archaean granites, gneisses and greenstones, as well as a Witwatersrand sedimentary succession and Ventersdorp lavas.[8,10] The Transvaal Supergroup comprises the Wolkberg, Chuinespoort, and Pretoria Groups (Fig. 1); however, as there is an erosional contact between the Wolkberg and Chuniespoort Groups, Coetzee[8] does not consider the Wolkberg group to be part of the Transvaal Basin *sensu stricto*.

 DOI 10.1179/037174505X82134

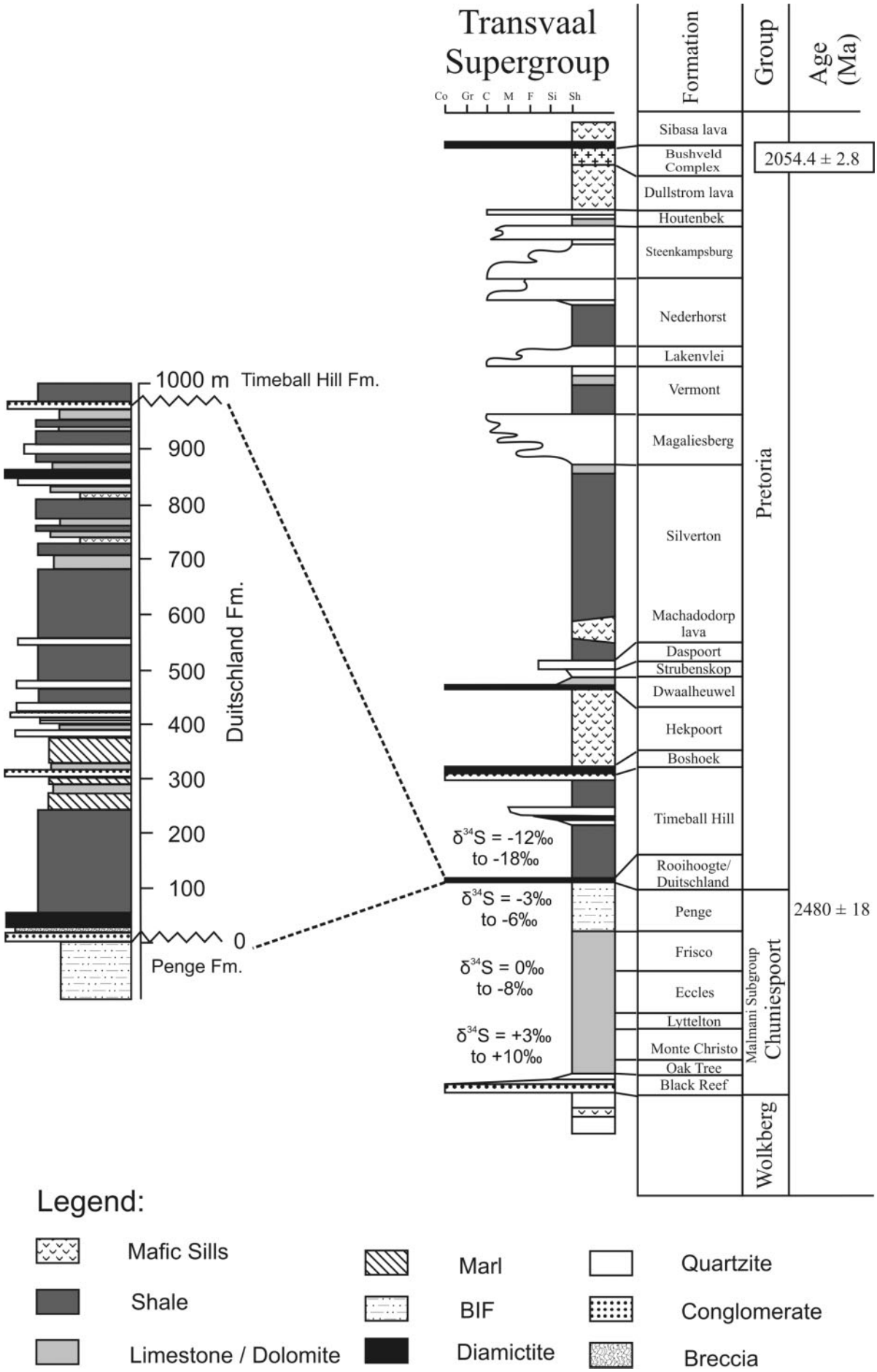

1 Stratigraphic column of the Transvaal Supergroup, showing detail of the Duitschland Formation[3,8]

In the southern sector of the Platreef, where this study is focused, the footwall is often comprised of Duitschland Formation which marks the base of the Pretoria Group and disconformably overlies the Chuniespoort Group. It comprises diamictite, an alternating sequence of fine-grained laminated shales; occasionally containing pyrite and dolomite, along with some minor sequences of quartzite and mudrock (Fig. 1). The formation is exposed in two areas near Mokopane and has a maximum thickness of 1000 m.[28] The Duitschland Formation is thought to have been deposited in a relatively shallow marine environment,[3,28] which is supported by the presence of stromatolites. Carbonaceous shales represent the deepest depositional environment within the formation.[28] The base of the formation is marked by a diamictite, and the top of the formation is characterised by an ivory-white dolomite containing bornite and chalcopyrite. It is bounded at its base in the north by the Penge Iron Formation which is composed predominantly of quartz, magnetite and hematite[8] and also contains subordinate carbonaceous shale beds. The top of the sequence in the study area is marked by Timeball Hill Formation which is composed of shale, quartzite, and diamictite.

Bushveld Complex

The Bushveld Complex (BC), which intruded into the Transvaal Supergroup, comprises the Rustenburg Layered Suite (RLS) – a thick sequence of layered mafic and ultramafic rocks ranging from dunite and pyroxenite, to anorthosite and pure oxide layers[9] – as well as the Bushveld Granites. The Bushveld Complex covers an area of approximately 65 000 km^2, with a thickness of 7–9 km. The rocks of the RLS occur in extensive layers of varying thickness, and despite their age of 2·05 Ga[14] have experienced no metamorphism, and only mild or local alteration.[9] The RLS comprises five major limbs – the western limb, the far western limb, the northern limb, the eastern limb (all of which outcrop at surface) and the south-eastern or Bethal limb, which is covered by younger sediments. The western and eastern limbs are the best known, being the most extensive, with average lengths of ~200 km. The northern limb is partially concealed beneath younger rocks of the Waterberg Supergroup, the far western limb is an eroded remnant, and the Bethal limb is only identifiable through a gravity high, with its location confirmed by borehole data.[9] The stratigraphy of the RLS is divided into five zones – the Marginal Zone, Lower Zone (LZ), Critical Zone (CZ), Main Zone (MZ), and Upper Zone (UZ).[9]

Northern limb

The northern limb occurs as a slightly sinuous, north-west striking sequence with a length of 110 km and a maximum width of 15 km,[1,34] and differs in several ways from the eastern and western limbs. Previously, not all of the zones of the Bushveld Complex were thought to be represented in the northern limb, where the existence of units from the Critical Zone were yet to be identified north of Mokopane (formerly Potgietersus) and units from the Lower Zone were thought to only be present south of Mokopane[4,16] and as satellite bodies. Current work, however, indicates that a Lower Zone component comprising pyroxenites and harzburgites occurs at the base of the succession south of Farm Tweefontein, as well as in satellite bodies.[22] Marginal Zone norite also occurs sporadically within the succession on farms Macalacaskop 243KR and Turfspruit 241KR. These sequences are followed by the Platreef itself, and it appears that the entire magmatic sequence has an overlapping relationship with the floor rocks, with each subsequent magmatic event being intruded over a wider area than the previous sequences.

The hanging-wall rocks of the Platreef are generally PGE-poor Main Zone comprising predominantly gabbronorite and are up to 2000 m in thickness.[34] The thickness of the MZ in the northern limb is much less than in the eastern and western limbs of the Bushveld Complex. This Main Zone is followed by Upper Zone cyclic units of magnetite, magnetite gabbro, gabbro and anorthosite, which are ~1500 m thick.[2] In the west, the hanging wall is a variety of Bushveld granites and metasedimentary rocks.[22]

An important feature of the northern limb is that the layered rocks have a transgressive relationship with the country rocks of the Transvaal Supergroup (*i.e.* the intrusion rests on progressively older rocks towards the north). To the south of the town of Mokopane, the floor rocks comprise Magaliesburg quartzites. Northwards, the floor rocks first comprise the Pretoria Group, the banded iron-formations and dolomites of the Chuniespoort Group, and finally the Archaean granites.[16] The entire layered sequence pinches out to the north.[4,16,34]

General geology of the Platreef

The Platreef, which is the major PGE-bearing layer of the northern limb, occurs at the base of the layered rocks. The Platreef comprises a 'complex series of medium-to-coarse-grained pyroxenites and norites that contains xenoliths of the floor rocks'.[12] It is observed as being a highly inhomogeneous body, comprising different rock types including pyroxenites, para-pyroxenites, feldspathic pyroxenites (pyroxenites with > 10% interstitial plagioclase), serpentinites, gabbronorites and norites. The Platreef itself has been equated with the Critical Zone and, specifically, the Merensky Reef, of the Bushveld Complex proper,[35,36] although other authors have regarded the Platreef as the base of the Main Zone.[33]

The Platreef also contains xenoliths of altered footwall, which vary depending on the footwall; however, the composition of these rafts is not always the same as the directly underlying footwall. For example, the hornfels rafts within the Platreef; that have a Duitschland Formation footwall of dolomitic marble; have a mineral composition of aluminous cordierite-spinel hornfels. These rafts comprise mainly cordierite, with disseminated green spinel, and accessory corundum, sillimanite and andalusite, that indicates a high-grade of metamorphism of a shale

protolith. Another example is the occurrence of calc–silicate rafts in the northern sector of the Platreef on the Farm Drenthe, where the direct footwall is Archaean granite.[12,22]

The base- and precious-metal mineralisation of the Platreef is unevenly distributed, and occurs over a zone that is up to 400 m thick.[22] The sulphides in the Platreef usually occur as a combination of pyrhhotite, pentlandite, chalcopyrite and, occasionally, pyrite and bornite, which exist as several different styles or phases of mineralisation. Massive sulphides are recorded in core up to several metres in thickness, and often contain a complex assemblage of sulphide minerals. Typically, these massive sulphides are dominated by pyrrhotite. Chalcopyrite usually occurs around the rims of the pyrrhotite, and has pentlandite associated with it. Pentlandite also occurs as veins, and as exsolution lamellae within the pyrrhotite. More rarely, these massive sulphides are dominated by chalcopyrite, which have pyrrhotite veins running through them. Associated with massive sulphides, and often within serpentinites are 'net-textured' sulphides that occur as a matrix to the silicate minerals, with samples having 50–80 modal percent sulphides. 'Net-textured' sulphides are dominated by pyrrhotite, with minor chalcopyrite and pentlandite.

Fine-to-medium-grained disseminated sulphides are common in the finer grained lithologies of the Platreef, and are often interstitial. These sulphides have a different modal mineralogy than that of the massive or 'net-textured' sulphides. They usually comprise approximately 50% pentlandite, 40% chalcopyrite, as well as pyrrhotite and occasional bornite. 'Blebby' sulphides also occur, and contain a similar combination of sulphide minerals to that of the interstitial sulphides. These blebby sulphides are often observed as pyrrhotite with chalcopyrite rims.

Sulphides also occur within the metamorphosed footwall of the Platreef, particularly within calc–silicates, but also occasionally within cordierite spinel hornfels. Typically, these sulphides are cubic pyrite, but pyrrhotite has also been observed, sometimes occurring in a cubic form. This is probably due to the conversion of pyrite to pyrrhotite during the metamorphism of the footwall. It should also be noted that mineralisation occurs around calc–silicate rafts within the Main Zone of the northern limb, especially in the northern sector of the Platreef, and shows similarities to that in the Platreef (*sensu stricto*).[12,22]

The sulphide mineralisation was thought to be of primarily magmatic origin by some authors;[33] however, evidence for post-magmatic fluid interaction[16] is also present. Buchanan *et al.*,[4] Harris and Chaumba,[16] and Armitage *et al.*[1] suggested that assimilation, or contamination, by sedimentary floor rocks, especially those rich in sulphur, may have contributed to the sulphide mineralisation of the Platreef. Petrographic studies indicate an association between sulphides and biotite, as well as the alteration of silicates in samples with high sulphide content. The degree of alteration associated with sulphides, as well as the presence of biotite, is probably due to an interaction between pre-existing silicate minerals, and an immiscible sulphide liquid or later fluid-rich phase.

It has previously been assumed that the Pt and Pd mineralisation within the Platreef was associated with sulphide mineralisation. Armitage *et al.*[1] noted that the occurrence of PGE mineralisation associated with alteration zones indicates 'syn- to post-magmatic crystallization or redistribution of PGE by hydrothermal fluids'. The authors also noted that the PGE mineralisation in the Platreef in the central sector is more complex than previously thought, and that several different mineralisation processes have been involved in its formation. A new detailed study using laser ablation-inductively coupled plasma–mass spectrometry has revealed that, while Pd, Ru, Rh and some Os and Ir are commonly hosted by sulphides, Pt generally is not.[21] In addition, a number of Pt-bearing minerals, including geversite ($PtSb_2$) and sperrylite ($PtAs_2$) and various Pt–Pd–Bi–Te-antimonide, Pd–Pt–Sb–Bi-telluride and Pd–Pt–Bi-telludide phases have been seen to occur in the silicates external to the sulphides. This may be linked to contamination. Hutchinson and McDonald[21] noted that where the degree of contamination was high, the Pt formed As and Sb complexes, which were subsequently expelled from the sulphide liquids. As a result of this, Pt was fractionated from Pd and the other platinum-group elements which remained within the sulphide minerals.

Previous stable isotope studies

The first sulphur isotope analyses conducted on the northern limb were by Liebenberg.[24] He recorded two $\delta^{34}S$ values for the farm Zwartfontein 818LR, both of which had approximate magmatic values of +0·7‰ (for a calc–silicate) and +1·9‰ (from a pegmatoidal norite; Fig. 3). Hulbert[19] presented data from Lower Zone pyroxenites and chromitites south of Mokopane, as well as pyroxenites, chromitites and anorthosites from the Critical Zone. These yielded $\delta^{34}S$ values from +0·96‰ to +7·54‰ (Fig. 3). He also analysed two samples of Upper Zone material from the northern sector of the Platreef on farm Molendraai, which also had $\delta^{34}S$ values of approximately +2‰ (Fig. 3). Hulbert interpreted these data as indicating that the majority of sulphur associated with sulphides is of mantle origin. Elevated $\delta^{34}S$ values were ascribed to an increased fo_2 which the author proposed was due to the release of volatiles from sedimentary material.[19]

The majority of the sulphur isotope data available for the Platreef itself prior to this work was presented by Buchanan *et al.*[4] and Buchanan and Rouse[5] and was for a variety of sulphide samples taken from Tweefontein and Turfspruit farms (Fig. 3). These samples indicated $\delta^{34}S$ values in pyrrhotite of +6‰ to +9‰, which they suggested might have originated from contamination by anhydrite within the Malmani Dolomite.[4] Sulphides from graphite layers on Farm Turfspruit yielded values of –2·42‰ to +2·0‰.[5]

Manyeruke and Maier[27] examined samples taken from a core on farm Townlands (Fig. 3), and identified three different units separated by hornfels

rafts, which they termed the Upper, Middle and Lower Platreef. Sulphur isotope values from this core indicated that the Upper and Lower Platreefs had elevated $\delta^{34}S$ values of about +8‰, whereas the Middle Platreef had $\delta^{34}S$ values of about +4‰. These elevated values were also attributed to the addition of sulphur of crustal origin.

Cameron[6] investigated sulphur isotope variations for the Transvaal Supergroup, specifically for the Timeball Hill shale, Penge Iron Formation, the Malmani Subgroup, and the Black Reef Quartzite in the eastern Bushveld. It is recorded that the majority of these lithologies have significantly negative $\delta^{34}S$ values. The Timeball Hill Formation yielded $\delta^{34}S$ values of –12‰ to –18‰, and the Penge Formation has $\delta^{34}S$ values of –3‰ to –6‰ (Fig. 1). Pyrite-bearing shales from the Malmani Subgroup showed some variations, with the upper three-quarters yielding $\delta^{34}S$ values of 0‰ to –8‰, and the lower quarter yielding values of +3‰ to +10‰. Pyrite in quartzites of the Black Reef Formation gave $\delta^{34}S$ values of about +3‰ (Fig. 1).

Li *et al.*[23] examined sulphur isotope variations for the Uitkomst Complex, which is considered to be a satellite body of the eastern Bushveld Complex. In the unmineralised lithologies of the complex, as well as the basal gabbro, $\delta^{34}S$ values are recorded as being close to magmatic (–0·9‰ to +2·6‰). However, in the sulphide-bearing harzburgites, the $\delta^{34}S$ values indicated a contribution from crustal sulphur (–2·6‰ to –7·1‰), which the authors proposed was probably from either the Malmani Subgroup or the Timeball Hill Formation.

Oxygen isotope work has been conducted both on the northern limb,[16,17] and on the eastern and western limbs of the Bushveld.[30,31] Schiffries and Rye[31] recorded $\delta^{18}O$ values from mineral separates within the RLS at approximately 1‰ higher than values expected for a basaltic magma. No systematic variation with stratigraphic height was observed. This was suggested to indicate RLS magmas were contaminated and were well mixed before emplacement. The slightly elevated $\delta^{18}O$ values could be attributed to the assimilation of Transvaal Supergroup rocks into the magma, *i.e.* up to 10–29% contamination.

This observation was supported by Harris *et al.*[17] who also found slight elevated $\delta^{18}O$ values, and no stratigraphic variation. This is thought to indicate that BC magmas were contaminated before emplacement, supporting the staging chamber hypothesis. However, the most likely contaminant is suggested to be the middle-to-lower crust, and not Transvaal rocks as previously proposed. This is also supported by a Sr–Nd isotope study conducted by Maier *et al.*[25]

Reid *et al.*[30] examined samples taken the footwall of the Merensky Reef as it occurs in a pothole formed in the Merensky Reef of the western limb of the Bushveld Complex. They found that their $\delta^{18}O$ data agreed well with that of Schiffries and Rye,[31] with $\delta^{18}O_{plag}$ values of approximately +7·1‰, and $\delta^{18}O_{opx}$ values of approximately +6·6‰. No variation with depth was observed by the authors. They also recorded a $\Delta_{plagioclase–pyroxene}$ = 0·5‰, indicating that magmatic processes were responsible for silicate formation. This is also in agreement with Schiffries and Rye.[31]

Harris and Chaumba[17] conducted stable isotope studies on plagioclase and pyroxenes taken from feldspathic pyroxenites of the Platreef at Sandsloot Mine in the northern limb. These samples (which were genuine magmatic feldspathic pyroxenites) indicated assimilation of Malmani Dolomite footwall.

METHODOLOGY

Sample selection

Sulphides for this study were collected through a vertical Platreef profile of 450 m and from sulphide-bearing footwall lithologies. Samples were chosen from selected cores on Farms Macalacaskop (AMK-21), Turfspruit (ATS-46, ATS-57, ITS-33) and Rietfontein (ARF-08) (Fig. 2). The cores selected had varying footwall lithologies including pyritic shales, sulphide-bearing dolomite of the Duitschland Formation and anhydrite-bearing dolomite of the Malamani Subgroup. Sulphides from the Platreef were collected systematically from top to bottom and included disseminated, blebby, net-textured and massive ore together with sulphides from hornfels xenoliths. Chosen samples were either crushed or

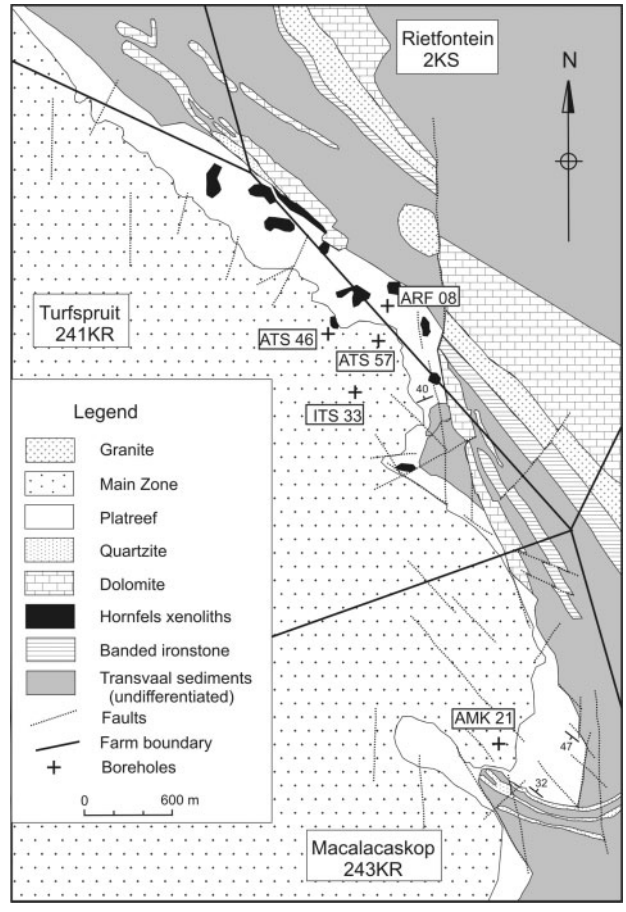

2 Geological map of the northern limb of the Bushveld Complex showing the location of boreholes used in this study

prepared into polished blocks. An oxygen isotope study was also conducted to compare any effects of crustal contamination on host rock silicates with those of sulphide minerals.

Sample preparation

Samples that were crushed were then milled, and sieved to –125+90 μm in size. These fractions were then washed and dried to remove any very fine material. Samples were also cleaned of any heavily magnetic minerals (*i.e.* magnetite or pyrrhotite) using a hand magnet, then separated according to magnetic susceptibility on a Frantz Isodynamic Separator using various amperages. Separates were then further cleaned to remove any remaining silicates using heavy liquid separation (bromoform) resulting in pure sulphide fractions. For samples where it was not possible to separate out pure sulphides, mineral separates were extracted by microdrill from polished blocks at University College London. This drill allows for the extraction of mineral separates on a small scale as its tip is approximately 50 μm in diameter.

Sulphur isotope analyses were conducted on pyrrhotite, pentlandite and chalcopyrite mineral separates from the Platreef, pyrrhotite and pyrite from hornfels within cores, as well as on pyrite and bornite from footwall material of the Duitschland Formation. Anhydrite samples from a dolomite, which occurs in the Central Sector of the Platreef, were also analysed for comparative purposes. Sulphur isotope analyses were conducted at the Environmental Isotope Laboratory of the iThemba Laboratories in South

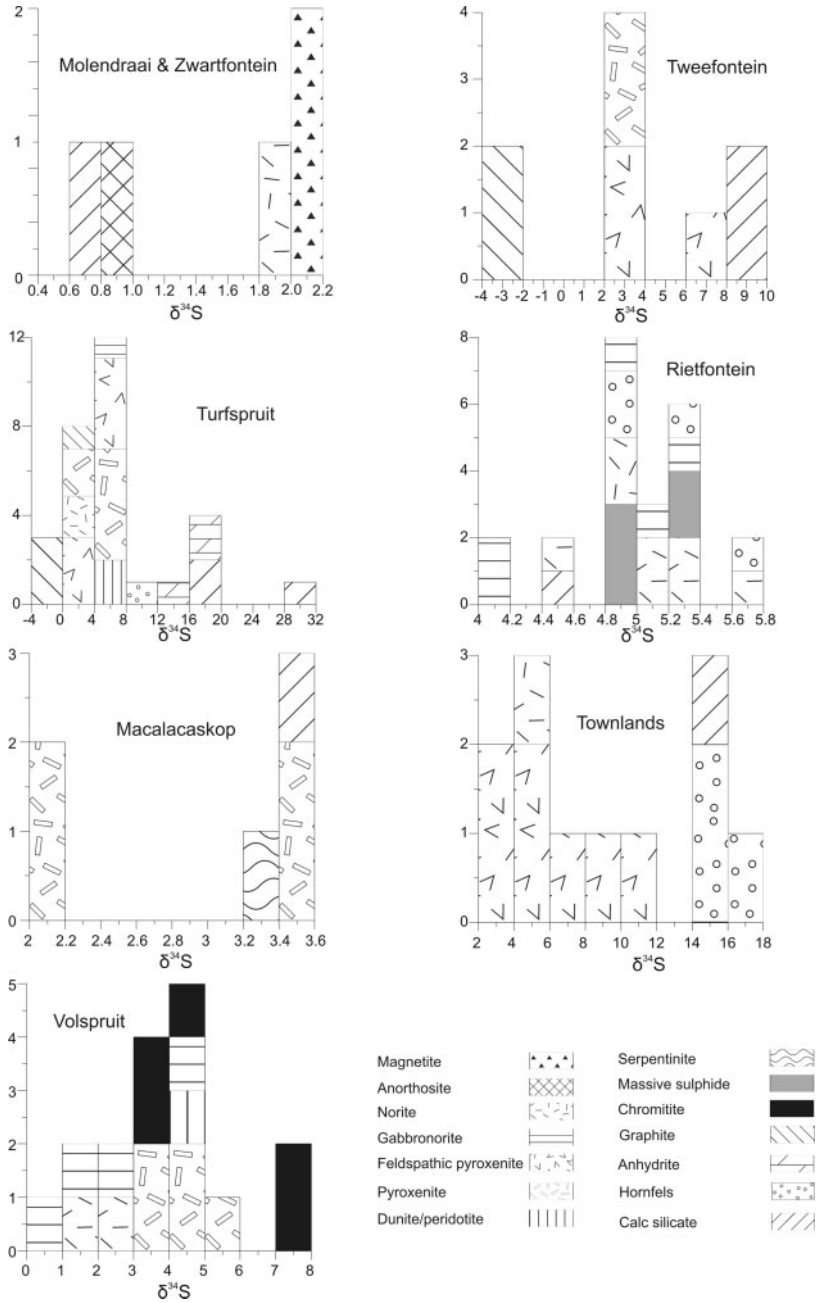

3 Histograms showing all of the sulphur isotope analyses for the northern limb of the Bushveld Complex. Data for Zwartfontein from Liebenberg;[24] data for Macalacaskop, Turfspruit and Rietfontein from this study; data for Tweefontein from Buchanan *et al.*[4] and Buchanan and Rouse;[5] data for Townlands from Manyeruke;[26] and data for Molendraai and Volspruit from Hulbert[19]

Table 1 Sulphur isotope data in per mil relative to CDT

Sample number	Rock type	Mineral	Sulphide/sulphate texture	$\delta^{34}S‰$ CDT
ARF 08/36.42	Cordierite-Spinel Hornfels	Pyrrhotite	Fine-grained disseminated	5·3
ARF 08/36.42	Cordierite-Spinel Hornfels	Chalcopyrite	Fine-grained disseminated	5·6
ARF 08/36.53	Cordierite-Spinel Hornfels	Pyrrhotite	Fine-grained disseminated	5·0
ARF 08/44.65	Norite	Pyrrhotite	Medium-grained disseminated	5·2
ARF 08/49.26	Norite	Pyrrhotite	Fine-grained disseminated	4·5
ARF 08/49.26	Norite	Chalcopyrite	Fine-grained disseminated	4·8
ARF 08/49.26	Norite	Pyrrhotite	Fine-grained disseminated	5·2
ARF 08/52.42	Gabbronorite	Pyrrhotite	Fine-grained disseminated	5·4
ARF 08/73.24	Gabbronorite	Pyrrhotite	Fine-grained disseminated	5·1
ARF 08/76.80	Cordierite-Spinel Hornfels	Pyrrhotite	Fine-to-coarse grained blebs	5·0
ARF 08/82.74	Gabbronorite	Pyrrhotite	Medium-grained disseminated	4·9
ARF 08/96.32	Gabbronorite	Pyrrhotite	Medium-grained disseminated	4·1
ARF 08/106.67	Gabbro	Pyrrhotite	Coarse-grained blebs	4·2
ARF 08/124.64	Massive Sulphide	Pyrrhotite	Massive sulphide	4·9
ARF 08/124.64	Massive Sulphide	Pyrrhotite	Massive sulphide	4·9
ARF 08/124.64	Massive Sulphide	Pyrrhotite	Massive sulphide	4·9
ARF 08/124.64	Massive Sulphide	Pyrrhotite	Massive sulphide	5·4
ARF 08/124.64	Massive Sulphide	Pyrrhotite	Massive sulphide	5·4
ARF 08/126.27	Norite	Pyrrhotite	Fine-to-coarse grained interstitial	5·6
ARF 08/129.78	Norite	Pyrrhotite	Medium-to-coarse grained blebs	5·0
ARF 08/129.78	Norite	Chalcopyrite	Medium-to-coarse grained blebs	5·4
ARF 08/130.89	Norite	Pyrrhotite	Very coarse grained bleb	5·3
ARF 08/153.46	Calc-Silicate	Pyrrhotite	Fine-grained disseminated	4·5
ATS 46/60.34	Pegmatoidal Norite	Pyrrhotite	Coarse-grained bleb	1·1
ATS 46/60.34	Pegmatoidal Norite	Chalcopyrite	Coarse-grained bleb	1·1
ATS 46/61.12	Feldspathic Pyroxenite	Pyrrhotite	Coarse-grained bleb	1·1
ATS 46/61.12	Feldspathic Pyroxenite	Chalcopyrite	Coarse-grained bleb	1·3
ATS 46/61.12	Feldspathic Pyroxenite	Pentlandite	Coarse-grained bleb	0·9
ATS 46/146.71	Feldspathic Pyroxenite	Pyrrhotite	Fine-to-medium grained disseminated	5·9
ATS 46/154.67	Gabbro Norite	Pyrrhotite	Net-textured vein	6·3
ATS 46/207.50	Hornfels	Pyrrhotite	Medium-grained bleb	9·7
ATS 46/316.62	Peridotite	Pyrrhotite	Medium-to-coarse grained interstitial	4·8
ATS 46/345.60	Dunite/Peridotite	Pyrrhotite	Net-textured	5·3
ATS 46/457.49	Pyroxenite	Pyrrhotite	Fine-grained interstitial	5·4
ATS 46/461.21	Feldspathic Pyroxenite	Chalcopyrite	Medium-grained interstitial	5·5
ATS 46/469.25	Calc-silicate	Pyrrhotite	Fine-grained disseminated	16·4
ATS 57/72.48	Pyroxenite	Chalcopyrite	Coarse-grained bleb	1·0
ATS 57/118.78	Pyroxenite	Pyrrhotite	Fine-to-coarse grained interstitial	2·2
ATS 57/180.64	Feldspathic Pyroxenite	Pyrrhotite	Fine-to-medium grained disseminated	4·5
ATS 57/218.39	Pyroxenite	Pyrrhotite	Net-textured	5·0
ATS 57/218.39	Pyroxenite	Chalcopyrite	Net-textured	4·9
ATS 57/221.39	Massive Sulphide/Pyroxenite	Pyrrhotite	Massive sulphides	5·3
ATS 57/221.39	Massive Sulphide/Pyroxenite	Pentlandite	Massive sulphides	5·4
ATS 57/268.15	Feldspathic Pyroxenite	Pyrrhotite	Fine-grained disseminated	4·6
ATS 57/325.32	Calc-silicate	Pyrrhotite	Coarse-grained bleb	28·2
ATS 57/325.32	Calc-silicate	Pyrrhotite	Coarse-grained bleb	27·7
ATS 57/325.32	Calc-silicate	Pyrrhotite	Coarse-grained bleb	28·7
ATS 57/335.07	Calc-silicate	Pyrite	Fine-grained disseminated	16·9
AMK 21/125.76	Pyroxenite	Pyrrhotite	Coarse-grained bleb	2·2
AMK 21/125.76	Pyroxenite	Pyrrhotite	Very coarse grained bleb	2·1
AMK 21/227.15	Serpentinite	Pyrrhotite	Interstitial	3·3
AMK 21/232.62	Pyroxenite	Pyrrhotite	Interstitial	3·6
AMK 21/232.62	Pyroxenite	Chalcopyrite	Interstitial	3·6
AMK 21/235.31	Calc-silicate	Pyrrhotite	Vein within chalcopyrite bleb	3·5
ITS 33/241.16	Feldspathic Pyroxenite	Pyrrhotite	Coarse grained interstitial	1·8
ITS 33/241.16	Feldspathic Pyroxenite	Chalcopyrite	Coarse grained interstitial	1·7
DL1	Dolomite	Bornite	Alteration vein	1·5
DL2	Shale	Pyrite	Medium-grained nodules along bedding planes	8·2
TN75	Anhydrite	Anhydrite	Vein	20·2
VK75-305	Anhydrite	Anhydrite	Vein	19·8

Sample prefixes ARF, ATS and AMK refer to Rietfontein, Turfspruit and Macalacaskop, respectively.

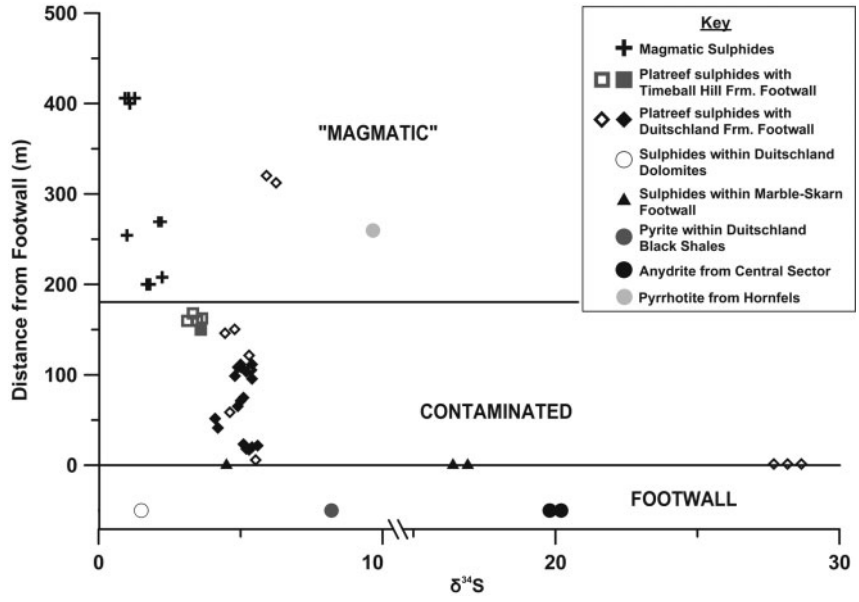

4 Diagram showing variation of $\delta^{34}S$ values with depth and increasing distance from the footwall, as well as $\delta^{34}S$ values from various sulphur-bearing footwalls of the northern limb

Africa, and microdrilled samples at Royal Holloway, University of London in the UK. Samples for sulphur isotope analysis in South Africa were prepared using the procedure outlined by Horstmann and Malinga[18] and analysed using a continuous-flow isotope ratio mass-spectrometer (GEO 20-20). Sulphur isotope analyses conducted in the UK were done using procedures outlined in Grassineau *et al.*[13] All sulphur isotope data are reported relative to Cañon Diablo Troilite (CDT).

Oxygen isotope analyses were undertaken on plagioclase and orthopyroxene separates from various lithologies of the Platreef, as well as on cordierite from footwall xenoliths within the Platreef. These minerals were hand-picked under a binocular macroscope using samples that had been crushed and sieved to –250+125 μm. These silicate separates were crushed to a fine powder, and placed in an oven at approximately 50°C to dry. Once dry, the sample was weighed out (~10 mg) and placed in a nickel reaction vessel (inside diameter ~12 mm) which was over-pressurised above atmosphere with dry nitrogen.[34] The extraction line consisted of ten reaction vessels, of which eight were used for samples, and two for standards.[15] The analysis thereafter follows the procedure outlined in Harris *et al.*[17] The analytical precision is estimated to be ± 0·1 per million based on the long-term average difference between duplicates of the MQ quartz standard.[17]

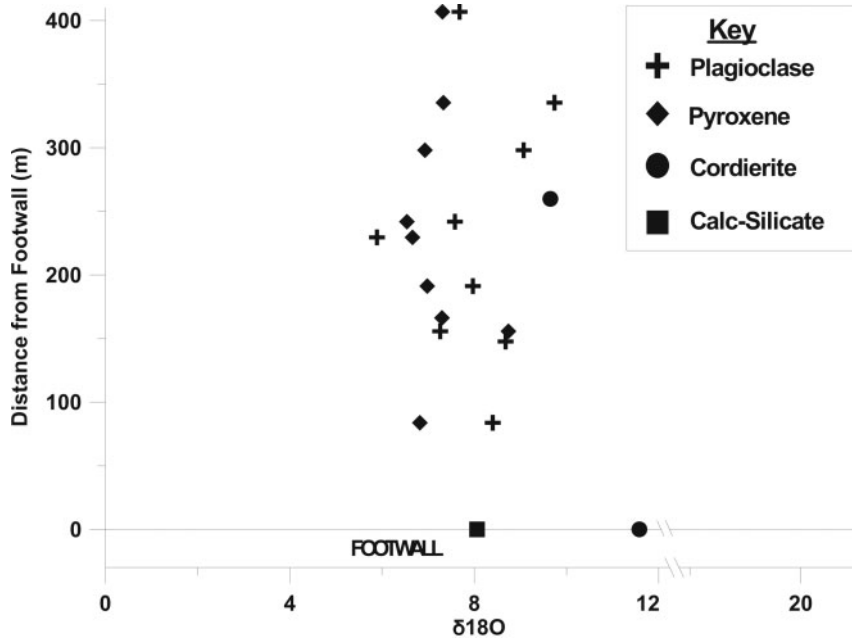

5 Diagram showing variation of $\delta^{18}O$ with depth and distance from footwall, as well as $\delta^{18}O$ values for footwall material that was analysed

Table 2 Details of all oxygen isotope analyses for this study (‰, V-SMOW), as well as the difference between $\delta^{18}O_{plag}$ and $\delta^{18}O_{opx}$ analyses ($\Delta_{plag-opx}$)

Sample number	Rock type	$\delta^{18}O_{plag}$	$\delta^{18}O_{opx}$	$\delta^{18}O_{cord}$	$\delta^{18}O_{calc-sil}$	$\Delta_{plag-opx}$
AMK021/90.25	Spotted Anorthosite	9·1	6·9			2·2
AMK021/222.06	Serpentinite		7·3			
AMK021/232.62	Pyroxenite	7·3	8·7			–1·4
AMK021/240.62	Pyroxenite	8·7				
AMK021/393.33	Metamorphosed quartzite			11·6		
ATS046/60.19	Norite–Leuconorite	7·7	7·3			0·4
ATS046/131.64	Feldspathic Pyroxenite	9·7	7·3			2·4
ATS046/207.25	Hornfels			9·7		
ATS046/275.80	Olivine. Feldspathic Pyroxenite	8·0	7·0			1·0
ATS046/383.23	Feldspathic Pyroxenite–Pyroxenite	8·4	6·8			1·6
ATS046/461.13	Feldspathic Pyroxenite					
ATS046/496.25	Calc-silicate				8·1	
ITS033/241.16	Feldspathic Pyroxenite	7·6	6·5			1·1
ITS033/253.44	Pyroxenite	5·9	6·7			–0·8

Abbreviations: plag, plagioclase; opx, orthopyroxene; cord, cordierite; calc-sil, calc-silicate.

RESULTS

Sulphur isotopes

Data obtained from Platreef sulphides varied according to the type of footwall lithology. On the Turfspruit farm, where the footwall is Duitschland Formation, $\delta^{34}S$ values can be separated into two distinct groups, one with an average of +5·2‰, the other with an average of +1·4‰ (Table 1; Fig. 3). These two groups occur at different depths in the sampled cores, with higher values occurring towards the base (Fig. 4). On the Rietfontein farm, where the footwall is also Duitschland Formation, $\delta^{34}S$ values all grouped together, with an average of +5·0‰ (Table 1; Fig. 3). Hornfels xenoliths from the two farms also split into two groups, with hornfels from the Rietfontein farm having an average $\delta^{34}S$ of +5·2‰, and a hornfels from the Turfspruit farm yielding a $\delta^{34}S$ value of +9·7‰ (Table 1; Fig. 3). Calc–silicates from the two farms generally showed two different sets of results, with pyrite and pyrrhotite within calc–silicates from farm Turfspruit having average $\delta^{34}S$ values of +16·6‰, and a pyrrhotite from farm Rietfontein, yielding an average $\delta^{34}S$ of +4·5‰. Analysis of a coarse-grained sulphide bleb which occurs within a calc–silicate at the base of core ATS 57 yielded anomalously high $\delta^{34}S$ values of +27·69‰ to +28·17‰.

Sulphides from magmatic Platreef rocks sampled from farm Macalacaskop, which has a footwall of Timeball Hill Formation quartzite, showed slightly less variation. Analyses yielded an average $\delta^{34}S$ value of +2·9‰ (Table 1), although a slight decrease in sulphur isotope values (from +3·6‰ to +2·2‰) is seen from the bottom to the top of the sampled core. A serpentinite from the same core yielded a $\delta^{34}S$ value of +3·3‰ and a pyrrhotite from the calc-silicate footwall has a $\delta^{34}S$ value of +3·6‰ (Table 1).

Footwall sedimentary sulphides taken from Farm Duitschland gave varying sulphur isotope values. Bornite from dolomite at the top of the Duitschland sequence yielded $\delta^{34}S$ values of +1·5‰, pyrite from the shales at the base of the sequence gave $\delta^{34}S$ values of +8·2‰, and anhydrite gave $\delta^{34}S$ values of between +19·8‰ and +20·2‰.

Oxygen isotopes

In the Platreef, some small variations of oxygen isotope data occur according to height above the footwall (Fig. 5). Recorded $\delta^{18}O$ values varying from +6‰ to +9‰ for plagioclase, and +6·5‰ to +8·5‰ for pyroxene (Table 2). Cordierite from hornfels rafts showed slightly higher $\delta^{18}O$ values with a maximum of +11·5‰ (AMK021/393.33, ATS046/207.25), whereas a calc–silicate from the direct footwall (ATS046/496.25) had a similar $\delta^{18}O$ as that of the Platreef itself (+8‰). The $\Delta_{plag-opx}$ values recorded by this study show a large variation from –1·48 to +2·41 (Table 2).

DISCUSSION AND CONCLUSIONS

Sulphur isotope analyses of sulphides from eclogites and associated kimberlites on the Kaapvaal Craton yield $\delta^{34}S$ values of +0·2‰ to +2·1‰.[33] This provides a viable range of $\delta^{34}S$ values for magmatic sulphides as they occur beneath Kaapvaal Craton. In this study, sulphides with values within this range were obtained from the top of cores from farms Macalacaskop and Turfspruit. Therefore, the group of $\delta^{34}S$ values that have an average of +1·4‰ can be said to be of magmatic origin and hence help to constrain a magmatic end member for the Platreef.

With increasing depth in the Platreef towards the footwall contact, these values increase from +1·4‰ to +5·2‰, which is seen clearly in Figure 4 where data are plotted against height above footwall contact. The only elevated $\delta^{34}S$ values more that 175 m above the footwall contact are related to a hornfels raft. This increase in $\delta^{34}S$ values towards the footwall contact seems likely to reflect an increasing contribution from crustal sulphur close to the floor. In the southern sector, the most likely source of crustal sulphur is from

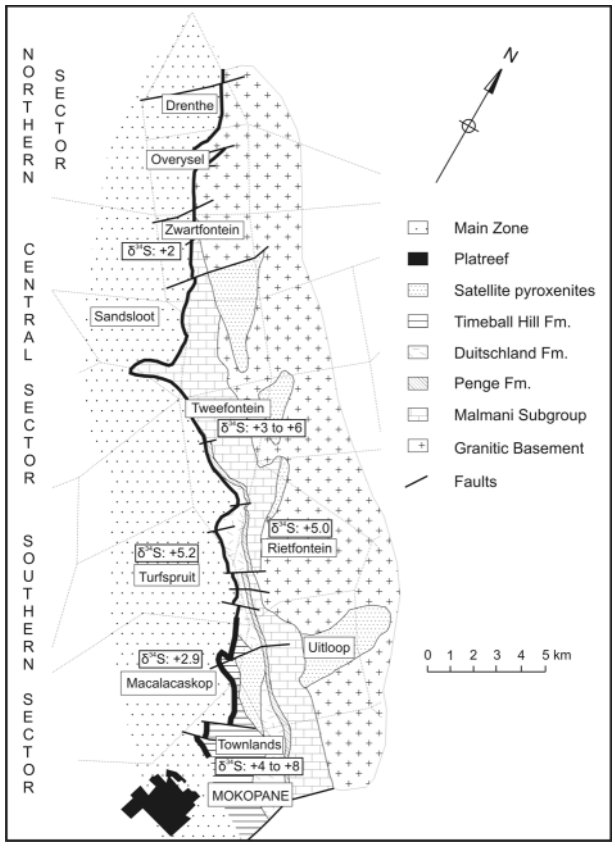

6 Diagram showing the geology of the Platreef with sulphur isotope data of the Platreef and equivalent lithologies. Map from P. Nex; data for Townlands from Manyeruke and Maier;[27] data for Macalacaskop, Turfspruit and Rietfontein from this study; data for Tweefontein from Buchanan *et al.*[4] and Buchanan and Rouse;[5] data for Zwartfontein from Liebenberg[24]

Duitschland Formation footwall, as $\delta^{34}S$ values for other lithologies within the Transvaal Supergroup are generally negative (Fig. 1). This contamination probably occurred through the release of sulphur- and other volatile- and trace element-enriched fluids from the pyrite-rich shale during metamorphism to aluminous cordierite spinel hornfels which occur as rafts in the southern sector of the Platreef. The whole-rock geochemistry of these rafts is similar to that of the shale in the Duitschland Formation.

When combined with data from previous work,[4,5,19,24,26] the data from this study indicates a variation of contaminated $\delta^{34}S$ values for the Platreef along strike (Fig. 6). When there is a quartzite footwall, sulphur isotope values are approximately +3‰, whereas with a footwall of Duitschland formation $\delta^{34}S$ values are approximately +5‰. In the central sector where the footwall is Malmani dolomites, sulphides have sulphur isotope values of +3‰ to +6‰, whereas on Archaean granites in the northern sector $\delta^{34}S$ values are +2‰. We propose that during metamorphism of footwall, volatiles, (including sulphur) are released into the magma. These volatiles travel through the system, causing sulphur saturation and the formation of an immiscible sulphide liquid which re-crystallises any pre-existing magmatic sulphides. The magmatic sulphides which occur at the top of the core have not been affected by these volatiles, and hence retain their primary sulphur isotope signature. Thus, whereas Buchanan *et al.*[4] and Buchanan and Rouse[5] proposed contamination of the Platreef by anhydrite, this study has shown that pyritic shales as well as anhydrite-bearing dolomites have contributed crustal sulphur to the Platreef magma.

The $\delta^{18}O$ data from this study agree in general with previous studies.[16,17,30,31] These datasets indicate the presence of crustal oxygen within the northern limb, and little variation with depth through the entire sequence, especially in contrast to the sulphur isotope data. This is to be expected, however, as oxygen is a major element, and sulphur is a trace element. Addition of a small amount of sulphur from a sedimentary source containing high $\delta^{34}S$ will be noticeable, but similar contamination of a magma

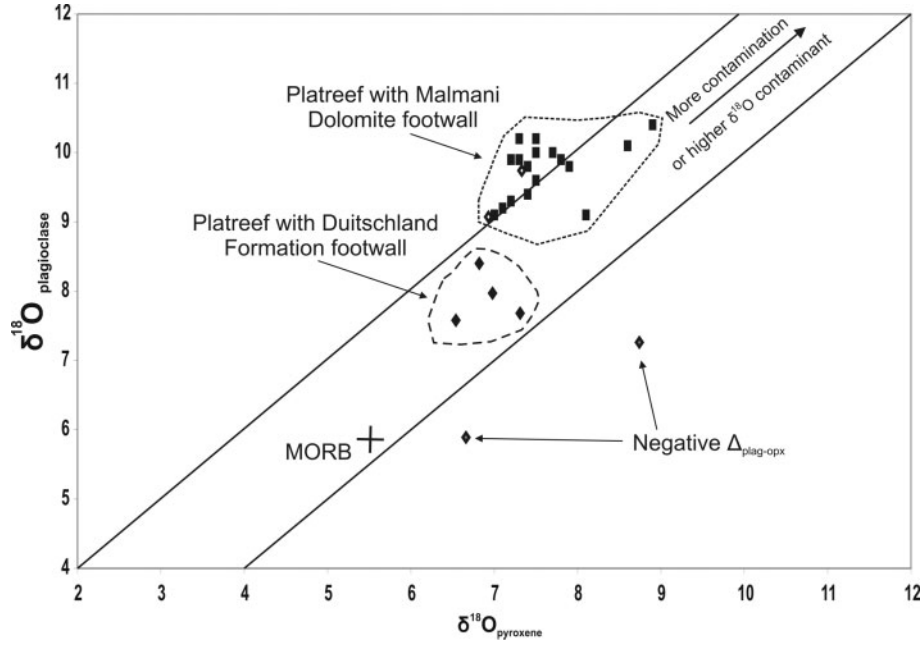

7 Diagram showing different oxygen isotope data for different sectors of the Platreef. Data for Malmani dolomite footwall from Harris and Chaumba[16]

with a $\delta^{18}O$ of 7‰ by a hornfels with a $\delta^{18}O$ of 10‰ will not make a noticeable difference. It is, however, important to note that the Platreef pyroxenites in contact with shale/quartzite have slightly higher $\delta^{18}O$ values than the RLS in general, and are also different to those recorded at Sandsloot (Fig. 7).[29] This indicates either a greater degree of crustal contamination at Sandsloot, or that contaminants at Sandsloot have higher $\delta^{18}O$ values. We believe that the latter of these two possibilities is the more likely, with $\delta^{18}O$ values for the dolomite footwall at Sandsloot being much higher than the $\delta^{18}O$ values for hornfels and quartzite in the south. This agrees with the conclusions reached by this study from the interpretation of sulphur isotope data.

Previous authors[16,17] have recorded $\Delta_{plag-px}$ values of approximately +0·5‰, indicating that silicate minerals were magmatic. These authors suggest that this indicates that contamination of the magma occurred pre-intrusion, probably in a staging chamber. However, the $\Delta_{plag-opx}$ values recorded in this study do not completely support the view that the silicate minerals in the Platreef were formed through magmatic processes. The data presented in this study suggest that some sub-solidus re-equilibration has occurred. This may be due to deuteric fluids moving through the northern limb in the final stages of its formation and possibly causing the re-crystallisation of certain silicate minerals. For example, this may be the result of a granitic component flushing through the system, which is now represented in the Platreef as quartzo-feldspathic veins.[21] This fluid is probably related to the volatile-rich fluid that assisted in the formation of the sulphides within the Platreef.

ACKNOWLEDGEMENTS

We would like to thank Ivanhoe Nickel and Platinum, and especially L. Schürmann for his support of this project in every way, and J. White for logistical support. We would also like to thank the NRF/THRIP for funding this project, and the IOM³ for providing E. Sharman-Harris an opportunity to travel to the UK to conduct analyses. Thanks also go to T. Atkinson at the Bloomsbury Environmental Isotope Facility, University College London for the use of their microdrill, and D. Lowry and N. Grassineau at Royal Holloway, University of London for sulphur isotope analyses. Thanks are due to P. Nex for his help with diagrams and other matters, and M. Tuchscherer for his unconditional support. Finally, we would like to thank the reviewers C. Li and A. Boyce, and the editor I. McDonald for their invaluable input in making this paper what it is.

REFERENCES

1. P. E. B. ARMITAGE, I. McDONALD, S. J. EDWARDS AND G. M. MANBY: 'Platinum-group element mineralisation in the Platreef and calc-silicate footwall at Sandsloot, Potgitersrus District, South Africa', *Appl. Earth Sci. (Trans. Inst. Min. Metall. B)*, 2002, **111**, B36–B45.
2. L. D. ASHWAL, S. J. WEBB and M. W. KNOPER: 'Physical and mineralogical properties of Bushveld rocks: magnetic susceptibility, density and mineral chemistry profiles in the 2950 m Bellevue drillcore, Northern Lobe', *South Afr. J. Geol.*, 2005, **108**, 199–232.
3. A. BEKKER, A. J. KAUFMAN, J. A. KARHU, N. J. BEUKES, Q. D. SWART, L. L. COETZEE and K. A. ERIKSSON: 'Chemostratigraphy of the Paleoproterozoic Duitschland Formation, South Africa: implications for coupled climate change and carbon cycling', *Am. J. Sci.*, 2001, **301**, 261–285.
4. D. L. BUCHANAN, J. NOLAN, P. SUDDABY, J. E. ROUSE, M. J. VILJOEN and J. W. J. DAVENPORT: 'The genesis of sulfide mineralization in a portion of the Potgietersrus Limb of the Bushveld Complex', *Econ. Geol.*, 1981, **76**, 568–579.
5. D. L. BUCHANAN and J. E. ROUSE: 'Role of contamination in the precipitation of sulphides in the Platreef of the Bushveld Complex', (eds. D. L. Buchanan and M. J. Jones), Sulphide deposits in mafic and ultramafic rocks, London, IMM, 1984, 141–146.
6. E. M. CAMERON: 'Sulphate and sulphate reduction in early Precambrian oceans', *Nature*, 1982, **296**, 145–148.
7. O. CATUMEANU and P. G. ERIKSSON: 'The sequence stratigraphic concept and the Precambrian rock record: an example from the 2.7–2.1 Ga Transvaal Supergroup, Kaapvaal Craton', *Precambr. Res.*, 1999, **97**, 215–251.
8. L. L. COETZEE: 'Genetic stratigraphy of the Paleoproterozoic Pretoria Group in the Western Transvaal', Unpublished MSc thesis, Rand Afrikaans University, Johannesburg, South Africa, 2001, 1–212.
9. H. V. EALES and R. G. CAWTHORN: 'The Bushveld Complex', (ed. R. G. Cawthorn), Layered intrusions, Amsterdam, Elsevier Science, 1996, 181–221.
10. P. G. ERIKSSON, W. ALTERMANN, O. CATUNEANU, R. VAN DER MERWE and A. J. BUMBY: 'Major influences on the evolution of the 2.67–2.1 Ga Transvaal basin, Kaapvaal craton', *Sed. Geol.*, 2001, **141/142**, 205–231.
11. I. FRIEDMAN and J. R. O'NEILL: 'Compilation of stable isotope fractionation factors of geochemical interest', (ed. M. Fleischer), Data of geochemistry, 6th edn, (Geol. Sruv. Prof. paper, 440-KK), 1977, 1–117.
12. S. B. GAIN and A. B. MOSTERT: 'The geological setting of the platinoid and base metal sulfide mineralization in the Platreef of the Bushveld Complex in Drenthe, north of Potgietersrus', *Econ. Geol.*, 1982, **77**, 1395–1404.
13. N. V. GRASSINEAU, D. P. MATTEY and D. LOWRY: 'Sulfur isotope analysis of sulfide and sulfate minerals by continuous flow-isotope ratio mass spectrometry', *Anal. Chem.*, 2001, **73**, 220–225.
14. R. E. HARMER: 'New precise dates on the acid phase of the Bushveld and their implications', Workshop on the Bushveld Complex, Burgersfort, South Africa, 2000.
15. C. HARRIS and A. J. ERLANK: 'The production of large-volume low-$\delta^{18}O$ rhyolites during the rifting of Africa and Antarctica: the Lebombo Monocline, southern Africa', *Geochim. Cosmochim. Acta*, 1992, **56**, 3561–3570.
16. C. HARRIS and J. B. CHAUMBA: 'Crustal contamination and fluid-rock interaction during the formation of the Platreef, northern limb of the Bushveld Complex, South Africa', *J. Petrol.*, 2001, **12**, 1321–1347.
17. C. HARRIS, J. J. M. PRONOST, L. D. ASHWAL and R. G. CAWTHORN: Oxygen and hydrogen isotope stratigraphy of the Rustenburg Layered Suite, Bushveld Complex: constraints on crustal contamination', *J. Petrol.*, 2005, **40**, 579–601.
18. U. E. HORSTMANN and O. MALINGA: 'Sulphur isotope analysis on a PDZ ANCA/GEO 20-20 continuous flow isotope ratio mass-spectrometer. Part I – Hardware', Report Stable Isotope Lab 2003–06, South Africa, Council for Geosciences, 2004.

19. L. J. HULBERT: 'A petrological investigation of the Rustenburg Layered Suite and associated mineralization south of Potgietersrus', Unpublished DSc thesis, University of Pretoria, South Africa, 1983.
20. D. HUTCHINSON, J. A. KINNAIRD and L. W. SCHÜRMANN: 'Complex multi-stage mineralisation history in the southern sector of the Platreef, Bushveld Complex, RSA', Geoscience Africa 2004, Abstract Volume, Johannesburg, University of the Witwatersrand, 2004, 293–294.
21. D. HUTCHINSON and I. MCDONALD: 'Breaking the rules. Divergent behavior of platinum and palladium in the Northern Limb of Bushveld Complex, RSA', 10th International Platinum Symposium, Abstract Volume, Oulu, 2005, 118–121.
22. J. A. KINNAIRD, D. HUTCHINSON, L. W. SCHÜRMANN, P. NEX and R. DE LANGE: 'Petrology and mineralisation of the southern Platreef: northern limb of the Bushveld Complex, South Africa', *Miner. Deposita*, 2005, In press.
23. C. LI, E. M. RIPLEY, W. D. MAIER and T. E. S. GOMWE: 'Olivine and sulphur isotopic compositions of the Uitkomst Ni–Cu sulfide ore-bearing complex, South Africa: evidence for sulfur contamination and multiple magma emplacements', *Chem. Geol.*, 2002, **188**, 149–159.
24. L. LIEBENBERG: 'The sulphides in the layered sequence of the Bushveld Igneous Complex', Unpublished DSc thesis, University of Pretoria, South Africa, 1968.
25. W. D. MAIER, N. T. ARNDT and E. A. CURL: 'Progressive crustal contamination of the Bushveld Complex: evidence from Nd isotopic analyses of the cumulate rocks', *Cont. Min. Petrol.*, 2000, **140**, 316–327.
26. T. D. MANYERUKE: 'The petrography and geochemistry of the Platreef on the farm Townlands, near Potgietersrus, northern Bushveld Complex', Unpublished MSc thesis, University of Pretoria, South Africa, 2003.
27. T. D. MANYERUKE and W. D. MAIER: 'The petrography and geochemistry of the Platreef on the farm townlands, near Potgietersrus, Northern Bushveld Complex', Geoscience Africa 2004, Abstract Volume, Johannesburg, University of the Witwatersrand, 2004, 411–412.
28. J. E. J. MARTINI: 'A copper-bearing bed in the Pretoria group in northeastern Transvaal', Geocongress 77, *Geol. Soc. South Afr. Special Pub.*, 1979, **6**, 65–72.
29. J. PRONOST: 'Effects de la contamination continentale des interactions fluids-roches sur le Platreef, complexe igne du Bushveld, Afrique du Sud', Unpublished PhD thesis, University Clermont Ferrand, France, 2005.
30. D. L. REID, R. G. CAWTHORN, F. J. KRUGER and M. TREDOUX: 'Isotope and trace-element patterns below the Merensky Reef, Bushveld Complex, South Africa: evidence for fluids?' *Chem. Geol.*, 1993, **106**, 171–186.
31. C. M. SCHIFFRIES and D. M. RYE: 'Stable isotopic systematics of the Bushveld Complex: I. Constraints of magmatic processes in layered intrusions', *Am. J Sci.*, 1989, **289**, 841–873.
32. H. TSAI: 'Mineral inclusions in diamond: premier, Jagersfontein and Finsch kimberlites, South Africa, and Williamson Mine, Tanzania', (eds. F. R. Boyd, H. O. A. Meyer), Kimberlites, diatremes and diamonds: their geology, petrology and geochemistry, American Geophysical Union, 1979, 16–26.
33. M. J. VAN DER MERWE: 'The layered Sequence of the Potgietersrus Limb of the Bushveld Complex. *Econ. Geol.*, **71**, 1976, 1337 – 51.
34. T. W. VENNEMANN and H. S. SMITH: 'The rate and temperature of reaction of ClF_3 with silicate minerals, and their relevance to oxygen isotope analysis', *Chem. Geol.*, 1990, **86**, 83–88.
35. P. A. WAGNER: 'The platinum deposits and mines of South Africa', London, Struik, 1929, 1–338.
36. J. A. WHITE: 'The Potgietersrus Prospect – Geology and exploration history', XVth CMMI Congress, Johannesburg, SAIMM, 1994, **3**, 173–181.

Authors

Elizabeth Sharman-Harris completed her BSc Honours specialising in geochemistry at the University of the Witwatersrand in 2004. She is currently completing her MSc at the same university looking at the sulphide mineralisation of the Platreef. This year, she won the Inaugural Institute of Materials, Minerals and Mining Young Persons' World Lecture Competition, held at the Institute's headquarters in London.

Judith Kinnaird is Co-Director of the Economic Geology Research Institute in the School of Geosciences, University of Witwatersrand. She was awarded an Honours BSc degree from the University of London, an MSc and PhD from the University of St Andrews in Scotland and is a chartered engineer. She has taught for the Open University in UK and University College Cork in Ireland. Prior to taking up a post in South Africa in 1999 she was an independent consultant for 6 years. She has worked on tin and columbite deposits in Nigeria, gem-bearing pegmatites in Namibia, Nigeria and Somaliland, uranium deposits in Namibia, lead–zinc deposits in Ireland, copper deposits in Ireland and Zambia, alluvial gold deposits in Mozambique and is currently working on the Platreef.

Chris Harris graduated from Oxford University with a BA in 1979 and DPhil in 1982. He is currently Associate Professor at the University of Cape Town and has been in charge of the Stable Isotope Laboratory in the Department of Geological Sciences since 1989.

Uwe Horstmann received his diploma (MSc in 1981) and doctorate (in 1986) in Geology from the University of Göttingen, Germany. His thesis involved K/Ar dating of sedimentary sequences of the Nama Group in Namibia. As a postdoctoral researcher, he worked on the geochemistry of banded iron-formation at the University of Stellenbosch. After a short stint as lecturer at the then University of Durban Westville, he joined the then Geological Survey of South Africa in 1991, later to become the Council for Geoscience. He was in charge of the stable isotope laboratory, working on a variety of isotope applications from ore-deposit research to environmental investigations. In 2005 he was appointed as head of the Environmental Isotope Group at iThemba Labs (Gauteng) for accelerator-based sciences.